

**APPLICATIONS OF QCD TO
SHADOWING, DECAY AND
FRAGMENTATION PHENOMENA**

by

Mohammad Ali Yusuf

Department of Physics
Quaid-i-Azam Univeresity
Islamabad, Pakistan

1996

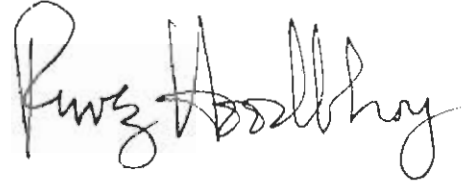
This work is submitted as a dissertation
in partial fulfilment of
the requirements for the degree of

DOCTOR OF PHILOSOPHY
in
PHYSICS

Department of Physics
Quaid-i-Azam University
Islamabad, Pakistan

Certificate

Certified that the work contained in this dissertation was carried out by Mr. Mohammad Ali Yusuf under my supervision.



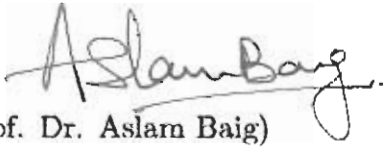
(Prof. Dr. Pervez A. Hoodbhoy)

Department of Physics

Quaid-i-Azam University

Islamabad, Pakistan.

Submitted through:



(Prof. Dr. Aslam Baig)

Chairman

Department of Physics

Quaid-i-Azam University

Islamabad, Pakistan.

Dedicated to the loving memory of my father who
wanted to see me a Ph.D but didn't live long enough.

Acknowledgments

First and foremost, I am grateful to my mentor for Ph.D, Prof. Dr. Pervez Hoodbhoy. His able guidance and deep understanding of physics provided the necessary support to conduct this research. I owe a lot to him not only in physics but in shaping my overall outlook as a liberal, rational minded student of science.

I am indebted to my parents and sisters for their encouragements and moral support during my studies. Seema deserves special thanks since she drew all the diagrams in Corel Draw on a short notice.

I am thankful to my colleagues for their support. In particular, I would like to mention my seniors, Rafia and Nzar, the members of the MAHAAN Group (Muncer, Adnan, Hafsa, Ayyaz, Ali Nuclear Group), Tariq and Raheel. Adnan deserves special thanks since he helped me a lot in sorting out many of the problems related to thesis completion.

During my years of Ph.D work at QAU two colleagues played a vital role in shaping my ideas. First and foremost is Hafsa. For many years she was the only friend available to discuss high energy physics. Second, my detailed discussions with Toor enabled me to understand some of the problems in other branches of physics.

I also wish to acknowledge the Pakistan Atomic Energy Commission and the Pakistan Science Foundation for providing the necessary financial support.

Finally, I owe much to my wife, Fauzia, and to my son, Haider. Without their patience, love, and tolerance over many years, this thesis could not have been completed. In future, my time with them will not be so measured.

(Mohammad Ali Yusuf)

Abstract

In this thesis I explore three hard processes where QCD plays a major role.

In the first problem, different hard nuclear processes are investigated for the possible measurement of the quadrupole gluon distribution, which exists only for hadrons with spin ≥ 1 . Choosing Li^3 as a typical light nucleus I use the convolution model and a QCD inspired parton recombination model to calculate cross section asymmetries. The effects of an exotic quadrupole gluon component upon asymmetries in prompt photon production and J/ψ leptonproduction are estimated. The calculated asymmetries are quite large even though the corresponding cross sections are very small. This raises the hope that this quadrupole asymmetry can ultimately be measured.

The second problem deals with the decay of hadrons, in particular Upsilon decay, which is one of the first applications of QCD and provides a test-bench to study many ideas of QCD. Since it is possible to measure the photon spectrum in the decay $\Upsilon \rightarrow \gamma + 2g$, one can test a theory against many data points. This is in contrast to the prediction of total decay rate which is a single number. I use a systematic gauge-invariant method, which starts directly from QCD and allows for an expansion in the quark relative velocity v , a small natural parameter for heavy quark systems. This technique is used to calculate the rate for an Upsilon meson to decay inclusively into a prompt photon. It is found that the inclusion of these $O(v^2)$ corrections tends to increase the photon rate in the middle z range and to lower it for larger z , a feature supported by the data.

In the third, and last problem, I calculate the fragmentation function for a charm quark to decay inclusively into S-wave charmonium states, including relativistic and binding energy corrections in powers of the quark relative velocity v . In this case the direct introduction of a gauge-link operator provides a quick route to arriving at gauge invariant matrix elements. I also use these fragmentation functions to estimate their contribution to the production rate of η_c and J/ψ in Z^0 decay. These corrections contribute about 38% to the integrated $c \rightarrow J/\psi + X$ fragmentation. For η_c these are found to be small.

List of publications

This thesis is based on the following publications

1. **On the possible measurement of gluon asymmetry in a spinning nucleus**
J. Phys. **G17**, 1637 (1991)
M. A. Yusuf and P.Hoodbhoy.
2. **Relativistic and Binding Energy Corrections To Direct Photon Production In Upsilon Decay**
Phys. Rev. **D54**, 1 (1996)
M. A. Yusuf and P.Hoodbhoy.
3. **Relativistic and Binding Energy Corrections to Heavy Quark Fragmentation Functions**
Submitted to Phys. Rev. **D**
M. A. Yusuf and Adnan Bashir.

Contents

1	Introduction	1
1.1	A Historical Prologue	1
1.2	The Standard Model	3
1.3	Perturbative QCD	4
1.4	A brief description of Ph.D. research	6
1.4.1	Gluon Distribution in a Spinning Nucleus	6
1.4.2	Decays of heavy quarkonia	7
1.4.3	Heavy quark fragmentation functions	8
2	Gluon Distribution in a Spinning Nucleus	12
2.1	The Convolution Model	15
2.2	The Parton Recombination Model	17
2.3	Prompt Photons in Hadron-Hadron Collisions	21
2.4	Leptoproduction of Heavy Mesons in Electron Hadron Collisions .	27
2.5	Conclusion	29
3	Decays of Quarkonia	31
3.1	Introduction	31

3.2	Formalism	33
3.3	Decay Rate	39
3.4	Numerical Work	43
3.5	Conclusion	45
4	Heavy Quark Fragmentation Functions	48
4.1	Kinematics	50
4.2	Formalism	51
4.3	Fragmentation Function for $c \rightarrow \eta_c$	55
4.4	Fragmentation Function for $c \rightarrow J/\psi$	57
4.5	QCD Evolution	58
4.6	Numerical Work	59
4.7	Conclusion	61
1	Gauge Invariance in Υ Decay	64
2	Matrix elements for 1^{--}	66
3	Hermitian Conjugate of Matrix Elements for 1^{--}	68
4	Mathematica programs	71

Chapter 1

Introduction

High-energy physics has made remarkable advances during the past few decades. The construction of new high energy accelerators around the world made it possible to perform more precise experiments which provide a large class of results to be compared with the theoretical predictions. On the theoretical side, the convergence of ideas due to developments in various sectors have brought to the subject a new coherence and have raised new issues. In this introductory chapter I shall begin with a quick historical review of the quark model and the achievements of Quantum Chromodynamics (QCD) and then go on to review the standard model of fundamental interactions and Perturbative QCD (PQCD [1]) in order to set stage for my own research work. The final section presents a brief summary of my Ph.D work in the area of perturbative Quantum Chromodynamics.

1.1 A Historical Prologue

By the end of 1964 some high energy physicists had started feeling that the large number of hadrons known at that time hint towards a possible deeper level of structure of hadrons. The first major theoretical step was taken by Gell-Mann[2] who proposed that all hadrons are made up of three basic entities for which he coined the name “quarks”. Using this model he succeeded not only

in classifying all the known hadrons but predicted the existence of a few more particles. They were later on discovered, providing experimental support to an otherwise theoretical model.

The concrete evidence for quarks however came in 1968 from SLAC where a couple of interesting observations were made when electrons were fired at proton targets. First the scattering involved large momentum transfers more frequently than anticipated [3]. This result suggested that there were discrete scattering centres within proton. Secondly, the distribution of scattered electrons in energy and angle exhibited a phenomenon called scale invariance. It was pointed out by Feynman that scaling could occur only if the scattering centres had no internal structure[4]. This paved the way to a successful parton model and its various predictions which agree well with the data.

A careful analysis of deep inelastic data reveals that quarks behave as if they are free inside a hadron. However isolated free quarks are never observed. This fact suggests that quarks are confined within hadrons due to a very strong force which increases with increasing distance. No rigorous theoretical demonstration of this effect is yet available, it is still a conjecture. However all the experiments support this view of confinement. Despite the fact that QCD has so far been unable to provide a sound theoretical basis for confinement its predictions agree well for high energy processes such as cross section in electron-positron annihilation into hadrons, structure functions in deeply inelastic lepton-nucleon scattering, fragmentation functions and the decay rates of quarkonia. Even the application of PQCD to nuclei seems to be in agreement with data. The simplest case of a deuteron is one such example. The data on $F_2(x, Q^2)$ of the deuteron from the NMC Collaboration are well fitted by a perturbative QCD calculation.

However there are many aspirations in the nonperturbative regime which remain unfulfilled. These include the derivation of the interaction among hadrons as a collective effect of the interactions among constituents, theoretical understanding of the details of fragmentation and decay phenomena etc. This last

problem can only be solved if one makes some reasonable model to describe the dynamics of decaying or produced hadron. I shall be discussing these processes in detail in the next few chapters. But before that, let's discuss the Standard Model of fundamental interactions which allows us to reliably calculate different cross sections and decay rates etc.

1.2 The Standard Model

The standard model[5] of fundamental interactions has proved to be an accurate description of nature at the highest energies available. This model is based upon the following elements:

- 1) the symmetry group $SU(3)_C \otimes SU(2)_L \otimes U(1)$,
- 2) the gauge principle,
- 3) the Higgs mechanism, and
- 4) the Yukawa couplings.

The result is a renormalizable theory which allows precise predictions from a few input parameters. There are three types of particles in this model,

- a) the gauge bosons,
- b) fermions (quarks and leptons) and,
- c) scalar higgs.

The gauge bosons associated with $SU(3)_C$ are called gluons whereas the gauge bosons of $SU(2)_L \otimes U(1)$ are W^\pm , Z^0 and photon. As the present work is concerned with QCD, I shall confine myself to the discussion of $SU(3)_C$.

The gluons are described by vector fields $A_\mu^i(x)$ with μ a vector index and i an $SU(3)_C$ color label for an **8** representation (or the adjoint representation) of the $SU(3)$ group. The quarks are described in terms of Dirac fields $\psi_{\alpha,r}^a$ where α is a Dirac spinor index, a is an $SU(3)$ color label for the **3** representation (or the fundamental representation of the $SU(3)_C$), and $r = u, d, s, c, b$ or t is the flavour label. The QCD lagrangian which is of interest to us, can be written in terms of

these fields :

$$L = -\frac{1}{2} \text{Tr} F_{\mu\nu} F_{\mu\nu} + \bar{\psi}_r (i\gamma \cdot D - m_r) \psi_r, \quad (1.1)$$

where

$$\begin{aligned} F_{\mu\nu} &= \partial_\mu A_\nu - \partial_\nu A_\mu - ig[A_\mu, A_\nu], \\ A_\mu &= \sum_{i=1}^8 \frac{\lambda^i}{2} A_\mu^i, \\ D^\mu &= \partial^\mu - iA^\mu, \end{aligned} \quad (1.2)$$

and λ^i are 3×3 matrices, called the Gell-Mann matrices, obeying the $SU(3)$ commutation relations for generators

$$\left[\frac{\lambda^i}{2}, \frac{\lambda^j}{2} \right] = if_{ijk} \frac{\lambda^k}{2}. \quad (1.3)$$

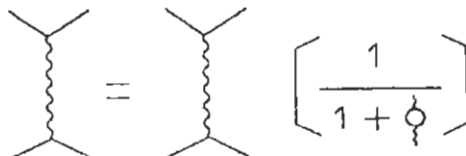
It should be noted that the above lagrangian contains gluon-gluon interactions which is a key feature of non-abelian gauge theories like QCD. I shall now go on to discuss perturbative QCD (PQCD) in the next section.

1.3 Perturbative QCD

In order to make accurate and sensible predictions in QCD it is important to understand the variation of effective color charge with the separation of the two charged particles (quarks or quark and antiquark). The whole perturbation theory relies on the value of the perturbation parameter which in this case is the coupling constant. Recall that in QED the renormalized running coupling constant is given by

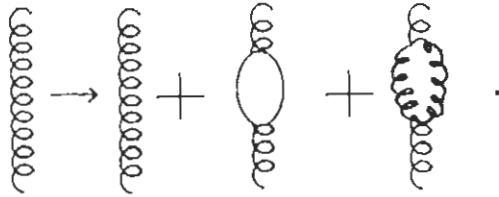
$$\alpha(Q^2) = \frac{\alpha(\mu^2)}{1 - \frac{\alpha(\mu^2)}{3\pi} \log\left(\frac{Q^2}{\mu^2}\right)}, \quad (1.4)$$

for large Q^2 . This incorporates all the corrections coming from 1,2,.. bubble diagrams like those shown below



contributing to any process involving photon exchange (like electron-positron scattering). It describes how the effective charge depends on the separation of the two charged particles. As Q^2 increases, the photon sees more and more charge until, at some astronomically large but finite Q^2 , the coupling constant is infinite. It increases from $1/137$ very slowly as Q^2 increases.

The Q^2 behaviour of QCD coupling, $\alpha_s(Q^2)$, turns out to be very different from that for $\alpha(Q^2)$. Because of the possibility of self interactions of gluons many more diagrams need to be considered here. For example:



It turns out that

$$\alpha_s(Q^2) = \frac{\alpha_s(\mu^2)}{1 + \frac{\alpha_s(\mu^2)}{12\pi}(33 - 2n_f) \log(\frac{Q^2}{\mu^2})}, \quad (1.5)$$

where n_f is the number of flavours. Only if $n_f > 16$ is the sign of the coefficient is the same as in QED. Therefore with increasing Q^2 the value of strong coupling constant decreases, making perturbative expansion more and more reliable. For sufficiently low Q^2 , the effective coupling will become large. It is usual to denote the Q^2 scale at which this happens by Λ^2 , where

$$\Lambda^2 = \mu^2 \exp\left(\frac{-12\pi}{(33 - 2n_f)\alpha_s(\mu^2)}\right). \quad (1.6)$$

Therefore I can rewrite the above equation as

$$\alpha_s(Q^2) = \frac{12\pi}{(33 - 2n_f) \log(\frac{Q^2}{\Lambda^2})}. \quad (1.7)$$

For Q^2 values much larger than Λ^2 , α_s is small and a perturbative description in terms of quarks and gluons interacting makes sense. When Q^2 is of order Λ^2 , one cannot make such a picture, since quarks and gluons will arrange themselves

into strongly bound hadrons. Thus Λ , which is a free parameter, is a boundary between a world of quasi-free partons and the world of hadrons. One expects it to be of the order of a typical hadron mass.

1.4 A brief description of Ph.D. research

In the following three sections I shall present a summary of my Ph.D. research.

1.4.1 Gluon Distribution in a Spinning Nucleus

The recent interest in the spin dependence of the gluon distribution was sparked by the observation that quarks inside a proton carry only a fraction of the total spin of the parent particle. This hints towards a significant gluon distribution inside a proton. Gluons are the analogues of $U(1)$ photon in a $SU(3)$ theory. Their role in a non-abelian theory is even more important due to the fact that they carry color charge and therefore their self interactions are possible. Although gluons do not interact directly with electrons or neutrinos, their effect can be seen indirectly in many processes. One such process which is studied is the prompt photon production in hadron-hadron collisions. This process is sensitive to the gluon distribution because of the dominance of Compton scattering. I have used a Li^7 target as a model to estimate the effects of the quark and gluon recombination. A parton recombination model handles the effects arising from the close proximity or overlap of neighbouring nucleons in a nucleus which affects the short distance physics of the partons. There is a possibility of leaking of a parton from a particular nucleon and its fusion with a parton of a neighbouring nucleon. Such effects are estimated easily using the model of Close et al[7]. The Li^7 target has a closed core of $J = 0$ with a single proton revolving around it with $l = 1, s = 1/2$ and $J = 3/2$. For such a system one can calculate both the crosssection and the crosssection asymmetry in terms of parton level crosssections and parton distributions.

Another process where gluons play a significant role at the tree level is the leptoproduction or photoproduction of heavy flavours. It is found that the gluon asymmetry in this case is considerably larger than the case of prompt photons. This gives us a hope that the gluon asymmetry will ultimately be measured.

1.4.2 Decays of heavy quarkonia

In the previous section I have discussed the total cross sections for two different processes involving hadrons in the initial state, without any concern about the final states. However there are many interesting questions about the configuration of final state hadrons. For example one might ask about the fate of a quark produced in the final state, or about the subsequent decay of hadronic states produced in high-energy collisions. With the present understanding of perturbative QCD it is possible to study these processes to some extent. It will be shown in the third and fourth chapters that both fragmentation and decay processes can be decomposed into a product of two parts: a ‘hard’ part calculable in PQCD and a soft part that can only be modelled at present. It turns out that this phenomenological description is quite adequate for many processes.

One of the earliest applications of quantum chromodynamics was to the decay of η_c and J/ψ mesons. Combined with radiative corrections, this provided the hope of measuring the strong coupling constant at reasonably large momentum transfers. The model that was used was essentially that of Weisskopf-Van Royen[7] for positronium decays, with appropriate modifications for color. In this model, the annihilating fermions are on-shell but are nevertheless confined by some potential. The problem with this model is that a fundamental symmetry of gauge theory, whether QED or QCD, is lost. Therefore there is a need to construct a proper theory of quarkonia which respects gauge invariance. In this work, I have used a systematic approach to incorporate gauge invariance by expanding in powers of the relative quark velocity. Gauge-invariance is then not destroyed even if the quarks are taken off-shell. This treatment automatically introduces

soft gluons in the expansion which are essential to restore gauge-invariance.

For sufficiently high quark mass one can use perturbation theory to compute the decay rate in terms of the wave function at the origin. This zeroth-order result requires modifications due to the fact that the relative velocity of bound heavy quarks is not zero but that $v^2 \approx 0.3$ for $c\bar{c}$ and ≈ 0.1 for $b\bar{b}$ states. The corrections of order v^2 come from:

- 1) non-zero binding energy of the two quarks in the quarkonium, and
- 2) a wavefunction correction which can be calculated in terms of the free parameter $\nabla^2\psi(0)$. It is found that the inclusion of these $O(v^2)$ corrections tends to increase the photon rate in the middle z range and to lower it for larger z , a feature supported by the data.

1.4.3 Heavy quark fragmentation functions

My interest in this area was initiated by the observation that in all existing treatments of fragmentation, color gauge invariance is not properly accounted for, even for twist-2 fragmentation functions. Effectively, all authors have implicitly assumed the size of the produced meson to be so small that the gauge-link between the quark and antiquark, which act as color sources, is a unit operator. This is valid only in the limit of infinitely massive quarks. But certainly this cannot be true for c or b quarks - even for the t quark this would be true only to a few percent.

The first step is to write down the amplitude which is given by the sum of all distinct Feynman diagrams leading from the initial state to the final state. Each diagram is then put into the form of a (multiple) loop integral with a kernel which is a product of a hard part and a soft part. The hard part is treated with perturbative QCD, and the soft part is analyzed into its different components with the use of Lorentz, \mathcal{C} , and \mathcal{P} symmetries.

It is found that for fragmentation processes, direct introduction of a link operator offers a quicker route to arriving at gauge-invariant matrix elements. While

these cannot be calculated ab-initio, they can be modeled in a non-relativistic model. Alternatively, they can be extracted from experiment by examining decay rates where large momentum transfers are involved.

The technique developed can be easily extended to calculate the fragmentation of a c (and b) quark to 1^{--} states etc. The state 1^{--} (J/ψ) is of particular importance as its decay into lepton pairs provides an easily identifiable experimental signature.

I have calculated the fragmentation function for a charm quark to decay inclusively into S-wave charmonium states, including relativistic and binding energy corrections in powers of the quark relative velocity v . Since the average value of v^2 for charmonium is about $1/3$, one expects the effect of $\mathcal{O}(v^2)$ terms not to be negligible. I found that in case of J/ψ these corrections contribute about 38% to the lowest order $c \rightarrow J/\psi + X$ result, but for η_c this contribution is small.

References

[1] There are many excellent accounts of QCD. Below is a short list :

- F. Halzen and A.D. Martin, "Quarks and Leptons", John Wiley and Sons, Inc, 1984.
- F.E. Close, "An Introduction to Quarks and Partons", Academic Press, 1979.
- R.D. Field, "Applications of Perturbative QCD", Addison-Wesley Publishing Company, Inc. (1989).
- V. Barger and R. Phillips, "Collider Physics", Addison-Wesley Publishing Company.
- T. Muta, "Foundations of Quantum Chromodynamics", World Scientific Pub Co Pte Ltd, 1987.
- W. Greiner and A. Schafer, "Quantum Chromodynamics", Springer-Verlag, 1995

[2] Gell-Mann, M. California Institute of Technology Report CTSL-20 (1961). (Reprinted in "The Eightfold Way", Gell-Mann and Ne'eman, Benjamin, New York, 1964.)

[3] Panofsky, W. in *Proceedings of International Symposium on High Energy Physics*, Vienna, 1968.

[4] Bjorken, J. D. in *Proceedings of 3rd International Symposium on Electron and Photon Interactions*, Stanford, California, 1967. Bjorken, J. D and

Paschos, E. A. Phys. Rev **185**, 1975 (1969). Feynman, R. P. Phys. Rev. Lett. **23**, 1415 (1969).

[5] There are innumerable texts discussing the standard model. See for example, J. F. Donoghue, E. Golowich, B. R. Holstein, “ Dynamics of the Standard Model”, Cambridge University Press, 1992.

[6] F.E. Close, J. Qiu and R.G. Roberts, Phys. Rev. **D40**, 2820 (1989).

[7] R. Van Royen and V.F.Weisskopf, Nuovo Cimento **50**, 617, 1967.

Chapter 2

Gluon Distribution in a Spinning Nucleus

The gluon asymmetry in a polarized proton has become the focus of considerable interest following the EMC measurements [1] of polarization asymmetry in the deep inelastic scattering of polarized muons on polarized protons. In this chapter I shall be discussing in detail the gluon distributions, specifically the polarized ones measurable in deep inelastic scattering (DIS) off nuclear targets. I will look for processes which may provide independent direct measurements of the spin dependence of the gluon density in a polarized nuclear target. The knowledge of $\Delta G(x, Q^2)$ is interesting in its own right and is necessary for extracting the correct behaviour of the spin dependent quark and antiquark distributions from the available DIS data.

Before going into the details of gluon distributions let us first look at the way gauge fields appear in a non-Abelian group. This will help us in understanding the self interactions of gluons - a process which plays a vital role in the gluon recombination model.

The non-interacting lagrangian density can be written as

$$\mathcal{L}_0 = \bar{\psi}(i\gamma^\mu\partial_\mu - m)\psi. \tag{2.1}$$

Invariance of the spinor fields under the infinitesimal local gauge transformations of the $SU(3)$ colour group, i.e., under

$$\psi(x) \rightarrow [1 - ig\alpha_a(x)T_a]\psi(x), \quad (2.2)$$

requires that the ordinary derivative be replaced by a covariant derivative D defined as

$$D_\mu = \partial_\mu - igT_a A_\mu^a, \quad (2.3)$$

where the auxiliary field (or the gauge field) A_μ transforms under the adjoint representation of the $SU(3)$ group, i.e.,

$$A_\mu^a(x) \rightarrow A_\mu^a(x) + \partial^\nu \alpha_a(x) + gf_{abc}\alpha_b(x)A_\mu^c(x), \quad (2.4)$$

and $T_a = \lambda_a/2$. The Lagrangian density then becomes

$$\mathcal{L}_q = \bar{\psi}(i\gamma^\mu D_\mu + m)\psi. \quad (2.5)$$

The gauge-invariant part in the lagrangian for the A field is

$$\mathcal{L}_g = -\frac{1}{4}F_a^{\mu\nu}F_{a\mu\nu}, \quad (2.6)$$

where the gluon field tensor is defined as

$$F_a^{\mu\nu} = \partial^\mu A_a^\nu - \partial^\nu A_a^\mu - gf_{abc}A_b^\mu A_c^\nu. \quad (2.7)$$

Therefore the total lagrangian density can be written as

$$\mathcal{L} = \mathcal{L}_q + \mathcal{L}_g. \quad (2.8)$$

It is straight-forward to see that the last term of the field strength tensor gives rise to self interactions of gluons. As the field tensor appears squared in the lagrangian, 3-gluon and 4-gluon interactions are also possible. The present experimental situation is that there are many indirect evidences of 3-gluon vertex but the 4-gluon vertex is still not easy to detect. I shall come back to the 3-gluon interactions in the section on the recombination model. This ends our very brief tour of the theoretical arguments behind the necessity of gluons and their self interactions in a non-abelian Yang-Mills theory.

Now consider the polarized gluon distributions in hadrons which is the subject of this chapter. For transverse gluons in a longitudinally polarized $J = 1/2$ hadron target, there is only one gluon asymmetry,

$$\Delta G(x, Q^2) = G_{\uparrow}^{\frac{1}{2}} - G_{\downarrow}^{\frac{1}{2}}, \quad (2.9)$$

where $\uparrow\downarrow$, denote gluon helicities and $1/2$ indicates positive helicity of the target. But in view of discussions [2, 3] of deep inelastic scattering from polarized $J \geq 1$ targets, it is worthwhile to ask what additional gluon asymmetries exist for higher spins and whether their measurement would be interesting and possible. From parity invariance $G_{\uparrow}^H = G_{\downarrow}^{-H}$ with $-J \leq H \leq J$. For $J = 1$ there are two independent asymmetries which can be chosen as

$$\Delta G = G_{\uparrow}^1 - G_{\downarrow}^1, \quad (2.10)$$

and

$$\Delta G = \frac{1}{2}(G_{\uparrow}^1 + G_{\downarrow}^{-1} - 2G_{\uparrow}^0). \quad (2.11)$$

The latter ‘‘quadrupole’’ asymmetry is interesting; it can be measured with an unpolarized probe (see below) and, paraphrasing the discussion for the quark distribution in [2], it can be easily seen to vanish for two independent nucleons in a relative s state. For p, d, f, \dots states it is small, of order $\langle P^2/M^2 \rangle$. Thus it is a good indicator of ‘‘exotic’’ gluons in a nucleus - i.e. the extent to which the nuclear gluon distribution is non-additive. For $J = 3/2$, the corresponding gluon asymmetry of interest is

$$\Delta G = \frac{1}{2}(G_{\uparrow}^{\frac{3}{2}} - G_{\uparrow}^{\frac{1}{2}} - G_{\downarrow}^{-\frac{1}{2}} + G_{\downarrow}^{-\frac{3}{2}}), \quad (2.12)$$

or, equivalently,

$$\Delta G = G_{\uparrow}^{\frac{3}{2}} - G_{\downarrow}^{\frac{1}{2}}, \quad (2.13)$$

where

$$G^H = \frac{1}{2}(G_{\uparrow}^H + G_{\downarrow}^{-H}).$$

The plan of this chapter is as follows. The first section discusses the convolution framework for the study of deep inelastic electron-nucleus scattering. Then

I shall focus on an aspect of perturbative QCD which is usually ignored. This is the fusion of quarks, antiquarks and gluons of two separate nucleons in a nucleus. In order to estimate the effects of this fusion on the nuclear gluon distribution two processes are chosen which involve gluons at tree level and hence are a useful probe of nuclear gluon distribution. These are discussed in the next two sections.

2.1 The Convolution Model

To study the deeply inelastic electron-proton scattering I use the probability of finding a quark inside a nucleon to compute the e-p scattering crosssection. But in the case of scattering off nuclear targets one has to deal with a more difficult problem. The essential argument of convolution model is that the probability distribution of a quark in a nucleus is the product of the probability distributions of a quark inside a nucleon and that of finding a nucleon inside a nucleus. This is shown schematically in figure 1. Denote,

$q_{\uparrow}^{\frac{1}{2}}(z) =$ Probability distribution of a quark with helicity \uparrow in a nucleon with helicity $s = \frac{1}{2}$ carrying light cone momentum fraction z of the nucleon,

$q_{\uparrow}^{JH}(x) =$ Probability distribution of a quark with helicity \uparrow in a nucleus with spin J , helicity H , carrying momentum fraction x of the nucleus, and

$f_s^{JH}(y) =$ Probability distribution of a nucleon with helicity s in a nucleus with spin J and helicity H ,

then the convolution model states that

$$q_{\uparrow}^{JH}(x) = \int \int dy dz \sum_s f_s^{JH}(y) q_{\uparrow}^s(z) \delta(x - yz). \quad (2.14)$$

Antiquark and gluon distributions $\bar{q}_{\uparrow}^{JH}(x)$ and $G_{\uparrow}^{JH}(x)$ are defined similarly. In order to calculate $f_s^{JH}(y)$, start with the definition [2, 3]

$$f_s^{JH}(y) = \frac{1}{2\pi} \int d\xi^- e^{-iy\lambda\xi^-/\sqrt{2}} \langle JH | \bar{\psi}(\xi^-) \gamma^1 \psi(0) | JH \rangle. \quad (2.15)$$

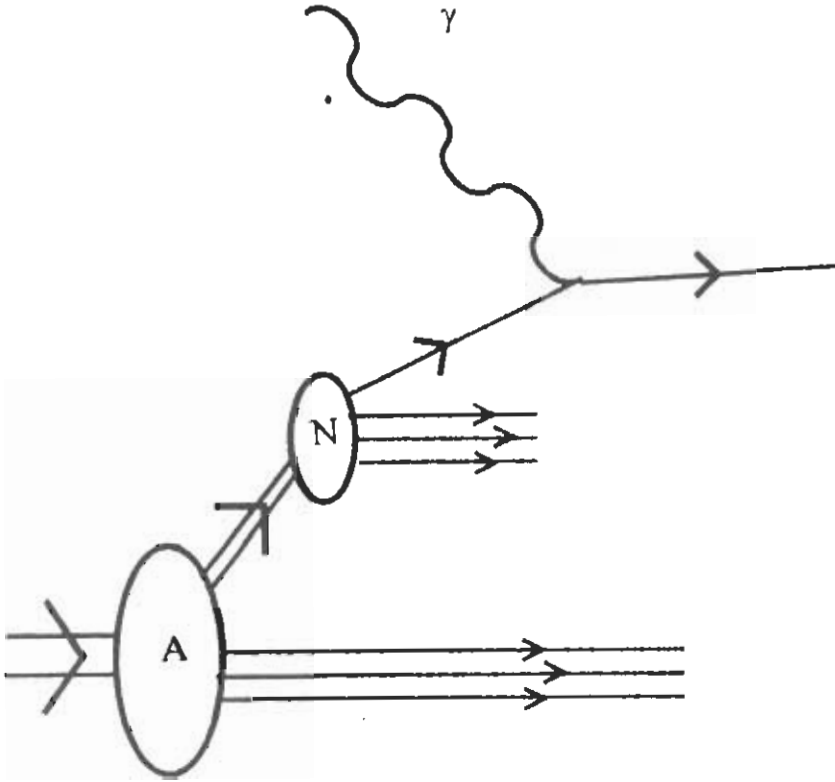


Figure 2.1: Convolution framework for DIS off nuclear target A

Next, insert a complete set of momentum states between the field operators, $\mathbf{1} = \int d^3p |p\rangle \langle p|$ and use translational invariance to get

$$f^{JH}(y) = \sqrt{2} \int d^3p \delta\left(y - \frac{E(p) + p^3}{M}\right) \bar{\psi}^{JH}(\vec{p}) \gamma^+ \psi^{JH}(p), \quad (2.16)$$

where the delta functions comes from the ξ^- integration. In the above $\psi^{JH}(\vec{p})$ is the momentum space Dirac wavefunction of a nucleon. One can further decompose $\psi^{JH}(\vec{p})$ into upper and lower components,

$$\psi^{JH}(\vec{p}) = \begin{pmatrix} \varphi^{JH}(\vec{p}) \\ \frac{\vec{\sigma} \cdot \vec{p}}{2m} \varphi^{JH}(\vec{p}) \end{pmatrix},$$

where I have also used the Dirac equation to write the lower component η^{JH} as

$$\eta^{JH}(\vec{p}) = \frac{\vec{\sigma} \cdot \vec{p}}{2m} \varphi^{JH}(\vec{p}), \quad (2.17)$$

upto corrections of the order of interaction energies divided by the nucleon mass.

One therefore arrives at the light-cone distribution function f^{JH} :

$$f^{JH}(y) = \int d^3p |\varphi^{JH}(\vec{p})|^2 \left(1 + \frac{p^3}{M} + \frac{|\vec{p}|^2}{4M^2}\right) \delta\left(y - \frac{E + p^3}{M}\right). \quad (2.18)$$

The above approximately includes binding of the nucleon since $p^0 = M - \epsilon$, as well as the leading order relativistic effect. Since $p^0 + p^3$ is quite close to M , the distribution peaks at around $y = 1$. This allows us to expand the delta function in a rapidly convergent series in $\delta(y - 1)$ and its derivatives. Also write $|\varphi^{\frac{3}{2}, \frac{3}{2}}(\vec{p})|^2$ in terms of spherical harmonics,

$$\varphi^{\frac{3}{2}, \frac{3}{2}}(\vec{p}) = C_{1, \frac{1}{2}}^{\frac{1}{2}, \frac{3}{2}} Y_{11}(\theta, \phi) \phi(p) \chi^{\frac{1}{2}, \frac{1}{2}}, \quad (2.19)$$

and similarly for $\varphi^{\frac{3}{2}, \frac{1}{2}}(\vec{p})$. In the above $\phi(p)$ is the radial wavefunction (in momentum space) of the single nucleon state (normalized so $\int p^2 |\phi(p)|^2 (1 + p^2/4M^2) dp = 1$). One finally arrives at the following simple expression,

$$f^{\frac{3}{2}, \frac{3}{2}}(y) - f^{\frac{3}{2}, \frac{1}{2}}(y) = -\frac{2}{15} \langle \frac{p^2}{M^2} \rangle \left[-2\delta'(y - 1) + \delta''(y - 1) \right], \quad (2.20)$$

where

$$\langle \frac{p^2}{M^2} \rangle \equiv \int_0^\infty dp \frac{p^2}{M^2} |\phi(p)|^2 \simeq 0.04. \quad (2.21)$$

The various quadrupole asymmetries are readily computed from the above,

$$\begin{aligned} \Delta G(x) &= G^{\frac{3}{2}} - G^{\frac{1}{2}} \\ &= -\frac{2}{15} \langle \frac{p^2}{M^2} \rangle \left(2 \left| \frac{d}{dy} \frac{G(x/y)}{y} \right|_{y=1} + \left| \frac{d^2}{dy^2} \frac{G(x/y)}{y} \right|_{y=1} \right). \end{aligned} \quad (2.22)$$

The quark and antiquark distributions are obtained similarly. However I need only the gluon asymmetry for my work.

2.2 The Parton Recombination Model

There is a modification to structure functions coming from an effect[7] which plays an important role when the nucleons in a nucleus are in close proximity. This is the leaking of partons of one nucleon into a neighbouring nucleon and their subsequent fusion with partons of that nucleon. This is shown schematically in Fig. 2. There are three possible situations, namely quark-gluon fusion, quark-antiquark fusion, and gluon-gluon fusion. The physical effects of such processes

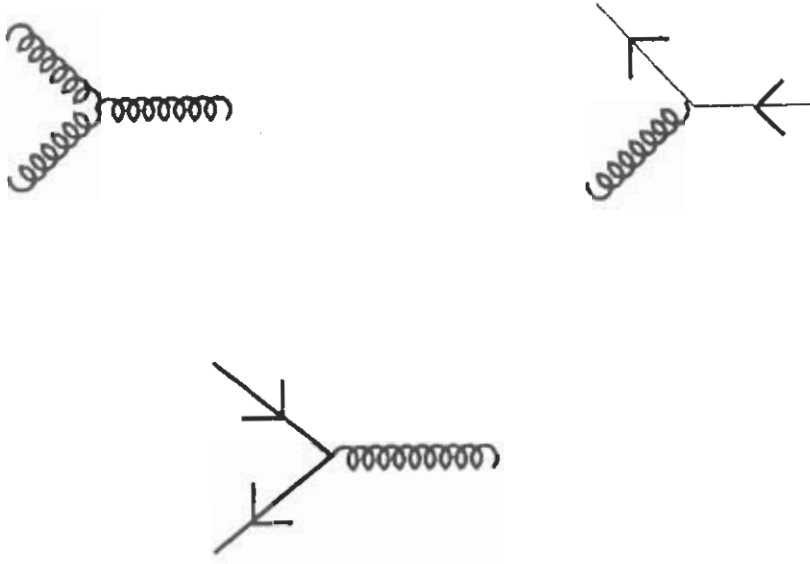


Figure 2.2: Three basic subprocesses contributing to $\delta x P(x)$.

are largely felt at small x and at large x . The reasons for this are very simple and easy to understand. As shown in figure 2c, two gluons may fuse together to form a single gluon. This reduces the gluon distribution in a nucleus at small x . This is called the gluon shadowing. A quark coming from a nucleon might be carrying a large fraction of the nucleon's momentum and therefore, after absorbing a gluon from another nucleon, will carry a momentum fraction > 1 . Thus nuclear structure functions extend beyond $x = 1$. However this occurs only when the spatial overlap between nucleons is appreciable. When viewed in the infinite momentum frame the nucleus is Lorentz contracted in the \hat{z} direction and has a longitudinal size $\Delta z_A 2R/\gamma \approx 2mR/P$, where m and P are the nucleon mass and momentum respectively. On the other hand, the longitudinal size of a sea parton (whether quark or gluon) is $\Delta z \simeq 1/xP$, where x is the fraction of the nucleon's momentum carried by the parton. For small x , Δz exceeds the size of the nucleus and shadowing occurs for $x \leq 1/2mR$ i.e. the nuclear parton distribution is no longer A times the nucleon parton distribution, $q^A \neq Aq^N$. For sufficiently small x the sea quarks and gluons from a given nucleon extend along the entire length of the nucleus in the z direction. The nuclear quark and gluon densities can be

written as

$$x P_A(x) = x P(x) + \delta x P(x), \quad (2.23)$$

where the first part corresponds to the convolution model and the second part corresponds to the correction coming from recombination effects. Three basic subprocesses illustrated in Fig. 2, gives rise to changes in $\delta x P(x)$. Using old-fashioned perturbation theory in the infinite momentum frame, all parton-parton fusion functions are readily calculated[7]. Consider the fusion of parton 1 with momentum fraction x_1 and parton 2 with momentum fraction x_2 to form parton 3 with momentum fraction x_3 . The modification to the quark density is

$$\begin{aligned} \delta q_i(x) = & \left[2 \begin{array}{c} \mathbf{x}_1 \\ \diagdown \\ \text{---} \\ \diagup \\ \mathbf{x}_2 \end{array} \begin{array}{c} \text{---} \\ \diagup \\ \mathbf{x} \end{array} - 2 \begin{array}{c} \mathbf{x} \\ \diagdown \\ \text{---} \\ \diagup \\ \mathbf{x}_2 \end{array} \begin{array}{c} \text{---} \\ \diagup \\ \mathbf{x} \end{array} - 2 \begin{array}{c} \mathbf{x} \\ \diagdown \\ \text{---} \\ \diagup \\ \mathbf{x}_2 \end{array} \begin{array}{c} \text{---} \\ \diagup \\ \mathbf{x} \end{array} \right] \\ & = 2K \left[\int dx_1 dx_2 q_i(x_1) G(x_2) \Gamma_{qq \rightarrow q}(x_1, x_2, x_1 + x_2) \right. \\ & \quad \left. (\delta(x - x_1 - x_2) - \delta(x - x_1)) \right. \\ & \quad \left. - \int dx_1 dx_2 q_i(x_1) \bar{q}_i(x_2) \Gamma_{q\bar{q} \rightarrow g}(x_1, x_2, x_1 + x_2) \delta(x - x_1) \right]. \quad (2.24) \end{aligned}$$

Similarly for antiquark distribution :

$$\begin{aligned} \delta \bar{q}_i(x) = & 2K \left[\int dx_1 dx_2 \bar{q}_i(x_1) G(x_2) \Gamma_{q\bar{q} \rightarrow q}(x_1, x_2, x_1 + x_2) \right. \\ & \quad \left. (\delta(x - x_1 - x_2) - \delta(x - x_1)) \right. \\ & \quad \left. - \int dx_1 dx_2 \bar{q}_i(x_1) \bar{q}_i(x_2) \Gamma_{q\bar{q} \rightarrow g}(x_1, x_2, x_1 + x_2) \delta(x - x_1) \right]. \quad (2.25) \end{aligned}$$

The diagrams contributing to gluon distribution are,

$$\begin{aligned} \delta G(x) = & \left[\begin{array}{c} \mathbf{x}_1 \\ \diagdown \\ \text{---} \\ \diagup \\ \mathbf{x}_2 \end{array} \begin{array}{c} \text{---} \\ \diagup \\ \mathbf{x} \end{array} - \begin{array}{c} \mathbf{x} \\ \diagdown \\ \text{---} \\ \diagup \\ \mathbf{x}_2 \end{array} \begin{array}{c} \text{---} \\ \diagup \\ \mathbf{x} \end{array} - \begin{array}{c} \mathbf{x}_1 \\ \diagdown \\ \text{---} \\ \diagup \\ \mathbf{x} \end{array} \begin{array}{c} \text{---} \\ \diagup \\ \mathbf{x} \end{array} \right] \\ & + 2 \begin{array}{c} \mathbf{x}_1 \\ \diagdown \\ \text{---} \\ \diagup \\ \mathbf{x}_2 \end{array} \begin{array}{c} \text{---} \\ \diagup \\ \mathbf{x} \end{array} - 2 \begin{array}{c} \mathbf{x}_2 \\ \diagdown \\ \text{---} \\ \diagup \\ \mathbf{x} \end{array} \begin{array}{c} \text{---} \\ \diagup \\ \mathbf{x} \end{array} - 2 \begin{array}{c} \mathbf{x}_2 \\ \diagdown \\ \text{---} \\ \diagup \\ \mathbf{x} \end{array} \begin{array}{c} \text{---} \\ \diagup \\ \mathbf{x} \end{array} \end{aligned}$$

$$\begin{aligned}
&= 2K \left[\frac{1}{2} \int d\mathbf{x}_1 d\mathbf{x}_2 G(x_1) G(x_2) \Gamma_{gq \rightarrow g}(x_1, x_2, x_1 + x_2) \right. \\
&\quad \left. (\delta(x - x_1 - x_2) - \delta(x - x_1) - \delta(x - x_2)) \right. \\
&\quad + \int d\mathbf{x}_1 d\mathbf{x}_2 \sum_i^f q_i(x_1) \bar{q}_i(x_2) \Gamma_{q \rightarrow q}(x_1, x_2, x_1 + x_2) (\delta(x - x_1 - x_2) \\
&\quad \left. - \int d\mathbf{x}_1 d\mathbf{x}_2 G(x_1) \sum_i^f (q_i(x_2) + \bar{q}_i(x_2)) \Gamma_{gq \rightarrow q}(x_1, x_2, x_1 + x_2) \delta(x - x_1) \right]. \quad (2.26)
\end{aligned}$$

The factor of two appears because the quark (or gluon) can come from either one of the two nucleons. The extent to which the core affects the nuclear parton asymmetries is determined by the dimensionless quantity K , which is given by

$$K = \frac{g^2}{Q_0^2} \int d^3R d^3r \rho_{core}(\mathbf{R}) \rho_n(\mathbf{r}) \delta^2(\mathbf{B} - \mathbf{b}). \quad (2.27)$$

In the above, the delta function restricts the impact parameters of the nucleons in the core and the valence nucleon to be equal. The core density $\rho_{core}(\vec{r})$ is taken to be a simple gaussian,

$$\rho_{core} = \frac{A_0}{(\pi R_0^2)^{3/2}} e^{-r^2/R_0^2}, \quad (2.28)$$

where A_0 is the total number of core nucleons and R_0 the core radius. For the valence nucleon density ρ_N , consider a harmonic oscillator wavefunction corresponding to the $p_{\frac{3}{2}}$ state,

$$\psi_{\frac{3}{2}1m} = N \left(\frac{r}{r_0} \right) e^{-\frac{1}{2}(r/r_0)^2} \mathcal{Y}_{\frac{3}{2}1m}(\hat{r}), \quad (2.29)$$

where N is a normalization constant, r_0 is the radius of the nucleon orbital, and $\mathcal{Y}_{jlm}(\hat{r})$ is vector spherical harmonic. This gives the valence nucleon density for $m = \frac{3}{2}$ and $ml = \frac{1}{2}$,

$$\rho_N^{m=\frac{3}{2}} = \left| \psi_{\frac{3}{2}1\frac{3}{2}} \right|^2 = \frac{r^2 e^{-(r/r_0)^2}}{r_0^5 \pi^{\frac{3}{2}}} \sin^2 \theta, \quad (2.30)$$

$$\rho_N^{m=\frac{1}{2}} = \left| \psi_{\frac{3}{2}1\frac{1}{2}} \right|^2 = \frac{r^2 e^{-(r/r_0)^2}}{3 r_0^5 \pi^{\frac{3}{2}}} (\sin^2 \theta + 4 \cos^2 \theta). \quad (2.31)$$

The shadowing parameter K^{JH} for a spin J nucleus with spin projection H is, therefore,

$$K^{\frac{3}{2}\frac{3}{2}} = \frac{g^2 A_0}{Q_0^2 \pi} \frac{R_0^2}{(r_0^2 + R_0^2)^2}, \quad (2.32)$$

$$K^{\frac{3}{2}\frac{1}{2}} = \frac{g^2 A_0}{Q_0^2 \pi} \left[\frac{R_0^2}{3(r_0^2 + R_0^2)^2} + \frac{2}{3(r_0^2 + R_0^2)} \right]. \quad (2.33)$$

For a numerical estimate of the shadowing parameters I have used a starting value of $\alpha(Q_0^2) = g^2/4\pi = 0.327$. Typically, $r_0 = 1.19(A^{1/3} - 0.44)^{\frac{1}{2}}$ and $R_0^2 = 1.83 r_0^2$.

The fusion functions $\Gamma_{gq \rightarrow q}(x_1, x_2, x_1 + x_2)$ etc., are very similar to the splitting functions appearing in the Altarelli-Parisi equation and are in fact related to them [7].

$$\Gamma_{gq \rightarrow g}(x_1, x_2, x_1 + x_2) = \frac{3}{4} \frac{x_1^2 x_2^2}{(x_1 + x_2)^4} \left[\frac{(x_1 + x_2)^2}{x_2^2} + \frac{(x_1 + x_2)^2}{x_1^2} + 1 \right],$$

$$\Gamma_{gq \rightarrow q}(x_1, x_2, x_1 + x_2) = \frac{1}{6} \frac{x_1 x_2}{(x_1 + x_2)^2} \left[\frac{1 + \left(\frac{x_2}{x_1 + x_2}\right)^2}{1 - \left(\frac{x_2}{x_1 + x_2}\right)} \right],$$

and

$$\Gamma_{qq \rightarrow g}(x_1, x_2, x_1 + x_2) = \frac{4}{9} \frac{x_1 x_2}{(x_1 + x_2)^2} \left[\frac{x_1^2 + x_2^2}{(x_1 + x_2)^2} \right]. \quad (2.34)$$

Once these fusion functions are known, it is straight forward to compute the crosssection for many different processes involving a nuclear target. In the next section I shall use them to calculate the crosssection for the production of prompt photons in p-N scattering. In section 5 they will be used to estimate the crosssection asymmetries for J/ψ production in e-N scattering.

2.3 Prompt Photons in Hadron-Hadron Collisions

It is well known that photons are produced copiously in hadronic collisions. These photons may come, e.g., from the electromagnetic decays of directly produced hadrons or they might be produced directly in high-energy interactions. The

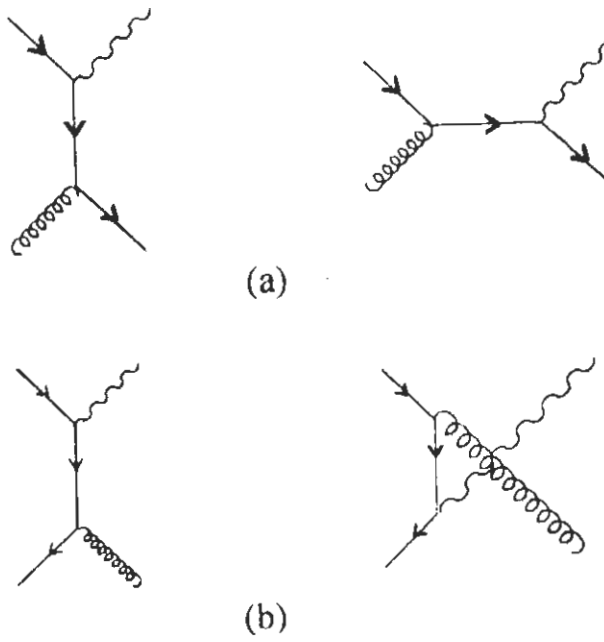


Figure 2.3: Lowest order Feynmann diagrams contributing to the process $pp \rightarrow \gamma X$ (a) Compton subprocess (b) Annihilation subprocess.

later variety of photons are called prompt photons or direct photons. In order to compare theoretical predictions against experimental data one needs to pick high energy processes which involve the gluon distribution directly. As the gluons carry no electric charge, gluon distributions are only indirectly measurable in lepton-hadron scattering. A more direct probe is provided by prompt photon production in hadron-hadron collisions, which is dominated by the quark-gluon Compton scattering diagrams of Fig.3a, with contamination only at the few percent level from quark-antiquark fusion Fig.3b. Since these investigations are exploratory, one can ignore the radiative corrections. The specific situation considered is an unpolarized proton beam striking a nuclear target with definite helicity H . According to the usual hard scattering model,

$$E_\gamma \frac{d\sigma_H(s, x_F, P_T)}{d^3 P_\gamma} = \sum_{a,b} \int dx_a dx_b P^a(x_a) P_H^b(x_b) E_\gamma \frac{d\hat{\sigma}_{ab}}{d^3 P_\gamma}, \quad (2.35)$$

where $E_\gamma d\hat{\sigma}_{ab}/d^3 P_\gamma$ is the subprocess $ab \rightarrow \gamma x$ crosssection, $P^a(x_a)$ is the spin-averaged density of parton a ($a = q, \bar{q}, G$) in an unpolarized proton and $P_H^b(x_b)$ is the spin-averaged density of parton b ($b = q, \bar{q}, G$) in the nuclear target with polarization H . The matrix elements for the two basic subprocesses are readily computed,

$$|M_{qg \rightarrow \gamma q}|^2 = -\frac{1}{3} \frac{s^2 + t^2}{s\hat{t}},$$

$$|M_{q\bar{q}\rightarrow\gamma q}|^2 = \frac{8}{9} \frac{\hat{t}^2 + \hat{u}^2}{\hat{t}\hat{u}}. \quad (2.36)$$

The parton level crosssections are expressible in terms of these as

$$E_\gamma \frac{d\hat{\sigma}(\hat{s}, x_F, P_T)}{d^3P_\gamma} = \alpha_{em} \alpha_s \frac{1}{\hat{s}} |M|^2 \delta(\hat{s} + \hat{t} + \hat{u}), \quad (2.37)$$

where the delta function

$$\delta(\hat{s} + \hat{t} + \hat{u}) = \frac{1}{x_a s + u} \delta\left(x_b + \frac{x_a t}{x_a s + u}\right), \quad (2.38)$$

can be used to eliminate the integration over x_b .

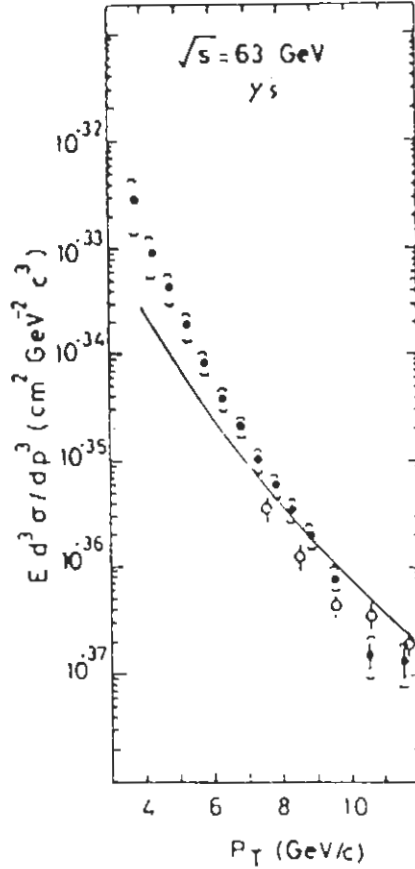


Figure 2.4: The invariant inclusive crosssection for prompt photon production in pp collisions at $\sqrt{s} = 63 \text{ GeV}$ near 90° in the center of mass [11,12]. Solid line shows our fit to the crosssection.

The limits for x_a integration are $x_{min} \leq x_a \leq 1$, with $x_{min} = -u/(s+t)$. Neglect all the masses to get

$$\begin{aligned}\hat{s} &= x_a x_b s, \\ \hat{t} &= x_a t, \\ \hat{u} &= x_b u.\end{aligned}\tag{2.39}$$

In CM frame

$$\begin{aligned}s &= 4P^2, \\ t &= -\frac{1}{2}s x_T T_c, \\ u &= -\frac{1}{2}s x_T \frac{1}{T_c},\end{aligned}\tag{2.40}$$

where

$$\begin{aligned}x_T &= \frac{2P}{\sqrt{s}} \\ T_c &= \tan(\theta_c/2).\end{aligned}\tag{2.41}$$

Although one could use a polarized deuterium target to explore the second gluon asymmetry discussed earlier, the low density of the deuteron makes a significant exotic gluon component unlikely. A more appealing possibility is Li^7 , which has $J = 3/2$. In the shell model, it consists of a single nucleon in the $1P_{3/2}$ level outside a closed spherical core. This ignores core polarization effects, but is adequate as a first approximation. The single nucleon thus carries all the spin of the nucleus. Our aim is to estimate the influence of the ‘‘quadrupole’’ gluon asymmetry, $\Delta G = G^{3/2} - G^{1/2}$, upon the prompt photon crosssection asymmetry. This entails making reasonable models for the parton asymmetries in the Li target.

As a first model assume that the parton asymmetries in Li can be obtained from the single nucleon by convolution,

$$P_{\uparrow}^{JH}(x) = \int \int dy dz \sum_{s=\pm 1/2} f_s^{JH}(y) P_{\uparrow}^s(z) \delta(x - yz).\tag{2.42}$$

In the above, $P = q \bar{q}$, or G , and f_s^{JH} is the light-cone probability distribution for a nucleon with helicity $s = \pm \frac{1}{2}$ in a nucleus with helicity H , $-J \leq H \leq J$.

For the gluon asymmetry :

$$\begin{aligned}\Delta G &= G^{\frac{3}{2}}(x) - G^{\frac{1}{2}}(x) \\ &= \int dy dz \left[f^{\frac{3}{2}\frac{3}{2}}(y) - f^{\frac{1}{2}\frac{3}{2}}(y) \right] G(z) \delta(x - yz),\end{aligned}\quad (2.43)$$

where $f^{\frac{3}{2}\frac{3}{2}} = f_{1/2}^{\frac{3}{2}\frac{3}{2}} + f_{-1/2}^{\frac{3}{2}\frac{3}{2}}$, etc. Note that only the spin-averaged gluon distribution in a nucleon enters in eq.5; this quantity is better known than the gluon asymmetry. The convolution model, with the Dirac nature of the nucleon taken into account properly [2, 3, 5], gives a definite prescription for $f^{\frac{3}{2}\frac{3}{2}}$, etc., in terms of the nuclear wavefunction.

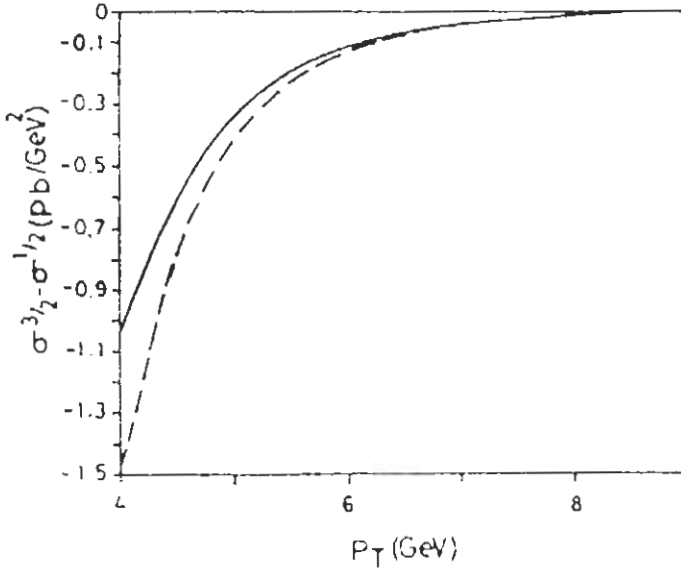


Figure 2.5: Prompt photoproduction asymmetry of $P_{beam} = 400$ GeV. Solid curve shows pure convolution model results, dashed curve shows results including fusion diagrams.

To numerically estimate the prompt photon crosssection asymmetry, I have used the Duke-Owens [6] set 1 of parton densities. As a check of their suitability and our tree-level computations, the p-p spin-averaged crosssection has been plotted in Fig. 4. The asymmetry is plotted in Fig. 5 and 6 for two different beam energies. As was stated at the outset, these are not expected to be large - the contributions come from Fermi motion at the $\langle P^2/M^2 \rangle$ level. Binding effects cancel out in the differences at this level of approximation.

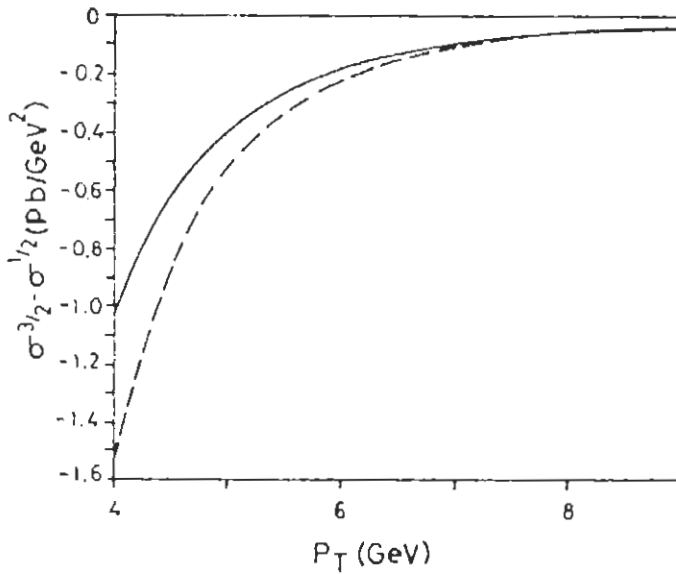


Figure 2.6: Same as Fig.3, at $P_{beam} = 2000$ GeV

Non-additive nuclear parton distributions could alter the above results. Non-additivity can be obtained in numerous ways; here I follow the parton recombination model (discussed earlier) developed by Close, Qiu, and Roberts [7], which is based upon the arguments of Mueller and Qiu [8] and which has been explored further in [1]. The numerical evaluation of the fusion corrections to the prompt photo production asymmetry is illustrated in Fig. 5 and 6, from which the difference relative to pure convolution is apparent.

The evaluation uses as input gluon and quark asymmetries, which requires a plausible model of nucleon structure [1]. Take the Li^7 core density to be $\sim \exp(-r^2/R_0^2)$ with $R_0 = 3.8$ fm, and the valence proton to be in the $1P_{3/2}$ state whose radial part is $\sim r \exp(-r^2/2r_0^2)$ with $r_0 = 1.44$ fm. I have taken $Q_0^2 \simeq P_T^2/4$ although this choice is open to the same criticism as in the original formulation[7] of the fusion model. The results however, should be qualitatively correct. As can be seen from figures 5 and 6, the difference in the prompt photon crosssections due to fusion are substantial although the crosssections themselves are small.

2.4 Leptoproduction of Heavy Mesons in Electron Hadron Collisions

A second useful probe of gluon distributions is the leptoproduction or photoproduction of heavy mesons [11]. The dominant (tree level) mechanism for this is $\gamma^* G \rightarrow Q\bar{Q}$, and is illustrated in Fig. 7.

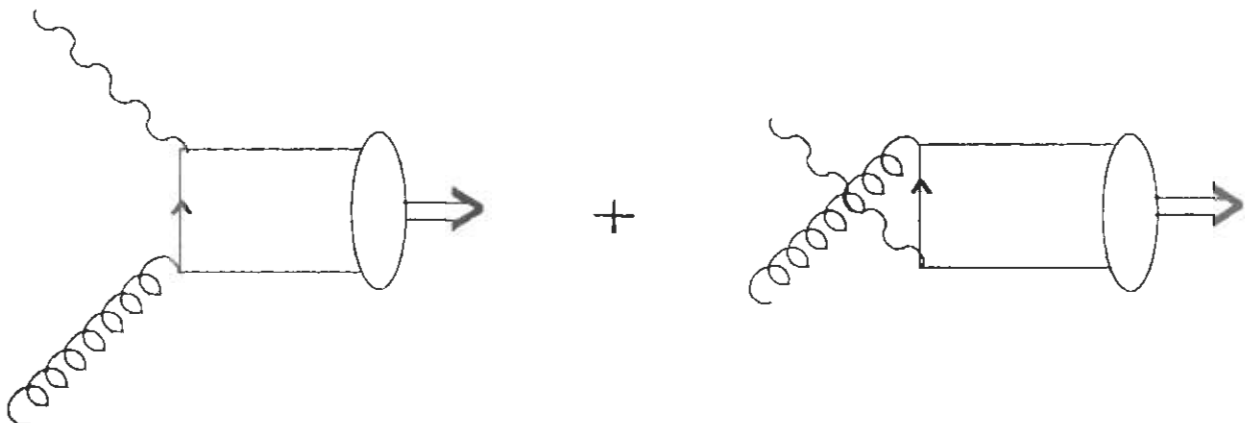


Figure 2.7: Lowest order Feynman diagrams contributing to the process $ep \rightarrow J/\psi + X$.

The outgoing heavy quarks are assumed to form through soft gluon interactions into the appropriate flavour meson with unit probability independent of the momenta. The total crosssection can be written as

$$\sigma(\gamma^* N \rightarrow c\bar{c} + X) = \int_{x_{min}}^1 dx G_{g/N}(x) \int_{\hat{t}_{min}}^{\hat{t}_{max}} \frac{d\hat{t}}{16\pi (\hat{s} + Q^2)^2} |\bar{M}(\hat{s}, \hat{t}, \hat{u})|^2, \quad (2.44)$$

where

$$\begin{aligned} x_{min} &= (\mu^2 + Q^2) / 2m_N \nu \\ \hat{t}_{min} &= -\frac{1}{2} (\hat{s} + Q^2 - 2m_c^2) - \frac{\hat{s} + Q^2}{2\hat{s}} [\hat{s} (\hat{s} - 4m_c^2)]^{1/2} \\ \hat{t}_{max} &= -\frac{1}{2} (\hat{s} + Q^2 - 2m_c^2) + \frac{\hat{s} + Q^2}{2\hat{s}} [\hat{s} (\hat{s} - 4m_c^2)]^{1/2}. \end{aligned} \quad (2.45)$$

Here $\hat{s} = (q_\gamma + q_g)^2 = -Q^2 + 2xM_N \nu \geq \mu^2$, with $\mu_{th} = 13(81) \text{ GeV}^2$ for $c(b)$ production. Also $\hat{s} + \hat{t} + \hat{u} = 2m_c^2 - Q^2$.

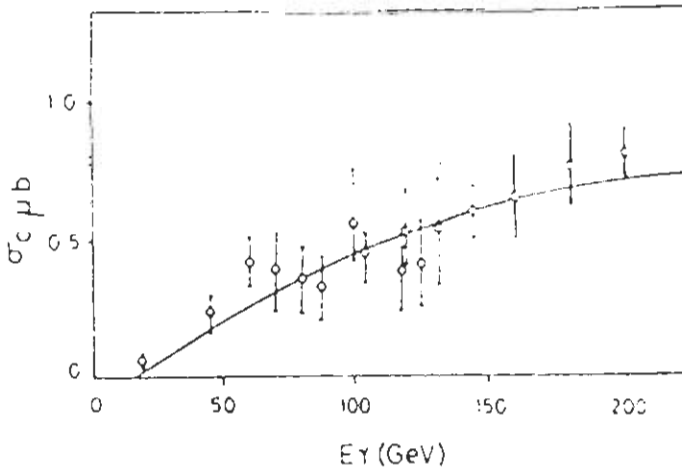


Figure 2.8: Charm production results from NA14' [10]. Solid line shows our fit to the crosssection.

The matrix element for the subprocess $\gamma g \rightarrow q\bar{q}$ can be written as

$$\begin{aligned}
 M &= \frac{2}{3} eg\bar{u}(p_c) \left[T_{ij}^b \frac{\not{\epsilon}_g(\not{q}_\gamma - p_c + m)\not{\epsilon}_\gamma}{t - m^2} + T_{ij}^b \frac{\not{\epsilon}_\gamma(\not{q}_g - p_c + m)\not{\epsilon}_g}{u - m^2} \right] u(p_c) \\
 &= \epsilon_g^\mu \epsilon_\gamma^\nu M_{\mu\nu}.
 \end{aligned} \tag{2.46}$$

Squaring and averaging over photon and gluon polarizations one gets

$$\begin{aligned}
 |\bar{M}|^2 &= \frac{11}{24} \left(\frac{2}{3} eg \right)^2 \frac{1}{(t - m^2)^2 (u - m^2)^2} \\
 &\quad \left(- 2(\hat{t} - \hat{u})^4 - 4(\hat{s} + Q^2)(\hat{t} + \hat{u})(\hat{t} - \hat{u})^2 - 4(\hat{s} + Q^2)^2 \right. \\
 &\quad \quad \left. \{(\hat{t} - \hat{u})^2 + 2(\hat{t} + \hat{u})^2\} - 12(\hat{s} + Q^2)^3(\hat{t} + \hat{u}) - 3(\hat{s} + Q^2)^4 \right. \\
 &\quad + \frac{Q^2}{(\hat{s} + Q^2)} \{2(\hat{t} - \hat{u})^4 + 8(\hat{s} + Q^2)(\hat{t} + \hat{u})(\hat{t} - \hat{u})^2 \\
 &\quad + 8(\hat{s} + Q^2)(\hat{t} - \hat{u})^2 - 2(\hat{s} + Q^2)^4\} \\
 &\quad \left. + \left(\frac{Q^2}{\hat{s} + Q^2} \right)^2 \{-2(\hat{t} - \hat{u})^4 + 2(\hat{s} + Q^2)^4\} \right).
 \end{aligned} \tag{2.47}$$

As a test of the distributions used, a comparison with the data [11] for spin-averaged leptonproduction of $\bar{c}c$ mesons from a proton target is shown in figure 8. Using the quadrupole gluon distributions in the convolution and fusion models discussed earlier, I have plotted in figure 9 the crosssection asymmetries for J/ψ production in the two models. Although both the asymmetries are rather small as compared to the spin-averaged crosssection, it is encouraging to note that they differ substantially - in fact appreciably more than the prompt photon asymmetry.

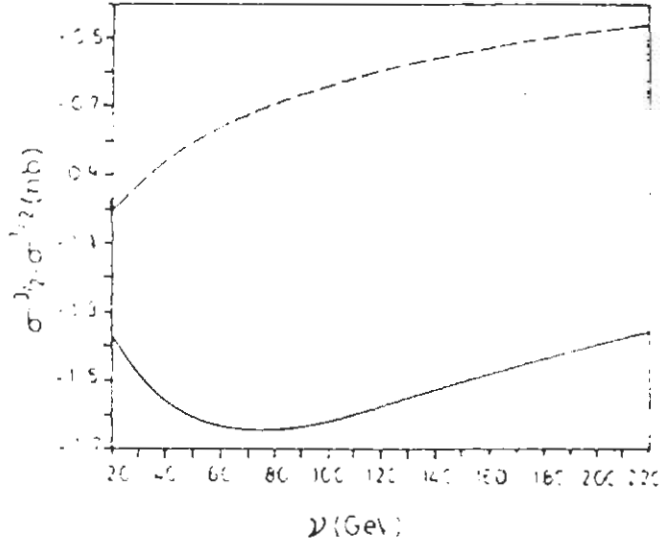


Figure 2.9: J/ψ production asymmetry at $Q^2 = -10 \text{ GeV}^2$. The solid curve shows pure convolution model results, dashed curve shows results including fusion diagrams.

2.5 Conclusion

In this chapter a calculation of the cross section asymmetries for two processes is presented. The processes chosen for this purpose are:

1. Prompt photon production in hadron-nucleus collisions, and
2. Leptoproduction of heavy mesons in electron-nucleus collisions

It is found that the cross section asymmetries for the first process are less than 10%. However the same quantity turns out to be significant in the case of leptoproduction, i.e., about 30%. This raises the hope that exotic gluon components of the nuclear wave function may be eventually measurable in high-flux fixed target polarization experiments.

References

- [1] EMC Collaboration, J. Asham et al, Phys. Lett. **B206**, 364 (1988).
- [2] P. Hoodbhoy, R. L. Jaffe and A. Manohar, Nucl. Phys. **B312**, 571 (1989).
- [3] R. L. Jaffe and A. Manohar, Nucl. Phys. **B321**, 343 (1989).
- [4] R. D. Field, "Applications of Perturbative QCD." Addison-Wesley Publishing Company, Inc. (1989).
- [5] R. L. Jaffe, in Relativistic dynamics and quark-nuclear physics, ed. M. B. Johnson and A. Picklesimer, Wiley, New York, 1986.
- [6] D. W. Duke and J. F. Owens, Phys. Rev. **D30**, 49 (1984).
- [7] F. E. Close, J. Qiu and R. G. Roberts, Phys. Rev. **D40** 2820 (1989).
- [8] A. H. Mueller and J. Qiu, Nucl. Phys. **B268**, 427 (1986); J. Qiu, Nucl. Phys. **B291**, 746 (1987).
- [9] R. Ali and P. Hoodbhoy, Phys. Rev. **D43**, 715 (1991).
- [10] R. W. Forty, Proceedings of the XXIV International Conference on High Energy Physics, Munich, 1988 eds. R. Kotthaus and J.H. Kuhn, Springer-Verlag 1989.
- [11] Anassonitzis, E., et al, Z. Phys. **C13**, 277 (1982).
- [12] Anassonitzis, E., et al, Proceedings of the XIII International Symposium on Multiparticle Dynamics, ed W.Kittle.

Chapter 3

Decays of Quarkonia

The study of heavy meson decays has been an important part of studies at various high energy physics laboratories around the world. This work was initiated by the MARK II and Crystal Ball Collaborations in the early 1980's. The first heavy meson which was studied at these laboratories was the J/ψ . Its discovery was announced in November 1974 by the MIT-BNL group at Brookhaven and the SLAC-LBL group at SLAC. Its successor, the Υ was discovered in 1977 at Fermilab. Both of these mesons are $SU(3)_c$ singlet states with $J^{PC} = 1^{--}(^3S_1)$.

3.1 Introduction

The hadronic decays of the Υ family of $b\bar{b}$ mesons proceed mainly through an intermediate state consisting of three gluons. In Fig.1, replacing one of the outgoing gluons with a photon, one obtains the leading order contribution to the production of direct photons, i.e. the photons which do not result from π^0 decay, etc. In principle, the spectrum of such photons provides an excellent test of perturbative quantum chromodynamics (QCD) because it yields a large number of data points against which theoretical predictions can be compared. This is in contrast to the prediction of a decay rate which is a single number. However, it is well known [1] that the photon spectrum $^3S_1 \rightarrow \gamma + X$, calculated at leading order [2], is

too hard when compared against experiment, both in J/Ψ and Υ decays. Such calculations yield an almost linearly rising spectrum in $z = 2E_\gamma/M$ with a sudden decrease at $z = 1$. A next-to-leading order calculation by Photiadis [3] sums leading logs of the type $\ln(1 - z)$ and yields a slight softening. However, the peak is still too sharp and close to $z = 1$. An earlier calculation by Field [4] predicts a much softer spectrum which fits the relatively recent data [5] rather well. This calculation uses a parton-shower Monte Carlo approximation wherein the two gluons recoiling against the direct photon acquire a non-zero invariant mass by radiating further bremsstrahlung gluons. This does not, therefore, qualify it as an ab-initio perturbative QCD calculation. In ref [2, 3, 4], the non-perturbative dynamics of the decaying hadron is described by a single parameter $\psi(0)$, the quark wavefunction at the origin. This leads to the assertion that the ratio of widths for the decay of quarkonia to prompt photons and hadrons is independent of quark dynamics.

One can compute the decay rate for $^3S_1 \rightarrow \gamma + X$ by taking into account the bound state structure of the decaying quarkonium state. Note that the description of hadron dynamics by $\psi(0)$ alone is correct only if one assumes that Q and \bar{Q} are exactly on-shell and at rest relative to each other. These assumptions are motivated by the fact that heavy quarkonia are weakly bound $Q\bar{Q}$ composites and v^2/c^2 is a small parameter. An improvement on these assumptions requires introduction of additional hadronic quantities, to be identified within the context of a systematically improved gauge-invariant theory for quarkonium decays. Such a formalism has been developed recently [2, 8] and applied to one and two particle decays. Here, I use the method outlined in ref [2] to the more complicated case of three particles and obtain the photon spectrum in the process $\Upsilon \rightarrow \gamma + X$. The total decay rates for $\Upsilon \rightarrow \gamma + 2g$ and $\Upsilon \rightarrow 3g$ are also calculated. It is found that the inclusion of binding and relativistic effects through two additional parameters, ϵ_B/M and $\nabla^2\psi(0)/M^2\psi(0)$, makes the computed spectrum substantially softer for large z . Although the discrepancy between theory and experiment is not totally resolved, it is considerably reduced.

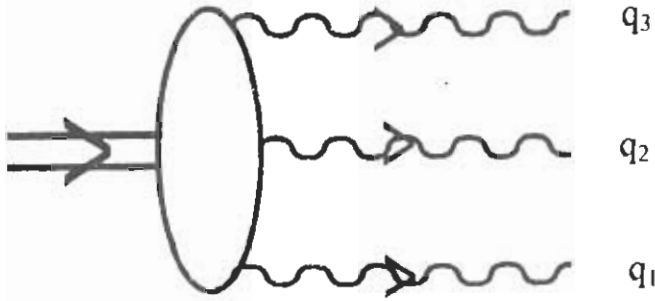


Figure 3.1: The decay ${}^3S_1 \rightarrow 3g$

3.2 Formalism

As shown in Fig. 3.1, q_i are the 4-momenta of outgoing bosons (photons and/or gluons) and P is the 4-momentum of the decaying quarkonium. In order to write the decay rate in a simple form, define a set of variables:

$$s_i = q_i - \frac{1}{2}P, \quad i = 1, 2, 3$$

and

$$\begin{aligned} s &= (P - q_1)^2 = M^2(1 - x_1) \\ t &= (P - q_2)^2 = M^2(1 - x_2) \\ u &= (P - q_3)^2 = M^2(1 - x_3) \quad , \end{aligned} \quad (3.1)$$

where $x_i = 2E_i/M$ are the dimensionless energy fractions such that $s+t+u = M^2$ and $x_1 + x_2 + x_3 = 2$.

The starting point of our approach is that the decay amplitude for ${}^3S_1 \rightarrow \gamma + X$ is given by the sum of all distinct Feynman diagrams leading from the initial to the final state, Fig. 3.1. The first step is to write a given diagram in the form of a (multipole) loop integral. As an example, consider one of the six leading order diagrams shown in Fig. 3.2

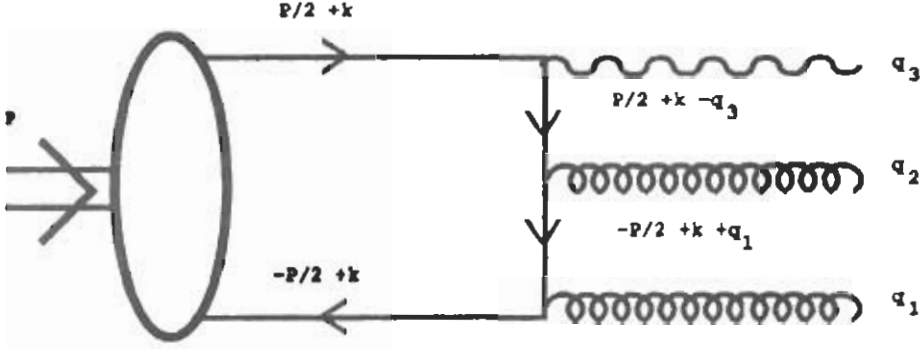


Figure 3.2: One of the six leading order diagrams

Omitting color matrices and coupling constants for brevity, the contribution of this diagram can be expressed as

$$T_{(0)}^{\mu_1\mu_2\mu_3} = -i \int \frac{d^4k}{(2\pi)^4} \text{Tr} [\gamma^{\mu_1} S_F(k + s_1) \gamma^{\mu_2} S_F(k - s_3) \gamma^{\mu_3} M(k)], \quad (3.2)$$

$M(k)$ is the usual, but obviously non-gauge invariant zero-gluon Bethe-Salpeter amplitude

$$M(k) = \int d^4x e^{ik \cdot x} \langle 0 | T [\bar{\psi}(-x/2) \psi(x/2)] | P, \epsilon \rangle. \quad (3.3)$$

In Eqs. 2-3, x^μ is the relative distance between quarks, k^μ is the relative momentum, $P^2 = M^2$, and $s_i = q_i - \frac{1}{2}P$. I define the binding energy as $\epsilon_B = 2m - M$ in terms of which the free quark propagator is

$$S_F(p) = (\not{p} - \frac{1}{2}M - \frac{1}{2}\epsilon_B)^{-1}. \quad (3.4)$$

Provided all propagators are considerably off-shell, they may be expanded in two small quantities ϵ_B/M and k/M :

$$S_F(k + s) = S_F(s) + k^\alpha \frac{\partial S_F}{\partial k^\alpha} + \frac{1}{2!} k^\alpha k^\beta \frac{\partial^2 S_F}{\partial k^\alpha \partial k^\beta} + \text{binding energy terms}. \quad (3.5)$$

Using the first term of the above expansion one gets

$$\begin{aligned} T_{(0),I}^{\mu_1\mu_2\mu_3} &= -i \int \frac{d^4k}{(2\pi)^4} \text{Tr} [\gamma^{\mu_1} S_F(s_1) \gamma^{\mu_2} S_F(-s_3) \gamma^{\mu_3} M(k)] \\ &= \text{Tr} [h^{\mu_1\mu_2\mu_3} M(0)], \end{aligned} \quad (3.6)$$

where

$$h^{\mu_1\mu_2\mu_3} = -i\gamma^{\mu_1} S_F(s_1)\gamma^{\mu_2} S_F(-s_3)\gamma^{\mu_3}, \quad (3.7)$$

and

$$M(0) = \int \frac{d^4k}{(2\pi)^4} M(k) = \langle 0|\bar{\psi}\psi|P\rangle. \quad (3.8)$$

Now expand S_F to $\mathcal{O}(k)$:

$$T_{(0),II}^{\mu_1\mu_2\mu_3} = -i \int \frac{d^4k}{(2\pi)^4} \text{Tr} \left[\gamma^{\mu_1} k^\alpha \frac{\partial S_F(s_1)}{\partial k^\alpha} \gamma^{\mu_2} S_F(-s_3) \gamma^{\mu_3} M(k) \right. \\ \left. + \gamma^{\mu_1} S_F(s_1) \gamma^{\mu_2} k^\alpha \frac{\partial S_F(-s_3)}{\partial k^\alpha} \gamma^{\mu_3} M(k) \right], \quad (3.9)$$

where

$$\int \frac{d^4k}{(2\pi)^4} k^\alpha M(k) = \int \frac{d^4k}{(2\pi)^4} d^4x \frac{1}{i} \partial^\alpha e^{ik \cdot x} M(k) \\ = i\partial^\alpha \langle 0|\bar{\psi}\psi|P\rangle \equiv M^\alpha(0). \quad (3.10)$$

Therefore

$$T_{(0),II}^{\mu_1\mu_2\mu_3} = \text{Tr} [\partial_\alpha h^{\mu_1\mu_2\mu_3} M^\alpha(k)] \quad (3.11)$$

Finally, on expanding to $\mathcal{O}(k^2)$:

$$T_{(0),III}^{\mu_1\mu_2\mu_3} = -i \int \frac{d^4k}{(2\pi)^4} \text{Tr} \left[\gamma^{\mu_1} \frac{1}{2} k^\alpha k^\beta \frac{\partial^2 S_F(s_1)}{\partial k^\alpha \partial k^\beta} \gamma^{\mu_2} S_F(-s_3) \gamma^{\mu_3} M(k) \right. \\ \left. + \gamma^{\mu_1} S_F(s_1) \gamma^{\mu_2} \frac{1}{2} k^\alpha k^\beta \frac{\partial^2 S_F(-s_3)}{\partial k^\alpha \partial k^\beta} \gamma^{\mu_3} M(k) \right. \\ \left. + \gamma^{\mu_1} k^\alpha \frac{\partial S_F(s_1)}{\partial k^\alpha} \gamma^{\mu_2} k^\beta \frac{\partial S_F(-s_3)}{\partial k^\beta} \gamma^{\mu_3} M(k) \right]. \quad (3.12)$$

Once again the integration can be performed easily,

$$\int \frac{d^4k}{(2\pi)^4} k^\alpha k^\beta M(k) = \langle 0|\bar{\psi} i \overleftrightarrow{\partial}^\alpha i \overleftrightarrow{\partial}^\beta \psi|P\rangle \equiv M^{\alpha\beta}(0) \quad (3.13)$$

and thus

$$T_{(0),III}^{\mu_1\mu_2\mu_3} = \text{Tr} \left[\partial_\alpha \partial_\beta \frac{1}{2} h^{\mu_1\mu_2\mu_3} M^{\alpha\beta}(k) \right]. \quad (3.14)$$

Addition of all the above contributions yields the expression

$$T_{(0)}^{\mu_1\mu_2\mu_3} = \text{Tr} [\langle 0|\bar{\psi}\psi|P\rangle h^{\mu_1\mu_2\mu_3} + \langle 0|\bar{\psi} \overleftrightarrow{\partial}_\alpha \overleftrightarrow{\partial}^\alpha \psi|P\rangle \partial^\alpha h^{\mu_1\mu_2\mu_3} \\ + \langle 0|\bar{\psi} \overleftrightarrow{\partial}_\alpha \overleftrightarrow{\partial}_\beta \psi|P\rangle \frac{1}{2} \partial^\alpha \partial^\beta h^{\mu_1\mu_2\mu_3} + \dots]. \quad (3.15)$$

I have defined $\overleftarrow{\partial} = \frac{1}{2}(\overleftarrow{\partial} - \overrightarrow{\partial})$ and $h^{\mu_1\mu_2\mu_3}$ is the “hard part” which combines terms from all six leading diagrams. It is easy to show that only three of the diagrams need to be evaluated because of the time-reversal symmetry. Thus

$$h^{\mu_1\mu_2\mu_3} = -2i[\gamma^{\mu_1} S_F(s_1)\gamma^{\mu_2} S_F(-s_3)\gamma^{\mu_3} + \gamma^{\mu_2} S_F(s_2)\gamma^{\mu_1} S_F(-s_3)\gamma^{\mu_3} + \gamma^{\mu_1} S_F(s_1)\gamma^{\mu_3} S_F(-s_2)\gamma^{\mu_2}] \quad (3.16)$$

where 2 accounts for the crossed diagram. The derivative of $h^{\mu_1\mu_2\mu_3}$ acts on the quark propagators and can be simplified by using the Ward identity

$$\partial^\alpha S_F = -S_F \gamma^\alpha S_F. \quad (3.17)$$

There are 12 one-gluon diagrams. One of these is depicted in Fig 3.3, which must be added as corrections to the no-gluon amplitude. However, in this case one needs to expand the relevant quantity only to first order in k . The amplitude has the general form:

$$T_{(1)}^{\mu_1\mu_2\mu_3} = \int \frac{d^4k}{(2\pi)^4} \frac{d^4k'}{(2\pi)^4} \text{Tr} M^\rho(k, k') H_\rho^{\mu_1\mu_2\mu_3}(k, k'), \quad (3.18)$$

where $M^\rho(k, k')$ is a generalized B-S amplitude

$$M^\rho(k, k') = \int d^4x d^4z e^{ik \cdot x} e^{ik' \cdot z} \langle 0 | T[\bar{\psi}(-x/2) A^\rho(z) \psi(x/2)] | P, \epsilon \rangle, \quad (3.19)$$

and $H_\rho^{\mu_1\mu_2\mu_3}$ is the hard part given by

$$H_\rho^{\mu_1\mu_2\mu_3}(k, k') = -2i[\gamma_1^{\mu_1} S_F(k - s_1 + k'/2)\gamma^{\mu_2} S_F(k - s_3 + k'/2)\gamma_\rho S_F(k - s_3 - k'/2)\gamma^{\mu_3} + \dots] \quad (3.20)$$

$A^\rho \equiv \frac{1}{2}\lambda^a A^{a\rho}$ is the gluon field matrix. The dots represent the other 11 diagrams, whereas the factor 2 again arises from the application of time reversal symmetry. The gluon which originates from the blob is part of the $Q\bar{Q}g$ Fock-state component of the meson. The momentum k' is bounded by $R^{-1} \lesssim k' \ll M$, where R is the meson's spatial size. Therefore, it is considered soft on the scale of the quark mass. Again, one may expand the propagators in $H_\rho^{\mu_1\mu_2\mu_3}(k, k')$ about $k = k' = 0$ to get

$$T_{(1)}^{\mu_1\mu_2\mu_3} = \text{Tr}[M^\rho H_\rho^{\mu_1\mu_2\mu_3} + M^{\rho,\alpha} \partial_\alpha H_\rho^{\mu_1\mu_2\mu_3} + M^{\rho,\alpha} \partial_\alpha H_\rho^{\mu_1\mu_2\mu_3} + \dots], \quad (3.21)$$

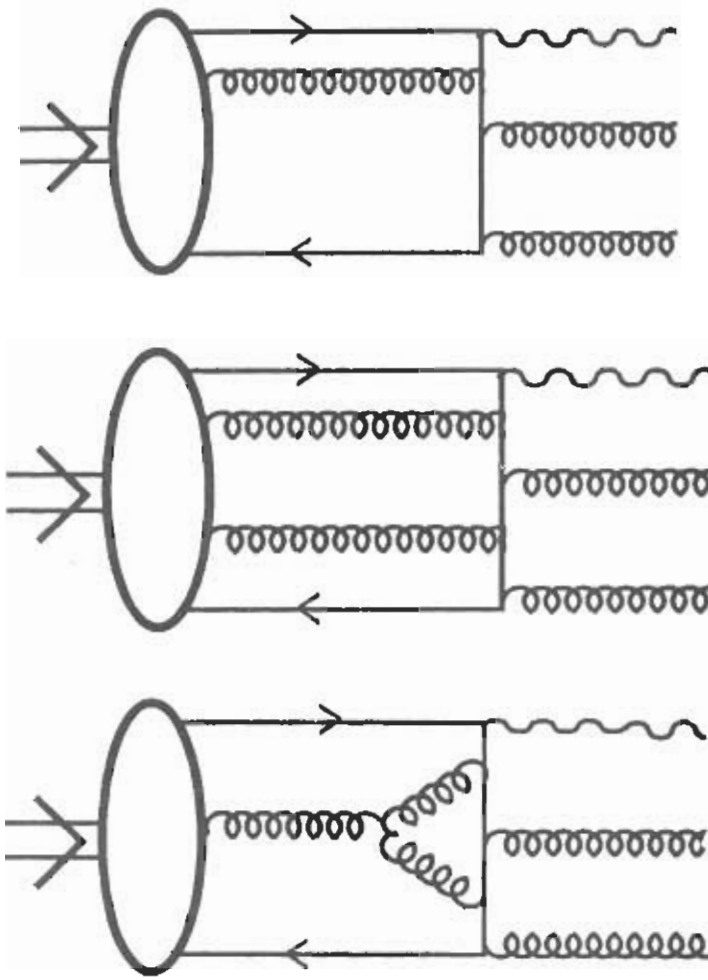


Figure 3.3: (a) One of the 12 one-gluon diagrams, (b) One of the 24 two-gluon diagrams, (c) One of the 12 gluon self-coupling diagrams.

where,

$$\begin{aligned}
 M^\rho &= \langle 0 | \bar{\psi} \psi A^\rho | P, \epsilon \rangle \\
 M^{\rho, \alpha} &= \langle 0 | \bar{\psi} \overleftrightarrow{\partial}^\alpha \psi A^\rho | P, \epsilon \rangle \\
 M'^{\rho, \alpha} &= \langle 0 | \bar{\psi} \psi i \overleftrightarrow{\partial}^\alpha A^\rho | P, \epsilon \rangle.
 \end{aligned} \tag{3.22}$$

The derivatives $\overleftrightarrow{\partial}^\alpha$ act only upon the quark operators.

The two soft-gluon contributions to the amplitude are handled similarly but are more complicated. Typical diagrams are illustrated in Fig 3.2(b,c) :

$$T_{(2)}^{\mu_1 \mu_2 \mu_3} = \int \frac{d^4 k}{(2\pi)^4} \frac{d^4 k'}{(2\pi)^4} \frac{d^4 k''}{(2\pi)^4} \text{Tr} M^{\rho\sigma}(k, k', k'') H_{\rho\sigma}^{\mu_1 \mu_2 \mu_3}(k, k', k''), \tag{3.23}$$

where $M_p(k, k', k'')$ is a generalized B-S amplitude,

$$M^{\rho\sigma}(k, k', k'') = \int d^4x d^4z d^4w e^{ik \cdot x} e^{ik' \cdot z} e^{ik'' \cdot w} \langle 0 | T[\bar{\psi}(-x/2) A^\rho(z) A^\sigma(w) \psi(x/2)] | P, \epsilon \rangle. \quad (3.24)$$

I shall not reproduce the remaining steps now as the principle is rather clear. The real purpose of considering the one-gluon and two-gluon amplitudes is to show that the sum of the amplitudes $T_0 + T_1 + T_2$ is a manifestly gauge-invariant expression upto two derivatives.

In the sum $T_0 + T_1 + T_2$ all ordinary derivatives combine with gluon fields to yield covariant derivatives and/or field strength tensors (see the appendix 1 for details). Hence

$$(T_0 + T_1 + T_2)^{\mu_1\mu_2\mu_3} = \text{Tr}[\langle 0 | \bar{\psi} \psi | P \rangle h^{\mu_1\mu_2\mu_3} + \langle 0 | \bar{\psi} i \vec{D}_\alpha \psi | P \rangle \partial^\alpha h^{\mu_1\mu_2\mu_3} + \langle 0 | \bar{\psi} i \vec{D}_\alpha i \vec{D}_\beta \psi | P \rangle \frac{1}{2} \partial^\alpha \partial^\beta h^{\mu_1\mu_2\mu_3} + \langle 0 | \bar{\psi} F^{\alpha\beta} \psi | P \rangle \frac{i}{2} \partial_\alpha H_\beta^{\mu_1\mu_2\mu_3} + \dots], \quad (3.25)$$

where $F^{\alpha\beta} = \partial^\alpha A^\beta - \partial^\beta A^\alpha + ig[A^\alpha, A^\beta]$ and $D_\alpha = \partial_\alpha - igA_\alpha$. The above is a sum of terms each of which is the product of a soft hadronic matrix element and a hard perturbative part. The hard amplitudes $h^{\mu\nu}(k)$, $H^{\mu\nu\alpha}(k, k')$ and their derivatives are all evaluated at $k = k' = k'' = 0$. Each term in the above equation is a product of a gauge invariant matrix element characteristic of the decaying hadron and a simple and calculable hard part.

To proceed, one can perform a Lorentz and CPT invariant decomposition of each of the hadronic matrix elements in Eq 3.25 (see appendix 2 for details). This is somewhat complicated and involves a large number of constants which characterize the hadron. Considerable simplification results from choosing the Coulomb gauge, together with the counting rules of Lepage et al.,[9]. The upshot of using this analysis is that, in this particular gauge, the gluons contribute at $O(v^3)$ to the reaction ${}^3S_1 \rightarrow \gamma + X$, and hence can be ignored. Even then there are too many parameters and one is forced to search for a dynamical theory describing the essential dynamics of a $Q\bar{Q}$ system. A possible but by no means unique description is provided by the Bethe-Salpeter equation with an instantaneous

kernel. This has been conveniently reviewed by Keung and Muzinich [11] and I use their expression for B-S amplitude in terms of the non-relativistic wavefunction $\psi(p)$ ¹. The momentum space B-S amplitude $\chi(p)$ satisfies the homogeneous equation,

$$\chi(p) = iG_0(P, p) \int \frac{d^4 p'}{(2\pi)^4} K(P, p, p') \chi(p'), \quad (3.26)$$

which, after making the instantaneous approximation $K(P, p, p') = V(\vec{p}, \vec{p}')$ and reduction to the non-relativistic limit yields

$$\chi(p) = \frac{M^{1/2}(M - 2E)(E + m - \vec{p} \cdot \vec{\gamma}) \not{\epsilon}(1 - \gamma_0)(E + m - \vec{p} \cdot \vec{\gamma})\phi(|\vec{p}|)}{4E(E + m)(p^0 + \frac{M}{2} - E + i\epsilon)(p^0 - \frac{M}{2} + E - i\epsilon)}. \quad (3.27)$$

The scalar wavefunction $\phi(|\vec{p}|)$ is normalized to unity,

$$\int \frac{d^3 p}{(2\pi)^3} |\phi(|\vec{p}|)|^2 = 1, \quad (3.28)$$

and,

$$E = \sqrt{\vec{p}^2 + m^2}. \quad (3.29)$$

Fourier transforming $\chi(p)$ to position space gives $\langle 0 | \bar{\psi}(-x/2) \psi(x/2) | P \rangle$. On contracting with appropriate gamma matrices, the coefficients can be extracted. Finally, to $\mathcal{O}(v^2)$, one has a rather simple result,

$$\begin{aligned} \langle 0 | \bar{\psi} \psi | P, \epsilon \rangle &= \frac{M^{1/2}}{2} \left(1 + \frac{\nabla^2}{M^2} \right) \phi \left(1 + \frac{\not{P}}{M} \right) \not{\epsilon} - \frac{M^{1/2} \nabla^2 \phi}{2 \cdot 3M^2} \left(1 - \frac{\not{P}}{M} \right) \not{\epsilon}, \\ \langle 0 | \bar{\psi} \vec{\partial}_\alpha \psi | P, \epsilon \rangle &= -\frac{1}{3} M^{3/2} \frac{\nabla^2 \phi}{M^2} \epsilon^\beta \left[-g_{\alpha\beta} + i\epsilon_{\mu\nu\alpha\beta} \frac{P^\nu}{M} \gamma^\mu \gamma^5 \right], \\ \langle 0 | \bar{\psi} \vec{\partial}_\alpha \vec{\partial}_\beta \psi | P, \epsilon \rangle &= \frac{M^{5/2}}{6} \frac{\nabla^2 \phi}{M^2} \left(g_{\alpha\beta} - \frac{P_\alpha P_\beta}{M^2} \right) \left(1 + \frac{\not{P}}{M} \right) \not{\epsilon}. \end{aligned} \quad (3.30)$$

3.3 Decay Rate

All the ingredients are now in place to calculate the decay $\Upsilon \rightarrow \gamma + 2g$. In squaring the amplitude obtained by substituting Eqs. 29 into Eq. 24, terms involving the

¹The analysis of ref [11] is wanting because it does not properly deal with the issue of gauge-invariance of the meson state. Further, while the binding energy is taken into account, the wavefunction corrections-which are essentially short-distance or relativistic effects-are not.

product of ϵ_B and $\nabla^2\phi$ may be neglected. I assume the emitted gluons to be massless and transverse and that they decay with unit probability into hadrons. Polarizations of the final-state particles are summed and the spin states of the initial meson are averaged over. Summing over final-state colors yields 2/3. Also, one must include a factor of 1/2 for identical gluons. The Lorentz invariant phase-space factor for 3 massless particles has a standard expression[12] which is best expressed in terms of the dimensionless energy fractions $x_i = 2E_i/M$.

Ignoring radiative radiative corrections for the moment, a tedious calculation² yields

$$\frac{d^2\Gamma}{dx_1 dx_2} = \frac{256}{9} e_q^2 \alpha_s^2 \alpha_e \frac{|\phi(0)|^2}{M^2} [\eta_0 f_0(s, t, u) + \eta_B f_B(s, t, u) + \eta_W f_W(s, t, u)], \quad (3.31)$$

where e_q is the quark charge and,

$$\eta_0 = 1, \quad \eta_B = \frac{\epsilon_B}{M}, \quad \eta_W = \frac{\nabla^2\phi}{M^2\phi}. \quad (3.32)$$

The function f_0 provides the standard, leading order result:

$$f_0(s, t, u) = \frac{M^4 (s^2 t^2 + t^2 u^2 + u^2 s^2 + M^2 s t u)}{(s - M^2)^2 (t - M^2)^2 (u - M^2)^2}. \quad (3.33)$$

The binding energy and wavefunction corrections, f_B and f_W respectively, are more complicated:

$$\begin{aligned} f_B(s, t, u) &= \frac{M^4}{2D} [-7 s t u (s^4 + t^4 + u^4) + 7 M^2 (s^3 t^3 + t^3 u^3 + u^3 s^3) \\ &+ (s^2 t^2 + t^2 u^2 + u^2 s^2) (s^3 + t^3 + u^3 + 15 s t u) \\ &+ M^2 s t u (s^3 + t^3 + u^3) + 29 M^2 s^2 t^2 u^2], \\ f_W(s, t, u) &= \frac{M^4}{3D} [141 s t u (s^4 + t^4 + u^4) - 85 M^2 (s^3 t^3 + t^3 u^3 + u^3 s^3) \\ &- 27 (s^2 t^2 + t^2 u^2 + u^2 s^2) \left(s^3 + t^3 + u^3 + \frac{205}{27} s t u \right) \\ &- 139 M^2 s t u (s^3 + t^3 + u^3) - 463 M^2 s^2 t^2 u^2]. \end{aligned} \quad (3.34)$$

²I used **Mathematica**[13], supplemented by the HIP package[10], for computation of traces and simplification of algebra

The denominator D is

$$D = (s - M^2)^3(t - M^2)^3(u - M^2)^3. \quad (3.35)$$

Integrating over the energies of the outgoing gluons for a fixed photon energy yields

$$\frac{d\Gamma}{dz} = \frac{256}{9} e_q^2 \alpha_e \alpha_s^2 \frac{|\phi(0)|^2}{M^2} [\eta_0 F_0(z) + \eta_B F_B(z) + \eta_W F_W(z)], \quad (3.36)$$

where $z = 2E_\gamma/M$ and,

$$F_0 = [1 + 4\xi - 2\xi^3 - \xi^4 - 2\xi^5 + 2\xi(1 + 2\xi + 5\xi^2) \log \xi] / (1 - \xi)^2(1 + \xi)^3,$$

$$F_B = [2 - 16\xi + 10\xi^2 - 48\xi^3 - 10\xi^4 + 64\xi^5 - 2\xi^6 + (1 - 3\xi + 14\xi^2 - 106\xi^3 + 17\xi^4 - 51\xi^5) \log \xi] / 2(1 - \xi)^3(1 + \xi)^4,$$

$$F_W = [-26 + 14\xi - 210\xi^2 + 134\xi^3 + 274\xi^4 - 150\xi^5 - 38\xi^6 + 2\xi^7 - (27 + 50\xi + 257\xi^2 - 292\xi^3 + 205\xi^4 - 78\xi^5 - 41\xi^6) \log \xi] / 3(1 - \xi)^3(1 + \xi)^5. \quad (3.37)$$

In the above equations, $\xi = 1 - z$. The integrated decay width is³,

$$\Gamma_{1 \rightarrow \gamma + 2g} = \frac{128}{9} (\pi^2 - 9) e_q^2 \alpha_e \alpha_s^2 \frac{|\phi(0)|^2}{M^2} \left(1 + a \frac{\alpha_s}{\pi} - 1.03\eta_B + 19.34\eta_W \right). \quad (3.38)$$

The F 's are plotted in Fig. 3.3.

Radiative corrections of $\mathcal{O}(\alpha_s)$ are of the same order in v^2/c^2 as the other corrections and were calculated[10] many years ago at an arbitrary mass scale μ ,

$$a = (11 - \frac{2}{3}n_f) \log \frac{\mu}{m_b} - 4.37 - 0.77n_f. \quad (3.39)$$

The parameters η_W and η_B are independent of each other in the present treatment. Note, however, that imposing the condition $\eta_W = \frac{1}{2}\eta_B$, the result Eq.

³Note that Eq. 22 does not take into account non-perturbative effects [16] which are significant in the part of the phase space where one of the quark propagators become soft, and where the gluon vacuum condensate plays a role.

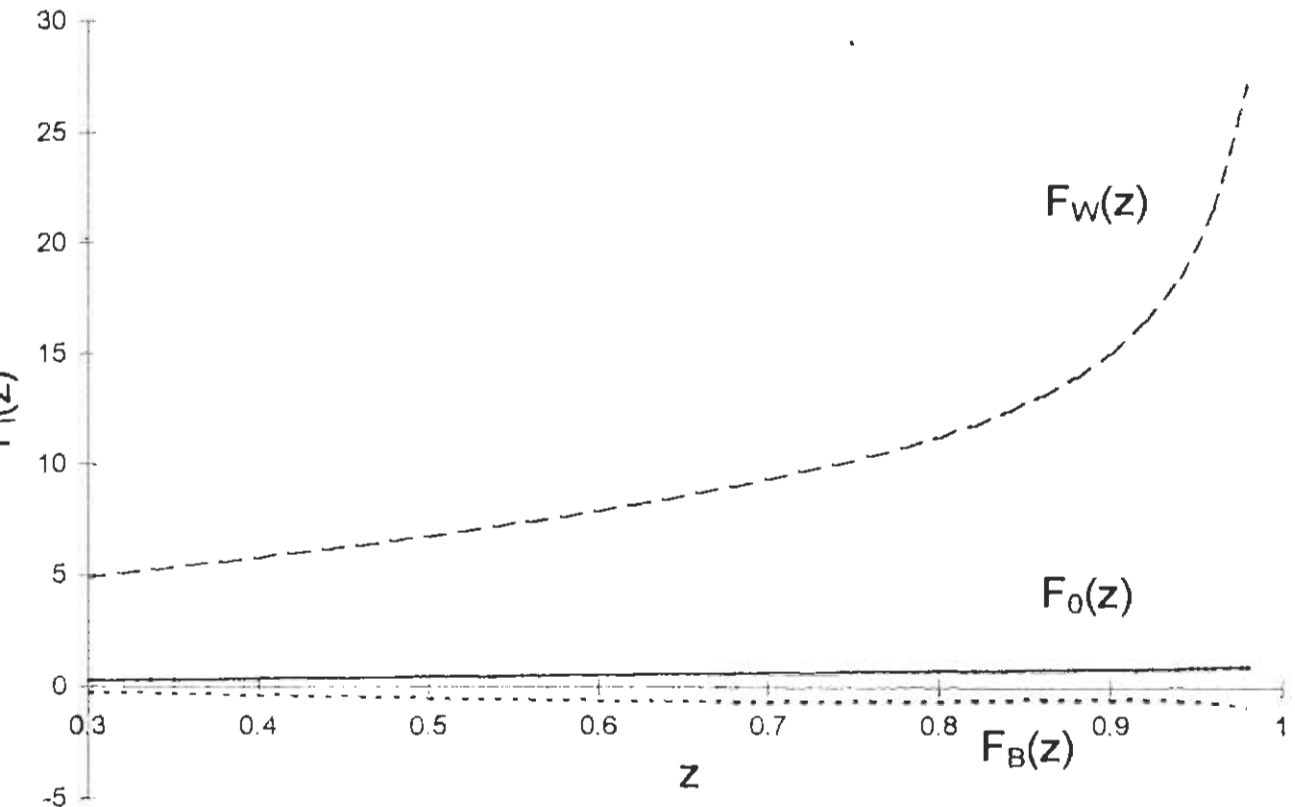


Figure 3.4: The functions F_0 , F_B and F_W plotted as a function of z

3.5 of Keung and Muzinich[10] is recovered. This latter condition is equivalent to $\frac{1}{M}\nabla^2\phi(0) = \frac{1}{2}\epsilon_B\phi(0)$, which is the Schrödinger equation for the relative motion of quarks in a potential which vanishes at zero relative separation. It is also worthy of note that the same condition emerges as a renormalization condition in the treatment of positronium by Labelle et al[15] (see their equations 11 and 12). However, in our treatment there is no principle which a priori constrains η_B to bear a fixed relation to η_W and therefore both will be considered as free parameters.

The application of Eq 3.38 must be done with caution because extraction of the direct photon decay rate from the data requires an extrapolation down to small photon energies. But in this energy range the prompt photons are heavily

contaminated by photons from π^0 decays. The 3 gluon rate is a more reliable quantity on experimental ground, and its theoretical expression is,

$$\Gamma_{1 \rightarrow 3g} = \left(\frac{5}{36} \frac{1}{Q_b^2} \frac{\alpha}{\alpha_s} \right) \Gamma_{1 \rightarrow \gamma, 2g} \quad (3.40)$$

3.4 Numerical Work

A numerical estimate for the correction factors requires the knowledge of η_B and η_W . I have chosen $m_b = 4.5$ which gives $\eta_B = -0.048$. Also take $\alpha_s = 0.20$ then η_W can be fixed by using the experimentally known numbers[5],

$$\begin{aligned} \Gamma(\Upsilon \rightarrow 2g + \gamma) &= 1.28 \pm 0.10 \text{ KeV.} \\ \Gamma(\Upsilon \rightarrow l\bar{l}) &= 1.34 \pm 0.04 \text{ KeV.} \end{aligned} \quad (3.41)$$

This analysis gives a range of values for η_W . The graphs are plotted in Fig. 3.5 at $\eta_W = -0.0059$. The binding, $F_B(z)$, and wave-function, $F_W(z)$, correction terms tend to cancel each other over part of the z region. The effect of final-state interaction corrections can be reasonably well estimated[3] provided one stays away from the end-point $z = 1$. In Fig. 3.5 comparison is made with the data, taken from ref.[6], with the prediction of this model appropriately folded with the experimental photon energy resolution (assumed to be Gaussian). The effect of the binding and wavefunction corrections calculated in this work is sizeable, and tends to increase the photon rate in the middle z range and to lower it for larger z . While this appears to be in the right direction, it would be highly desirable to have more precise data. The experimental data points are taken from Ref [6]. It should be noted that these values of η_B and η_W give a correction term consistent with the estimate made in Ref [11]. The shape of the curve depends on the values of η_B and η_W . A large negative value of η_B and a small value for η_W is favoured by the experimental data points.

The correction coming from a sum of leading logs of $1 - z$ has already been calculated [3] to all orders in perturbation theory. This correction modifies our

results somewhat in the large z region. The $\mathcal{O}(\alpha_S)$ radiative correction in the decay width is additive and is also included here. This correction is smaller than the $\mathcal{O}(v^2)$ terms. The inclusion of all these $\mathcal{O}(v^2)$ corrections causes the decay spectrum to increase in the region $.5 < z < .8$ and removes the sharp peak in the large z region. While this appears to be in the right direction, it would be highly desirable to have more precise data.

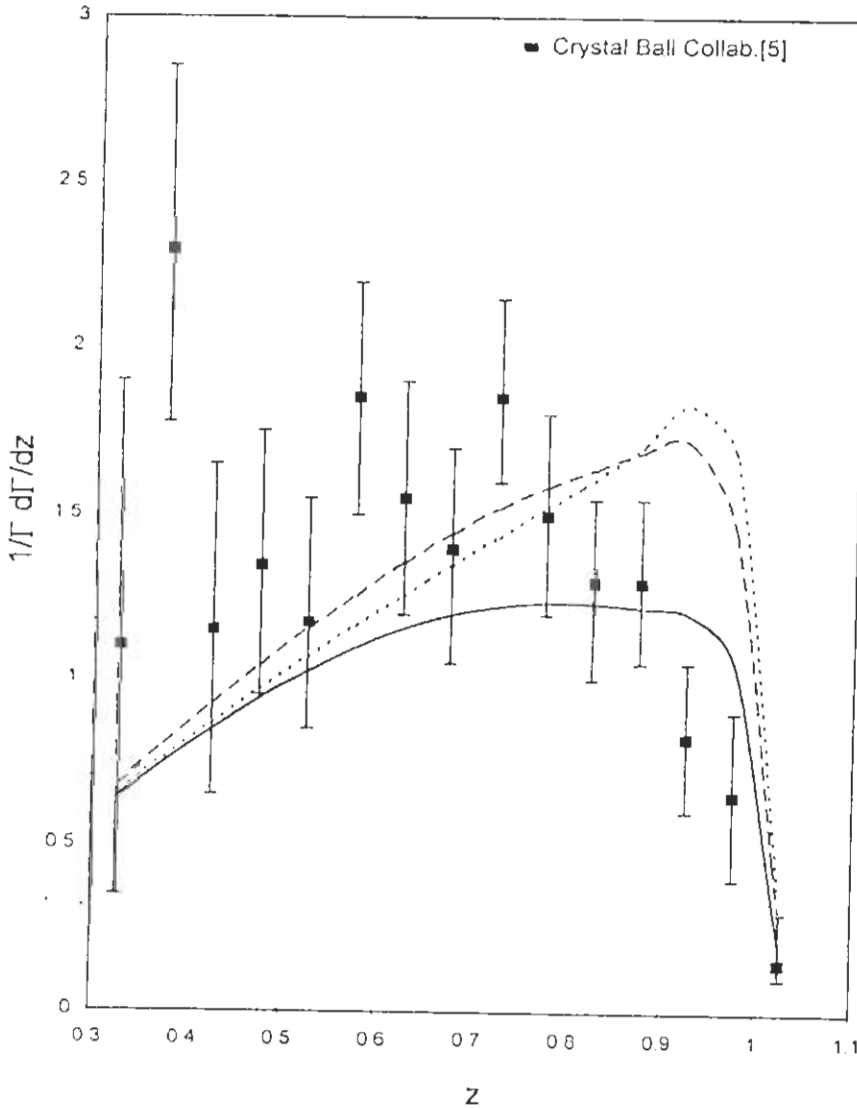


Figure 3.5: Zeroth order QCD result (dashed line) and our corrected spectrum (solid line) with $\eta_B = -.133$ and $\eta_W = -.056$. The data is taken from Ref [5]

3.5 Conclusion

The approach adopted in this work for calculating the amplitude for $\Upsilon \rightarrow \gamma + X$ is to take the sum of all distinct Feynman diagrams leading from the initial quarkonium state to the final state. Each diagram is put into the form of a (multipole) loop integral with a kernel which is a product of a hard part and a soft part. The hard part is treated with perturbative QCD, and the soft part is analyzed into its different components with the use of Lorentz \mathcal{C} and \mathcal{P} symmetries. Use of the QCD equations of motion enables separation of these components according to their importance in powers of v . At the last step, a specific commitment to dynamics is made and the B-S equation is used to express the components in the form of wavefunctions. However, the un-regularized value of $\nabla^2\phi(0)$ is singular at the origin $\nabla^2\phi(0) \sim M\phi(0)/r$. As is clear from the uncertainty principle, the local kinetic energy becomes very large at short distances and the expansion in powers of v breaks down. This difficulty was circumvented by imagining that annihilation takes place in a diffused region of size $O(1/m)$, i.e. $\phi(0)$ and $\nabla^2\phi(0)$ are quantities renormalized at this scale, and hence should be considered as adjustable parameters. The numerical investigation showed that varying these parameters within reasonable limits leads to substantial improvement in the intermediate z region but is insufficient to reproduce the data near $z = 1$, once again underscoring the importance of final-state interactions between collinear gluons.

References

- [1] For a review, see Gerhard A. Schuler, "Quarkonium Production And Decays", CERN-TH. 7170/94, submitted to Phys. Rep.
- [2] S.Brodsky, G.P.Lepage, and P.B.Mackenzie, Phys. Rev. **D28** 228 (1983).
- [3] Douglas M. Photiadis, Phys.Lett.164B 160 (1985).
- [4] R.D.Field, Phys.Lett. **B133** 248 (1983).
- [5] Review of particle properties, Phys.Rev.**D50**, 1994
- [6] Bizzeti et al, Crystal Ball Collaboration, Phys. Lett. **B267** 286 (1991).
- [7] Hafsa Khan and Pervez Hoodbhoy, "Systematic Gauge Invariant Approach To Heavy Quarkonium Decays", Phys.Rev. **D53** 1, 1996.
- [8] G.T.Bodwin, E.Braaten and G.P.Lepage, ANL-HEP-PR-94-24, July 1994.
- [9] G.P.Lepage, L.Magnea, C.Nakleh, U.Magnea, K.Hornbostel, preprint CLNS 92/1136, OHSTPY-HEP-T-92-001, Feb. 1992.
- [10] P.B.Mackenzie and G.P.Lepage, Phys. Rev. Lett 47, 1244 (1981).
W.Kwong, P.B.Mackenzie, R.Rosenfield, and J.L.Rosner, Phys. Rev. **D37**, 3210 (1988).
- [11] W.Y.Keung and I.J.Muzinich, Phys.Rev **D27** 1518 (1983).
- [12] C.Itzykson and J.Zuber, "Quantum Field Theory", p.237, McGraw-Hill, 1980.

- [13] S.Wolfram, "MATHEMATICA - A System for Doing Mathematics by Computer", Second edition, Addison-Wesley Publishing Company, 1991.
- [14] A. Hsieh and E. Yehudai, "HIP: Symbolic high-energy physics calculations", preprint SLAC-PUB 5576.
- [15] P. Labelle, G.P. Lepage and U. Magnea, Phys.Rev.Lett. 72, 2006 (1994).
- [16] M.B. Voloshin, Sov.J.Nucl.Phys. **40** 662 (1984).

Chapter 4

Heavy Quark Fragmentation Functions

Charmonium is possibly one of the simplest strongly bound systems that exist. Theoretical description of its decay and formation involves both perturbative and non-perturbative aspects of QCD. The large mass of the heavy quarks sets a mass scale large enough so that perturbative QCD, alongwith a non-relativistic potential model of the bound state, serve as a natural starting point to study these processes. Factorisation theorems of perturbative QCD separate the production process of charmonium in two steps, the production of a parton, a process which is calculable within perturbative QCD, and the subsequent splitting, called fragmentation, of that parton into charmonium state plus other partons. Fragmentation has proved to be a very useful concept as the fragmentation functions are universal, i.e. they are independent of the process responsible for producing the fragmenting parton. It has also been a major realisation in heavy quarkonium production that fragmentation processes dominate at sufficiently large transverse momenta.

The fragmentation function $f(z, \mu)$ gives the probability for a parton with invariant mass less than μ to split into the quarkonium state with longitudinal momentum fraction z . Until a few years ago, most predictions for fragmentation

functions were based on the color singlet model. This model assumes that the $c\bar{c}$ pair, which will subsequently bind into charmonium, is produced in the color singlet state. It also assumes that the relative momentum of the quark and the anti-quark is small compared to m_c and hence can be neglected because otherwise c and \bar{c} are likely to fly apart and never form charmonium.

The deviations of the predictions of the color singlet model from some recent data on the production of charmonium forced a reexamination of this model. The model is clearly incomplete. For one thing, it was assumed that a $c\bar{c}$ pair produced in the color octet state will never bind to form charmonium. This is of course not true as a color octet state can always make a transition to the color singlet state by emitting a gluon. The other assumption that the relativistic corrections, which take into account the relative velocity v of the charm and the anti-charm, are negligible is not true for charmonium since the estimated average value of v^2 is about $1/3$, suggesting that the relativistic corrections of order $(v^2)^n$ can be expected to be more important than perturbative corrections of order α_s^{2n} .

Whereas the role of the color octet model in physical processes such as Z^0 decay has been studied [4, 5], the relativistic and binding energy corrections have so far not been included. In this chapter the relativistic corrections to the fragmentation functions of a charm quark to decay into η_c and J/ψ are calculated. The Virial theorem suggests that the binding energy correction, arising from the fact that the mass of charmonium is not the exact sum of the masses of the constituent quarks, is of the same order of magnitude as the relativistic correction. So the binding energy correction to the fragmentation function are also calculated.

The issue of the absence of gauge invariance in much of the earlier work on processes involving heavy quarks has earlier been addressed and resolved in references [1, 2, 8] where this key property of a gauge theory has been systematically restored in the study of quarkonia decay. Here the same shall be done for fragmentation processes. However, it is found that direct introduction of a link operator offers a quicker route to arriving at gauge-invariant matrix elements.

The fragmentation function $f(z, \mu)$ will be calculated at the scale $\mu = (3m)^2$. Switching off the relativistic and binding energy corrections, the results obtained by Braaten et al. [6] are reproduced. Altarelli-Parisi equations are used to evolve these functions to the scale $\mu = (M_z/2)^2$ appropriate for Z^0 decay. One can also use the knowledge of the fragmentation functions to find the relativistic and binding energy corrections to the branching ratios of Z^0 decay into η_c and J/ψ . This is done in the last section.

4.1 Kinematics

I shall use the light cone coordinates in which a four-vector is written as

$$V^\mu = (V^+, V^-, V_\perp),$$

with

$$V_1 \cdot V_2 = V_1^+ V_2^- + V_1^- V_2^+ - V_1^\perp \cdot V_2^\perp \quad \Rightarrow \quad V^2 = 2V^+ V^- - V_\perp^2.$$

First define an auxiliary vectors n^μ such that $n^2 = n^+ = 0$. P^μ is the 4-momentum of the quarkonium. Choose a frame in which its 3-momentum is along the z-direction. One can then define $P^\mu = p^\mu + \frac{1}{2} M^2 n^\mu$, M being the quarkonium mass and p^μ a null vector such that $p^- = 0$ and $p \cdot n = 1$. A convenient choice for n^μ and p^μ is

$$p^\mu = (\mathcal{P}, 0, \vec{0}_\perp), \quad n^\mu = (0, 1/\mathcal{P}, \vec{0}_\perp) \quad , \quad (4.1)$$

where \mathcal{P} has been adjusted to be the forward momentum P^+ of the outgoing charmonium. A simple calculation yields

$$P^\mu \equiv (\mathcal{P}, M^2/2\mathcal{P}, \vec{0}_\perp) \Rightarrow P^2 = M^2,$$

$$l^\mu \equiv \left(\left(\frac{1}{z} - 1 \right) \mathcal{P}, \frac{x + m^2}{2 \left(\frac{1}{z} - 1 \right) \mathcal{P}}, \vec{l}_\perp^2 \right) \Rightarrow l^2 = m^2. \quad (4.2)$$

All the remaining dot products can now be calculated

$$\begin{aligned}
 P \cdot l &= \frac{x + m^2}{2(1/z - 1)} + \frac{M^2}{2} \left(\frac{1}{z} - 1 \right), \\
 P \cdot n &= 1, \\
 l \cdot n &= \left(\frac{1}{z} - 1 \right). \tag{4.3}
 \end{aligned}$$

4.2 Formalism

As pointed out earlier, Braaten et.al., [6] have calculated the leading order contribution to the charm quark fragmentation function. However the technique used by them is different from the one used in this work. They started with the assertion that the fragmentation contribution to the inclusive decay rate of the Z^0 into charmonium is the term that survives in the limit $M_Z/m_c \rightarrow \infty$. The differential decay rate for the production of a J/ψ of energy E can be written as,

$$d\Gamma(Z^0 \rightarrow \psi(E) + X) = \sum_i \int_0^1 dx d\hat{\Gamma}(Z^0 \rightarrow i(E/z) + X, \mu) f_{i \rightarrow \psi}(z, \mu). \tag{4.4}$$

where the sum is over partons of type i and z is the longitudinal momentum fraction of the J/ψ relative to the parton. Extraction of the fragmentation function from the above expression is then made possible by expanding in powers of m_c/M_Z . The problem with this technique is that it is very difficult to generalize it and calculate the correction terms.

The starting point of the present work is the definition of fragmentation function in terms of matrix elements of field operators at light cone separation[3] i.e.,

$$\hat{f}(z) = \frac{z}{4} \sum_X \int \frac{d\lambda}{2\pi} e^{-i\lambda/z} Tr [\not{n}(0) |\psi(0)\rangle PX \langle PX | \bar{\psi}(\lambda n) | 0 \rangle] , \tag{4.5}$$

where z is the momentum fraction of the fragmenting quark carried by quarkonium in the forward direction. In lowest order of α_s , the inclusive sum over X

is restricted to c and \bar{c} . First use translational invariance to shift the quark field operator from λn to 0:

$$\hat{f}(z) = \frac{z}{4} \int \frac{d\lambda}{2\pi} \frac{d^3l}{(2\pi)^3} e^{-i\lambda/z} e^{i(P+l)\cdot\lambda n} \text{Tr} [\not{\epsilon}(0) |\psi(0)\rangle \langle Pl| \langle Pl| \bar{\psi}(0)\rangle |0\rangle] . \quad (4.6)$$

The summation over X has been replaced with integration over l , the four-momentum of the undetected outgoing quark. Using the fact that this quark is on mass-shell, one can write the integration over l as

$$\begin{aligned} \int \frac{d^3l}{(2\pi)^3} &= \int \frac{d^4l}{(2\pi)^4} (2\pi) \delta(l^2 - m^2) \\ &= \int \frac{dl^+ dl^- d^2l_\perp}{(2\pi)^4} (2\pi) \delta(l^2 - m^2). \end{aligned} \quad (4.7)$$

Integration over λ yields another delta function $\delta\left(\frac{1}{z} - \frac{P^+ + l^+}{P^+}\right)$. These two delta functions allow us to integrate over l^+ and l^- , leaving behind the integration over l_\perp :

$$\hat{f}(z) = \frac{z^2}{64\pi^2(1-z)} \int dl_\perp^2 \text{Tr} [\not{\epsilon}(0) |\psi(0)\rangle \langle Pl| \langle Pl| \bar{\psi}(0)\rangle |0\rangle] , \quad (4.8)$$

where $d^2l_\perp = \pi dl_\perp^2$.

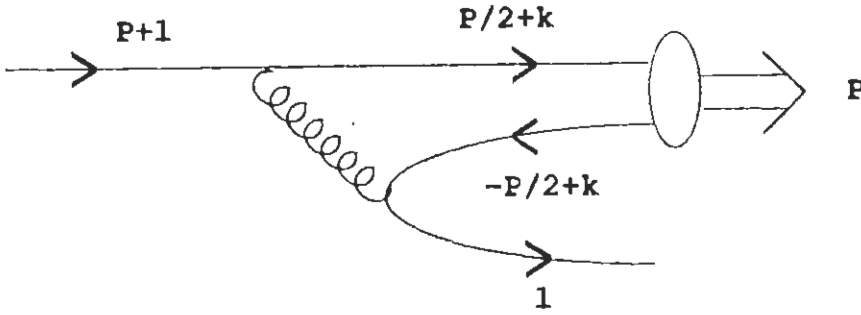


Figure 4.1: Feynman diagram contributing to the fragmentation of a c quark into charmonium

The leading order contribution to the amplitude comes from Fig.4.1, and is given by,

$$\langle Pl| \bar{\psi}(0)\rangle |0\rangle = \int \frac{d^4k}{(2\pi)^4} \bar{u}(l) (-i\gamma^\mu) M(k) (-i\gamma^\nu) iS_F(P+l) iD_{\mu\nu}(k - \frac{P}{2} + l), \quad (4.9)$$

where the color indices have been suppressed¹. The Bethe-Salpeter amplitude $M(k)$ is

$$M(k) = \int d^4x e^{ik \cdot x} \langle P | \psi(x/2) e^{i \int_{-x/2}^{x/2} A(\xi) d\xi} \bar{\psi}(-x/2) | 0 \rangle, \quad (4.10)$$

where the gauge invariance has been ensured by introducing the gauge link operator $\xi = e^{i \int_{-x/2}^{x/2} A(\xi) d\xi}$ [11]. The gluon propagator is

$$D_{\mu\nu}(q) = \left(-g_{\mu\nu} + \frac{q_\mu n_\nu + q_\nu n_\mu}{q \cdot n} \right) \frac{1}{q^2}, \quad (4.11)$$

in the light-cone gauge.

Since the relative velocity of heavy quarks is much less than the scale set by their mass, one can expand $D_{\mu\nu}(k - P/2 + l)$ in powers of k , the relative momentum :

$$\begin{aligned} D_{\mu\nu}(k - P/2 - l) &= D_{\mu\nu}(k - P/2 - l)|_{k=0} + k^\alpha \frac{\partial}{\partial k^\alpha} D_{\mu\nu}(k - P/2 - l)|_{k=0} \\ &+ \frac{1}{2!} k^\alpha k^\beta \frac{\partial}{\partial k^\alpha} \frac{\partial}{\partial k^\beta} D_{\mu\nu}(k - P/2 - l)|_{k=0} \quad , \end{aligned} \quad (4.12)$$

The above expansion permits us to write the amplitude as follows

$$\begin{aligned} \langle Pl | \bar{\psi}(0) | 0 \rangle &= \int \frac{d^4k}{(2\pi)^4} \left[\bar{u}(l) \gamma^\mu M(k) \gamma^\nu S_F(P+l) D_{\mu\nu}(P/2-l) \right. \\ &+ \bar{u}(l) \gamma^\mu M^\alpha(k) \gamma^\nu S_F(P+l) k_\alpha D_{\mu\nu,\alpha}(P/2-l) \\ &\left. + \bar{u}(l) \gamma^\mu M^{\alpha\beta}(k) \gamma^\nu S_F(P+l) k_\alpha k_\beta D_{\mu\nu,\alpha\beta}(P/2-l) \right] \quad , \end{aligned} \quad (4.13)$$

where

$$\begin{aligned} D_{\mu\nu,\alpha} &\equiv \partial_\alpha D_{\mu\nu} \quad , \\ D_{\mu\nu,\alpha\beta} &\equiv \partial_\alpha \partial_\beta D_{\mu\nu} \quad . \end{aligned} \quad (4.14)$$

The integration over k can be performed very easily

$$\int \frac{d^4k}{(2\pi)^4} M(k) = \int \frac{d^4x}{(2\pi)^4} e^{ik \cdot x} \langle P | \psi(x/2) \xi \bar{\psi}(-x/2) | 0 \rangle$$

¹The color factor for the leading order diagram turns out to be 16/27

$$= \langle P|\psi(0)\bar{\psi}(0)|0\rangle,$$

$$\begin{aligned} \int \frac{d^4k}{(2\pi)^4} k_\alpha M(k) &= \int \frac{d^4k}{(2\pi)^4} d^4x \frac{1}{i} \partial_\alpha e^{ik \cdot x} \langle P|\psi(x/2)\not{x}\bar{\psi}(-x/2)|0\rangle \\ &= i\partial_\alpha \langle P|\psi(x/2)\not{x}\bar{\psi}(-x/2)|0\rangle|_{x=0} \\ &= \langle P|\psi(0)i\vec{D}_\alpha \bar{\psi}(0)|0\rangle, \end{aligned}$$

$$\begin{aligned} \int \frac{d^4k}{(2\pi)^4} k_\alpha k_\beta M(k) &= \int \frac{d^4k}{(2\pi)^4} d^4x \frac{1}{i} \partial_\alpha \frac{1}{i} \partial_\beta e^{ik \cdot x} \langle P|\psi(x/2)\not{x}\bar{\psi}(-x/2)|0\rangle \\ &= i\partial_\alpha i\partial_\alpha \langle P|\psi(x/2)\not{x}\bar{\psi}(-x/2)|0\rangle|_{x=0} \\ &= \langle P|\psi(0)i\vec{D}_\alpha i\vec{D}_\alpha \bar{\psi}(0)|0\rangle, \end{aligned} \quad (4.15)$$

with

$$\vec{D}^\alpha = \frac{1}{2} \left(\overleftarrow{\partial}^\alpha - \overrightarrow{\partial}^\alpha \right) - iyA^\alpha. \quad (4.16)$$

So finally

$$\begin{aligned} \langle Pl|\bar{\psi}(0)|0\rangle &= [\bar{u}(l)\gamma^\mu M(0)\gamma^\nu S_F(P+l)D_{\mu\nu}(P/2-l) \\ &+ \bar{u}(l)\gamma^\mu M^\alpha(0)\gamma^\nu S_F(P+l)D_{\mu\nu,\alpha}(P/2-l) \\ &+ \bar{u}(l)\gamma^\mu M^{\alpha\beta}(0)\gamma^\nu S_F(P+l)D_{\mu\nu,\alpha\beta}(P/2-l)] , \end{aligned} \quad (4.17)$$

where

$$\begin{aligned} M(0) &\equiv \langle P|\psi\bar{\psi}|0\rangle, \\ M^\alpha(0) &\equiv \langle P|\psi i\vec{D}^\alpha \bar{\psi}|0\rangle, \\ M^{\alpha\beta}(0) &\equiv \frac{1}{2!} \langle P|\psi i\vec{D}^\alpha i\vec{D}^\beta \bar{\psi}|0\rangle. \end{aligned} \quad (4.18)$$

The fragmentation function can now be written as

$$f(z) = \frac{M^2}{64\pi^2} \frac{z^2}{1-z} \int dx \mathcal{T}, \quad x = l_\perp^2/M^2 \quad (4.19)$$

where

$$\mathcal{T} = \text{Tr} [\not{A} S_F \gamma^\alpha \bar{M} \gamma^\beta (\not{V} + m) \gamma^\mu M \gamma^\nu S_F] D_{\mu\nu} D_{\alpha\beta}$$

$$\begin{aligned}
& + \text{Tr} [\not{A} S_F \gamma^\alpha \bar{M} \gamma^\beta (\not{V} + m) \gamma^\mu M^\nu \gamma^\nu S_F] D_{\mu\nu,\rho} D_{\alpha\beta} \\
& + \text{Tr} [\not{A} S_F \gamma^\alpha \bar{M}^\rho \gamma^\beta (\not{V} + m) \gamma^\mu M \gamma^\nu S_F] D_{\mu\nu} D_{\alpha\beta,\rho} \\
& + \text{Tr} [\not{A} S_F \gamma^\alpha \bar{M} \gamma^\beta (\not{V} + m) \gamma^\mu M^{\rho\sigma} \gamma^\nu S_F] D_{\alpha\beta} D_{\mu\nu,\rho\sigma} \\
& + \text{Tr} [\not{A} S_F \gamma^\alpha \bar{M}^{\rho\sigma} \gamma^\beta (\not{V} + m) \gamma^\mu M \gamma^\nu S_F] D_{\alpha\beta,\rho\sigma} D_{\mu\nu} \quad . \quad (4.20)
\end{aligned}$$

The above result should also be multiplied with the color factor for the Feynman diagram shown in Fig. [1], which turns out to be (averaging over initial and summing over final colors) :

$$\begin{aligned}
\text{C.F} &= \frac{1}{3} \left| \frac{1}{\sqrt{3}} \delta_{ab} \left(\frac{\lambda^J}{2} \right)_{ab} \left(\frac{\lambda^J}{2} \right)_{ac} \right|^2 \\
&= \frac{1}{3} \left| \frac{1}{2\sqrt{3}} \left(3\delta_{dc} - \frac{1}{3}\delta_{dc} \right) \right|^2 \\
&= \frac{1}{3} \frac{16}{9} \quad , \quad (4.21)
\end{aligned}$$

where the factor 1/3 comes from averaging over initial quark colors.

To proceed one can perform a Lorentz and CPT invariant decomposition of each of the hadronic matrix elements in Eq. 4.18. However the evaluation of the hadronic matrix elements for the decay of mesons has been detailed in Ref. [2, 7, 8]. Their hermitian conjugation and trivial algebraic manipulation yields the matrix elements considered in this work. I shall list them in the next two sections where the corresponding fragmentation functions are also calculated. The details can be found in the appendix 3.

4.3 Fragmentation Function for $c \rightarrow \eta_c$

As outlined in the previous section, one can calculate the hadronic matrix elements in Eq. 4.18, for both η_c and J/ψ . For η_c :

$$\begin{aligned}
\langle P | \psi \bar{\psi} | 0 \rangle &= \frac{M^{1/2}}{2} \gamma_5 \left(1 + \frac{\not{\nabla}^2}{M^2} \right) \phi(0) \left(1 + \frac{\not{P}}{M} \right) - \frac{M^{1/2}}{2} \gamma_5 \frac{\nabla^2 \phi(0)}{M^2} \left(1 - \frac{\not{P}}{M} \right) \\
\langle P | \psi i \overleftarrow{D}^\alpha \bar{\psi} | 0 \rangle &= \frac{i}{3} M^{1/2} \frac{\nabla^2 \phi(0)}{M^2} \gamma_5 \sigma^{\alpha\beta} P_\beta
\end{aligned}$$

$$\langle P|\psi i\vec{D}^{\vec{\alpha}} i\vec{D}^{\vec{\beta}} \bar{\psi}|0\rangle = \frac{1}{6}M^{5/2}\frac{\nabla^2\phi(0)}{M^2}\gamma_5\left(g^{\alpha\beta} - \frac{P^\alpha P^\beta}{M^2}\right)\left(1 + \frac{\not{P}}{M}\right), \quad (4.22)$$

where $\phi(0)$ is the quarkonium wavefunction at the origin. Using these values of the matrix elements, the fragmentation function², including the binding energy correction coming from $m = M/2 + \epsilon_B/2$ can be computed :

$$\begin{aligned} \hat{f}_{c\rightarrow\eta_c}(z, 3m) &= \frac{64\alpha_s^2(3m)}{81\pi}\frac{|R(0)|^2}{M^3}\{f_0(z) + \eta_B f_B(z) + \eta_W f_W(z)\} \\ &= \hat{f}_0(z, 3m) + \eta_B \hat{f}_B(z, 3m) + \eta_W \hat{f}_W(z, 3m), \end{aligned} \quad (4.23)$$

where

$$\begin{aligned} f_0(z) &= \frac{z(1-z)^2(48 + 8z^2 - 8z^3 + 3z^4)}{(2-z)^6}, \\ f_B(z) &= \frac{4z^2(1-z)^2(-48 + 48z - 40z^2 + 12z^3 - 5z^4)}{(2-z)^8}, \\ f_W(z) &= \frac{8z(1-z)^2(96 + 144z - 528z^2 + 296z^3 - 102z^4 + 43z^5 - 9z^6)}{3(2-z)^8} \end{aligned}$$

$$\hat{f}_i(z, 3m) = \frac{64\alpha_s^2(3m)}{81\pi}\frac{|R(0)|^2}{M^3}f_i(z) \quad (i = 0, B, W) \quad (4.24)$$

and

$$\eta_B = \frac{\epsilon_B}{M} \quad \eta_W = \frac{\nabla^2 R(0)}{M^2 R(0)}, \quad (4.25)$$

where $R(0)$ is the radial wavefunction, related to $\phi(0)$ as $\phi(0) = R(0)/4\pi$. In the absence of relativistic and binding energy corrections, the results obtained by Braaten et al. [6] are recovered. It is straightforward to obtain the fragmentation probability by integrating Eq. (4.23) over z :

$$\int_0^1 dz f_{c\rightarrow\eta_c}(z, 3m_c) = \frac{64\alpha_s^2}{27\pi}\frac{|R(0)|^2}{M^3}(F_0 + \eta_B F_B + \eta_W F_W), \quad (4.26)$$

where

²I used **Mathematica**[9], supplemented by the **HIP** package[10], for computation of traces and simplification of algebra.

$$\begin{aligned}
F_0 &= \frac{773}{30} - 37 \log 2, \\
F_B &= -\frac{5639}{105} + \frac{232}{3} \log 2, \\
F_W &= -\frac{100304}{315} + \frac{4136}{9} \log 2.
\end{aligned} \tag{4.27}$$

4.4 Fragmentation Function for $c \rightarrow J/\psi$

In an identical fashion, one can repeat the above calculation for the fragmentation of a c quark to a 1^{--} state, the J/ψ . The corresponding matrix elements can be derived, as before, from the ones evaluated for the relevant decay process in ref[8].

$$\begin{aligned}
\langle P, \epsilon | \psi \bar{\psi} | 0 \rangle &= \frac{1}{2} M^{1/2} \left(1 + \frac{\nabla^2}{M^2} \right) \phi \not{\epsilon} \left(1 + \frac{\not{P}}{M} \right) - \frac{1}{6} M^{1/2} \frac{\nabla^2 \phi}{M^2} \not{\epsilon} \left(1 - \frac{\not{P}}{M} \right), \\
\langle P, \epsilon | \psi i \overleftrightarrow{D}^{\alpha} \bar{\psi} | 0 \rangle &= \frac{1}{3} M^{3/2} \frac{\nabla^2 \phi}{M^2} \epsilon_{\beta}^{\alpha} \left[g^{\alpha\beta} + \frac{i}{M} \epsilon^{\mu\nu\alpha\beta} P_{\nu} \gamma_{\mu} \gamma_5 \right], \\
\langle P, \epsilon | \psi i \overleftrightarrow{D}^{\alpha} i \overleftrightarrow{D}^{\beta} \bar{\psi} | 0 \rangle &= \frac{1}{6} M^{5/2} \frac{\nabla^2 \phi}{M^2} \left(g^{\alpha\beta} - \frac{P^{\alpha} P^{\beta}}{M^2} \right) \not{\epsilon} \left(1 + \frac{\not{P}}{M} \right).
\end{aligned} \tag{4.28}$$

With these values of matrix elements,

$$\begin{aligned}
\hat{f}_{c \rightarrow J/\psi}(z) &= \frac{64}{27\pi} \alpha_s (3m_c)^2 \frac{|R(0)|^2}{M^3} [f_0(z) + \eta_B f_B(z) + \eta_W f_W(z)] \\
&= \hat{f}_0(z, 3m) + \eta_B \hat{f}_B(z, 3m) + \eta_W \hat{f}_W(z, 3m),
\end{aligned} \tag{4.29}$$

where

$$\begin{aligned}
f_0(z) &= \frac{z(1-z)^2(16-32z+72z^2-32z^3+5z^4)}{(2-z)^6}, \\
f_B(z) &= -\frac{4z^2(1-z)^2(48-144z+152z^2-28z^3+13z^4-2z^5)}{3(z-2)^8}, \\
f_W(z) &= \frac{8z(1-z)^2(96-272z+592z^2-552z^3+338z^4-115z^5+15z^6)}{3(2-z)^8}
\end{aligned} \tag{4.30}$$

and all the other symbols have the same meaning as before with the only difference that M now stands for the mass of J/ψ instead of η_c . As before, the evaluation of the decay rate of Z^0 to J/ψ would require the total fragmentation probability, which can be obtained by integrating Eq. (4.29) over z :

$$\int_0^1 dz f_{c \rightarrow J/\psi}(z, 3m_c) = \frac{64\alpha_S^2 |R(0)|^2}{27\pi M^3} (F_0 + \eta_B F_B + \eta_W F_W), \quad (4.31)$$

where

$$\begin{aligned} F_0 &= \frac{1189}{30} - 57 \log 2, \\ F_B &= \frac{2327}{35} - 96 \log 2, \\ F_W &= \frac{54308}{63} - \frac{3728}{3} \log 2. \end{aligned} \quad (4.32)$$

4.5 QCD Evolution

The Altarelli-Parisi evolution equations,

$$\mu \frac{\partial}{\partial \mu} \hat{f}_{c \rightarrow \eta_c}(z, \mu) = \frac{\alpha_S(\mu)}{2\pi} \int_z^1 \frac{dy}{y} P_{c \rightarrow c}(z/y) \hat{f}_{c \rightarrow \eta_c}(y, \mu) \quad (4.33)$$

can now be used to evolve the fragmentation function evaluated at the scale $\mu = (3m)^2$ to $\mu = (M_Z/2)^2$. $P_{c \rightarrow c}(x)$ is the Altarelli-Parisi function for the splitting of a charm quark into another charm quark with longitudinal momentum fraction x :

$$P_{cc}(x) = \frac{4}{3} \frac{1+x^2}{(1-x)_+} + 2\delta(1-x), \quad (4.34)$$

where the subscript $+$ has its usual meaning, and

$$\alpha_S(Q^2) = \frac{12\pi}{(33 - 2n_f)t} \equiv \frac{2\pi C}{t}, \quad t = \ln(Q^2/\Lambda^2)$$

Multiplying the A-P equation by x^{n-1} and integrating over x from 0 to 1, one gets

$$m_n(Q^2) = m_n(Q_0^2) \left[\frac{\ln(Q^2/\Lambda^2)}{\ln(Q_0^2/\Lambda^2)} \right]^{C_{\gamma_n}}, \quad (4.35)$$

where $m_n(Q^2)$ is the moment of the fragmentation function

$$m_n(Q^2) = \int dx x^{n-1} f(x, \mu) \quad (4.36)$$

and

$$\gamma_n = \frac{4}{3} \left[-\frac{1}{2} + \frac{1}{n(n+1)} - 2 \sum_{j=2}^n \frac{1}{j} \right]. \quad (4.37)$$

The evolution equation is therefore solved easily assuming a polynomial fit for the evolved fragmentation function. Using the Altarelli-Parisi equation, I have evolved the fragmentation function for η_c and J/ψ at the scale $\mu = (3m)^2$ to the scale $\mu = (M_Z/2)^2$, Fig. (2) and Fig. (3) respectively.

Taking into consideration only the contribution of charm quark and anti-quark, the total decay rate for inclusive η_c production at leading order in α_s through Z^0 decay is given by :

$$\Gamma(Z^0 \rightarrow \eta_c + X) = 2\Gamma(Z^0 \rightarrow c\bar{c}) \int_0^1 dz \hat{f}_{c \rightarrow \eta_c}(z, M_Z/2), \quad (4.38)$$

where a factor of 2 has been included to incorporate the effect of anti-quark fragmentation. It is important to note that at leading order in α_s , the fragmentation probability $\int_0^1 dz \hat{f}_{c \rightarrow \eta_c}(z, \mu)$ does not evolve with scale μ , and one may write :

$$\Gamma(Z^0 \rightarrow \eta_c + X) = 2\Gamma(Z^0 \rightarrow c\bar{c}) \int_0^1 dz \hat{f}_{c \rightarrow \eta_c}(z, 3m) \quad (4.39)$$

4.6 Numerical Work

In order to produce numerical estimation for corrections to fragmentation functions, the values used for various parameters are: $\alpha_s = 0.19$, $m = 1.43$ GeV, $|R(0)_{\eta_c}|^2 = 0.936$ GeV³, $|R(0)_{J/\psi}|^2 = 0.978$ GeV³, $\nabla^2 R/R = -0.7$ GeV², $M_Z = 91$ GeV, $M_{\eta_c} = 2.98$ GeV, $M_{J/\psi} = 3.097$ GeV. The choice of the parameters α_s , $|R(0)|^2$, and $\nabla^2 R/R$ is discussed in ref[2]. The fragmentation functions have been depicted in Figs. (2,3).

One of the first applications of the fragmentation ideas was to charmonia production at LEP. After calculating the lowest order fragmentation functions, Braaten, Cheung and Yuan [6] calculated the branching fraction $\text{Br}(Z^0 \rightarrow \eta_c(J/\psi)) = \Gamma(Z^0 \rightarrow \eta_c(J/\psi) + X)/\Gamma(Z^0 \rightarrow c\bar{c})$. I generalize the above results to incorporate the binding energy and relativistic corrections as well. For η_c ,

$$\text{Br}(Z^0 \rightarrow \eta_c) = \frac{\Gamma_0(Z^0 \rightarrow \eta_c + X)}{\Gamma(Z^0 \rightarrow c\bar{c})} [1 - 0.84\eta_B + 0.95\eta_W], \quad (4.40)$$

where Γ_0 is the color-singlet decay rate in the absence of relativistic and binding energy corrections. For the values of parameters chosen above, the branching ratio without and with the corrections is 2.32×10^{-4} and 2.22×10^{-4} respectively.

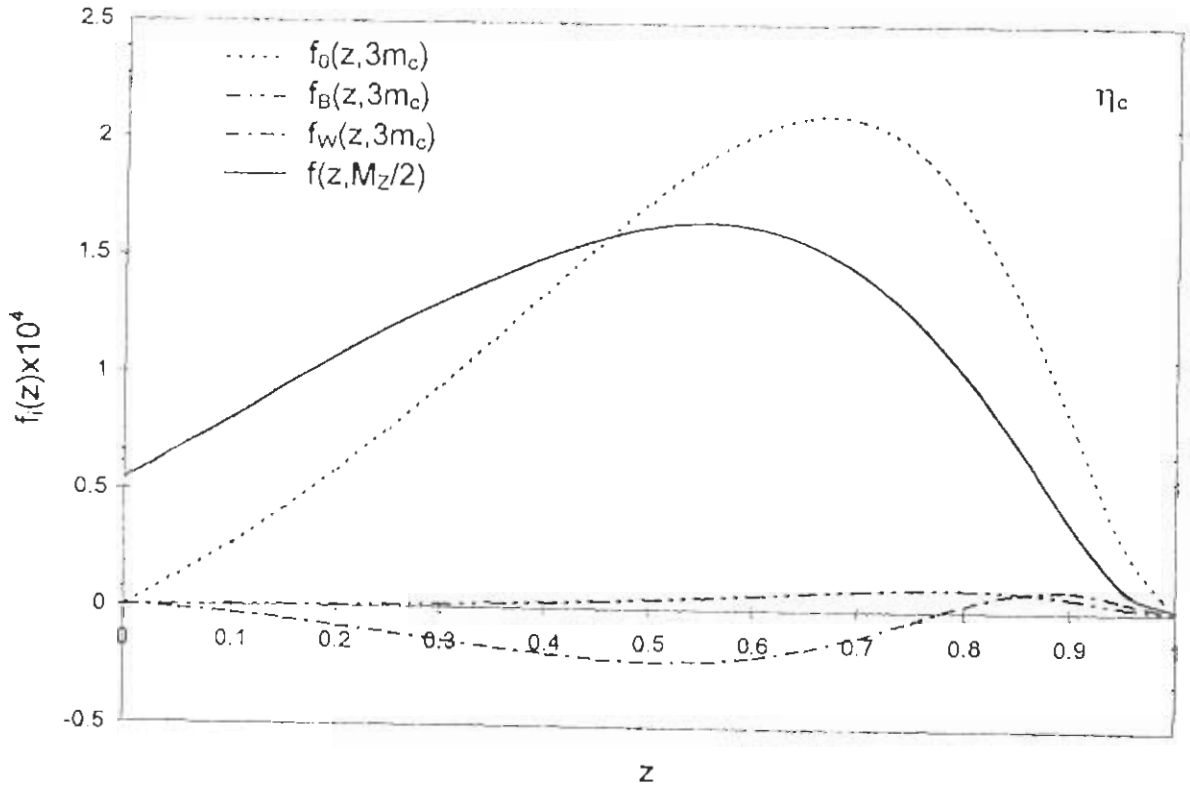


Figure 4.2: The functions f_0 , f_B & f_W at $Q^2 = (3m)^2$ for $c \rightarrow \eta_c$. The solid line shows the complete fragmentation function f at $Q^2 = (M_Z/2)^2$

For J/ψ ,

$$\text{Br}(Z^0 \rightarrow J/\psi) = \frac{\Gamma_0(Z^0 \rightarrow (J/\psi) + X)}{\Gamma(Z^0 \rightarrow c\bar{c})} [1 - 0.45\eta_B + 5.5\eta_W] . \quad (4.41)$$

The binding and relativistic corrections modify the color-singlet branching ratio of Braaten et al. from 2.22×10^{-4} to 1.36×10^{-4} , an effect of around 38%, which is not surprising on the grounds that v^2/v^2 is expected to be around 1/3 for charmonium. Therefore, the $\mathcal{O}(v^2)$ corrections seem to affect the decay of Z^0 into J/ψ much more than into η_c .

4.7 Conclusion

Relativistic and binding energy corrections of $\mathcal{O}(v^2)$ to the fragmentation functions for charm quark splitting into η_c and J/ψ are calculated. It is shown how these corrections can be expressed in terms of various bound state matrix elements of gauge-invariant quark and gluon operators. In the absence of the said corrections, these results reduce to the leading order result of Braaten et al., [6], as expected. The modified fragmentation functions are used to estimate the contribution of relativistic and binding energy corrections to the corresponding branching ratios in $Z^0 \rightarrow \psi c\bar{c}$ decays. Since the average value of v^2 for charmonium is about 1/3, one expects the effect of $\mathcal{O}(v^2)$ terms not to be negligible. It is found that in case of J/ψ , these corrections contribute about 38% to the lowest order $c \rightarrow c J/\psi$ result, though for η_c this effect does not exceed more than a few percent.

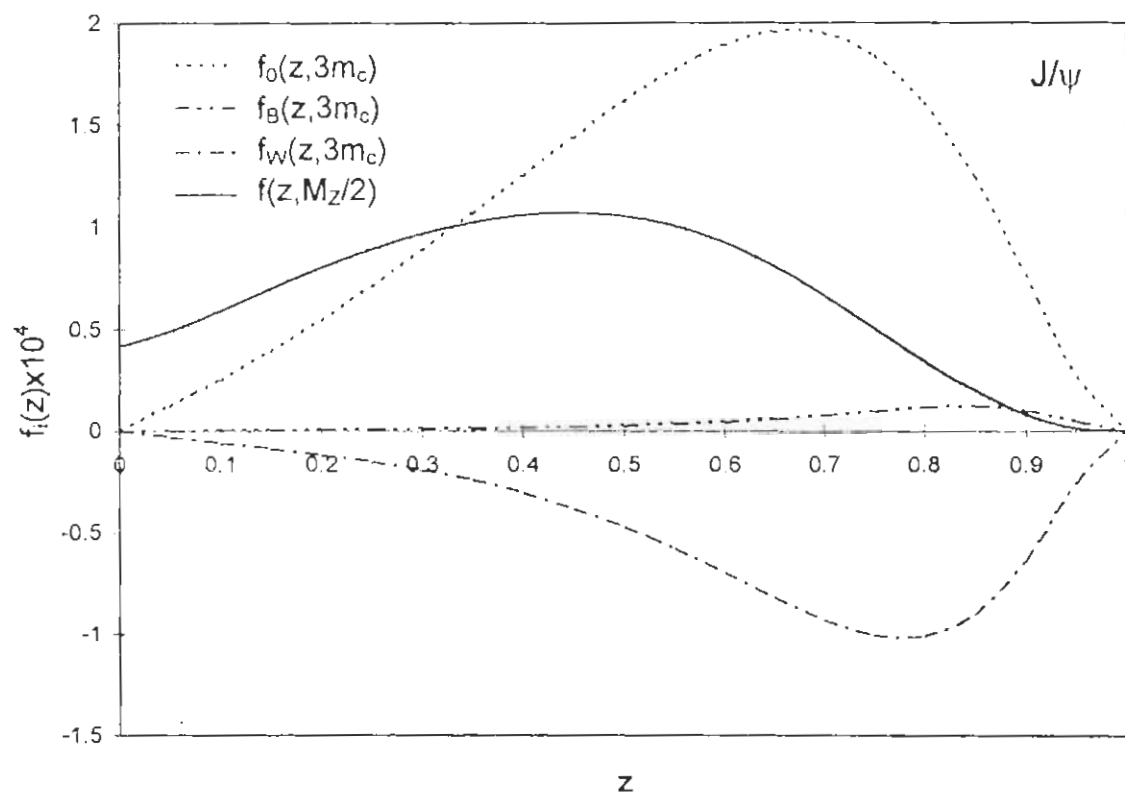


Figure 4.3: The functions f_0 , f_B & f_W at $Q^2 = (3m)^2$ for $c \rightarrow J/\psi$. The solid line shows the complete fragmentation function f at $Q^2 = (M_Z/2)^2$

References

- [1] R. Ali and P. Hoodbhoy, *Phys. Rev.* **D51**, 2302 (1995).
- [2] H. Khan and P. Hoodbhoy, *Phys. Rev.* **D53**, 1 (1996).
- [3] X. Ji, *Phys. Rev.* **D49**, 114 (1994).
- [4] K. Cheung, Wai-Yee Keung, and T.C. Yuan, *Phys. Rev* **D76**, 877 (1996).
- [5] P. Cho, Caltech preprint no. CALT-68-2020 (1995).
- [6] E. Braaten, K. Cheung and T.C. Yuan, *Phys. Rev.* **D48**, 4230 (1993).
- [7] M.A. Yusuf, Ph.D thesis, Quaid-e-Azam University, Islamabad, Pakistan (1996).
- [8] M.A. Yusuf and P. Hoodbhoy, *Phys. Rev.* **D54**, 1 (1996).
- [9] S.Wolfram, "MATHEMATICA - A System for Doing Mathematics by Computer", Second edition, Addison-Wesley Publishing Company, 1991.
- [10] A. Hsieh and E. Yehudai, "HIP: Symbolic high-energy physics calculations", preprint SLAC-PUB 5576.
- [11] Wai-Yee Keung and I.J. Muzinich, *Phys. Rev.* **D27**, 1518 (1983).
- [12] J.H. Kühn and H. Schneider, *Phys. Rev.* **D24**, 2996 (1981); *Z. Phys.* **C11**, 263 (1981).
- [13] M. Consoli and J.H. Field, Report No. UGVA-DPNC 1994/12-164, 1994 (unpublished).

Appendix 1

Gauge Invariance in Υ Decay

In this section I shall show that the different terms arising in the expansion of the amplitudes in Υ decay can be combined into gauge invariant parts. The zero-gluon amplitude can be written as

$$T_0^{\mu_1\mu_2\mu_3} = \int \frac{d^4k}{(2\pi)^4} \text{Tr} \{M(k)h^{\mu_1\mu_2\mu_3}(k)\}. \quad (1.1)$$

Expand the hard part in powers of k ,

$$h^{\mu_1\mu_2\mu_3}(k) = \sum_n \frac{1}{n!} k^{\alpha_1} \dots k^{\alpha_n} U_{\alpha_1 \dots \alpha_n}^{\mu_1\mu_2\mu_3}, \quad (1.2)$$

where

$$U_{\alpha_1 \dots \alpha_n}^{\mu_1\mu_2\mu_3} = \frac{\partial}{\partial k^{\alpha_1}} \dots \frac{\partial}{\partial k^{\alpha_n}} h^{\mu_1\mu_2\mu_3}(k)|_{k=0}. \quad (1.3)$$

Insert Eq. 2 in Eq. 1 and integrate by parts to get

$$T_0^{\mu_1\mu_2\mu_3} = \text{Tr} \sum_n \mathcal{M}^{\alpha_1 \dots \alpha_n} U_{\alpha_1 \dots \alpha_n}^{\mu_1\mu_2\mu_3}, \quad (1.4)$$

where

$$\mathcal{M}^{\alpha_1 \dots \alpha_n} = \frac{1}{n!} \langle 0 | \bar{\psi} i \overleftrightarrow{\partial}^{\alpha_1} \dots i \overleftrightarrow{\partial}^{\alpha_n} \psi | P \rangle. \quad (1.5)$$

Now look at the one-gluon amplitude

$$T_1^{\mu_1\mu_2\mu_3} = \int \frac{d^4k}{(2\pi)^4} \frac{d^4k'}{(2\pi)^4} \text{Tr} [M^\rho(k, k') H_\rho^{\mu_1\mu_2\mu_3}(k, k')]. \quad (1.6)$$

Expand the hard part in powers of k ,

$$H^{\mu_1\mu_2\mu_3\rho}(k, k') = \sum_{n,l} \frac{1}{n!l!} k^{\alpha_1} \dots k^{\alpha_n} k'^{\beta_1} \dots k'^{\beta_l} V_{\alpha_1 \dots \alpha_n \beta_1 \dots \beta_l}^{\mu_1\mu_2\mu_3\rho} \quad (1.7)$$

where

$$V_{\alpha_1 \dots \alpha_n \beta_1 \dots \beta_l}^{\mu_1\mu_2\mu_3\rho} = \frac{\partial}{\partial k^{\alpha_1}} \dots \frac{\partial}{\partial k^{\alpha_n}} \frac{\partial}{\partial k'^{\beta_1}} \dots \frac{\partial}{\partial k'^{\beta_l}} H^{\mu_1\mu_2\mu_3\rho}(k, k')|_{k \dots k' = 0}. \quad (1.8)$$

Insert Eq. 2 in Eq. 1 and integrate by parts over k, k' to get

$$T_1^{\mu_1\mu_2\mu_3} = \text{Tr} \sum_{n,l} \mathcal{M}_\rho^{\alpha_1 \dots \alpha_n \beta_1 \dots \beta_l} V_{\alpha_1 \dots \alpha_n \beta_1 \dots \beta_l}^{\mu_1\mu_2\mu_3\rho} \quad (1.9)$$

where

$$\mathcal{M}_\rho^{\alpha_1 \dots \alpha_n \beta_1 \dots \beta_l} = \frac{1}{n!l!} \langle 0 | \bar{\psi} i \overleftarrow{\partial}^{\alpha_1} \dots i \overleftarrow{\partial}^{\alpha_n} \psi i \partial^{\beta_1} \dots i \partial^{\beta_l} A_\rho | P \rangle. \quad (1.10)$$

The derivatives $i \overleftarrow{\partial}^{\alpha}$ act only upon the quark operators.

The two-gluon amplitude can be written as

$$T_2^{\mu_1\mu_2\mu_3} = \int \frac{d^4k}{(2\pi)^4} \frac{d^4k'}{(2\pi)^4} \frac{d^4k''}{(2\pi)^4} \text{Tr} \left[M^{\rho\rho'}(k, k', k'') H_\rho^{\mu_1\mu_2\mu_3} \rho'(k, k', k'') \right]. \quad (1.11)$$

In this case one needs to keep only the first term in the expansion around $k = k' = k'' = 0$.

The various terms in the expansions above can be combined together by using the Ward identity, i.e,

$$\frac{\partial}{\partial p^\alpha} S_F(p) = -S_F(p) \gamma^\alpha S_F(p). \quad (1.12)$$

This gives rise to many useful relations. For example,

$$V^{\mu_1\mu_2\mu_3\rho} = -g U^{\mu_1\mu_2\mu_3\rho} \quad (1.13)$$

allows us to combine the $n = 1$ term in the Eq. 4 and the $n = l = 0$ term in Eq. 9 into gauge invariant sum containing $\langle 0 | \bar{\psi} i \overleftarrow{D}^{\alpha} \psi | P \rangle$, where $i \overleftarrow{D}^{\alpha} = \frac{1}{2} \left(i \overleftarrow{\partial}^{\alpha} - i \overrightarrow{\partial}^{\alpha} \right) - ig A^\alpha$. Similarly the leading order term in the hard two-gluon amplitude is just the second order term in the zero-gluon amplitude, etc. Also note that the $n = 0, l = 1$ term in Eq. 9 gives the abelian part of the field strength tensor whereas the gluon self interaction diagrams give rise to the non-abelian part, $ig[A_\alpha, A_\beta]$, thereby forming the complete non-abelian field strength tensor $F_{\alpha\beta}$.

Appendix 2

Matrix elements for 1^{--}

Any 4×4 matrix can be expanded in terms of 16 Dirac matrices. For the 1^{--} state the most general decomposition of the matrix element $\langle 0 | \bar{\psi}(-x) \psi(x) | P, \epsilon \rangle$ can be written as

$$\langle 0 | \bar{\psi}_i(-x) \psi_j(x) | P, \epsilon \rangle = a \mathbf{1}_{ji} + b_\mu \gamma_{ji}^\mu + c_\mu (\gamma^\mu \gamma_5)_{ji} + d_{\mu\nu} (\sigma^{\mu\nu})_{ji} + e (\gamma_5)_{ji}. \quad (2.1)$$

The numbers a, b_μ, \dots, e can be projected out from the above equation.

$$a = \frac{1}{4} \langle 0 | \bar{\psi}(-x) \psi(x) | P, \epsilon \rangle, \quad (2.2)$$

$$b_\mu = \frac{1}{4} \langle 0 | \bar{\psi}(-x) \gamma_\mu \psi(x) | P, \epsilon \rangle, \quad (2.3)$$

$$c_\mu = \frac{1}{4} \langle 0 | \bar{\psi}(-x) \gamma_5 \gamma_\mu \psi(x) | P, \epsilon \rangle, \quad (2.4)$$

$$d_{\mu\nu} = \frac{1}{8} \langle 0 | \bar{\psi}(-x) \sigma_{\mu\nu} \psi(x) | P, \epsilon \rangle, \quad (2.5)$$

$$e = \frac{1}{4} \langle 0 | \bar{\psi}(-x) \gamma_5 \psi(x) | P, \epsilon \rangle. \quad (2.6)$$

From Lorentz invariance, each entry listed above can be a function of only three vector quantities, x^α, P^α and ϵ^α . I shall keep terms of $O(x^2)$ because only matrix elements with at most two derivatives are needed.

Lorentz invariance restricts a to be

$$a(M^2, P \cdot x, x^2, x \cdot \epsilon) = a_0 + a_1 P \cdot x + a_2 \epsilon \cdot x + a_3 x^2 + a_4 P \cdot x \epsilon \cdot x + a_5 (P \cdot x)^2 + a_6 (\epsilon \cdot x)^2 \quad (2.7)$$

To reduce the number of free parameters even further I shall use \mathcal{C} and \mathcal{P} invariance.

$$\begin{aligned}\mathcal{C}|P, \epsilon\rangle &= -|P, \epsilon\rangle, \\ \mathcal{P}|P, \epsilon\rangle &= +|\tilde{P}, \tilde{\epsilon}\rangle,\end{aligned}\tag{2.8}$$

Also

$$\begin{aligned}\mathcal{C}\bar{\psi}(-x/2)\mathcal{C}^{-1} &= \psi^T(-x/2)C, \\ \mathcal{C}\psi(x/2)\mathcal{C}^{-1} &= C\bar{\psi}^T(x/2), \\ \mathcal{P}\bar{\psi}(-x/2)\mathcal{P}^{-1} &= \bar{\psi}(-\tilde{x}/2)\gamma_0, \\ \mathcal{P}\psi(x/2)\mathcal{P}^{-1} &= \gamma_0\psi(\tilde{x}/2),\end{aligned}\tag{2.9}$$

where C is the charge conjugation operator, $C = i\gamma^2\gamma^0$, such that

$$C^T C = C^{-1} C = C^\dagger C = -C^2 = 1.\tag{2.10}$$

Therefore $C\gamma_\mu C = \gamma^T$. It is now straightforward to see that due to \mathcal{C} invariance $a_0 = a_3 = a_4 = a_5 = a_6 = 0$, whereas \mathcal{P} invariance does not restrict the number of free parameters. This leaves us with two unknowns such that $a = a_1 P \cdot x + a_2 \epsilon \cdot x$. Similarly I can write

$$b_\mu = b_1 x_\mu + b_2 P_\mu + b_3 \epsilon_\mu + b_4 \epsilon_{\mu\nu\alpha\beta} x^\nu P^\alpha \epsilon^\beta.\tag{2.11}$$

where the constants b_i can once again be written in terms of the scalars used for the calculation of a . Similar techniques give answer for one and two derivative matrix elements :

$$\begin{aligned}\langle 0|\bar{\psi}(-x/2)\psi(x/2)|P, \epsilon\rangle &= a_1 \not{x} + a_2 \not{P} \not{x}, \\ \langle 0|\bar{\psi}(-x/2)i \vec{\partial}_\alpha \psi(x/2)|P, \epsilon\rangle &= c\epsilon^\beta \left[-g_{\alpha\beta} + i\epsilon_{\mu\nu\alpha\beta} \frac{P^\nu}{M} \gamma^\mu \gamma^5 \right], \\ \langle 0|\bar{\psi}(-x/2)i \vec{\partial}_\alpha i \vec{\partial}_\beta \psi(x/2)|P, \epsilon\rangle &= d_{\alpha\beta} \left[\not{x} + \frac{1}{M} \not{P} \not{x} \right],\end{aligned}\tag{2.12}$$

Let us now write the matrix element with all the indices explicitly shown,

$$\langle 0 | \bar{\psi}_i(-x/2) \psi_j(x/2) | P, \epsilon \rangle |_{x=0} = b_1 \epsilon_\mu (\gamma^\mu)_{ji} + b_2 P_\mu \epsilon_\nu (\gamma^\mu \gamma^\nu)_{ji} \quad (3.3)$$

On taking the hermitian conjugate,

$$\langle P, \epsilon | \psi_j^\dagger(x/2) (\bar{\psi}_i(-x/2))^\dagger | 0 \rangle |_{x=0} = b_1 \epsilon_\mu^* (\gamma^\mu)_{ji}^* + b_2 P_\mu \epsilon_\nu^* (\gamma^\mu \gamma^\nu)_{ji}^* \quad (3.4)$$

Now

$$\begin{aligned} \bar{\psi}_i(-x/2) &= \psi_k^\dagger(-x/2) (\gamma^0)_{ki}, \\ (\bar{\psi}_i(-x/2))^\dagger &= (\gamma^0)_{ki}^* \psi_k(-x/2), \end{aligned} \quad (3.5)$$

Therefore I can write

$$\langle P, \epsilon | \psi_j^\dagger(x/2) (\gamma^0)_{ki}^* \psi_k(-x/2) | 0 \rangle |_{x=0} = b_1 \epsilon_\mu^* (\gamma^\mu)_{ji}^* + b_2 P_\mu \epsilon_\nu^* (\gamma^\mu \gamma^\nu)_{ji}^* \quad (3.6)$$

Next I use the following identities

$$(\gamma^0)^\dagger = \gamma^0 \Rightarrow ((\gamma^0)^\dagger)_{ik} = (\gamma^0)_{ik} \Rightarrow (\gamma^0)_{ki}^* = (\gamma^0)_{ik} \quad (3.7)$$

$$(\gamma^{\mu\dagger})_{ij} = (\gamma^0 \gamma^\mu \gamma^0)_{ij} \Rightarrow (\gamma^{\mu*})_{ji} = (\gamma^0)_{ik} (\gamma^\mu \gamma^0)_{kj} \quad (3.8)$$

$$((\gamma^\mu \gamma^\nu)^\dagger)_{ij} = \gamma^{\nu\dagger} \gamma^{\mu\dagger} = (\gamma^0 \gamma^\nu \gamma^0 \gamma^\mu \gamma^0)_{ij} \Rightarrow (\gamma^\mu \gamma^\nu)_{ji}^* = (\gamma^0)_{ik} (\gamma^\nu \gamma^\mu \gamma^0)_{kj} \quad (3.9)$$

Using these identities, cancelling γ_{ik}^0 from both sides and multiplying with γ_{jl}^0 one arrives at

$$\langle P, \epsilon | \bar{\psi}(x/2) \psi(-x/2) | 0 \rangle |_{x=0} = b_1 \not{\epsilon} + b_2 \not{\epsilon} \not{P}. \quad (3.10)$$

In a similar fashion I derive the following

$$\begin{aligned} \langle P, \epsilon | \bar{\psi}(x/2) i \overleftrightarrow{\partial}_\alpha \psi(-x/2) | 0 \rangle |_{x=0} &= \epsilon^{\beta\gamma} \left[-g_{\alpha\beta} - i \epsilon_{\mu\nu\alpha\beta} \frac{P^\nu}{M} \gamma^\mu \gamma^5 \right], \\ \langle P, \epsilon | \bar{\psi}(x/2) i \overleftrightarrow{\partial}_\alpha i \overleftrightarrow{\partial}_\beta \psi(-x/2) | P, \epsilon \rangle |_{x=0} &= d_{\alpha\beta} \left[\not{\epsilon} + \frac{1}{M} \not{\epsilon} \not{P} \right]. \end{aligned} \quad (3.11)$$

Notice that the above is still not in the right form. What I need is

$$I_1 = \int \frac{d^4 k}{(2\pi)^4} M(k) = \int \frac{d^4 k}{(2\pi)^4} d^4 x e^{ik \cdot x} \langle P | \psi(x/2) \bar{\psi}(-x/2) | 0 \rangle \quad (3.12)$$

Now use the anticommutation relation

$$\{\psi(x), \bar{\psi}(y)\} = \gamma^0 \delta(\vec{x} - \vec{y}) \quad (3.13)$$

to get

$$I_1 = - \int \frac{d^4 k}{(2\pi)^4} M(k) = \int \frac{d^4 k}{(2\pi)^4} d^4 x e^{ik \cdot x} \langle P | \bar{\psi}(-x/2) \psi(x/2) | 0 \rangle, \quad (3.14)$$

where I have used the fact that $\langle P | 0 \rangle = 0$. Now change $x \rightarrow -x$ and $k \rightarrow -k$.

$$I_1 = - \int \frac{d^4 k}{(2\pi)^4} M(k) = \int \frac{d^4 k}{(2\pi)^4} d^4 x e^{ik \cdot x} \langle P | \bar{\psi}(x/2) \psi(-x/2) | 0 \rangle, \quad (3.15)$$

Therefore one can write

$$\begin{aligned} M(0) &= -b_1 \not{\epsilon} - b_2 \not{\epsilon} \not{P} \\ M_\alpha(0) &= c \epsilon^{\beta\gamma} \left[-g_{\alpha\beta} - i \epsilon_{\mu\nu\alpha\beta} \frac{P^\nu}{M} \gamma^\mu \gamma^5 \right] \\ M_{\alpha\beta}(0) &= -\frac{1}{2!} d_{\alpha\beta} \left[\not{\epsilon} + \not{\epsilon} \frac{\not{P}}{M} \right] \end{aligned} \quad (3.16)$$

Appendix 4

Mathematica programs

The three attached programs calculate different quantities for Υ decay and charm quark fragmentation.

- Program 1. Calculates the amplitude for a J/ψ to decay into three photons. Zero derivative + binding energy corrections are calculated.
- Program 2. Takes the no-differentiation amplitude for the Υ decay, dissects it, calculates the squared amplitude, and then calculates the decay rate.
- Program 3. It calculates the interference term and the decay rate.
- Program 4. This program calculates the leading order η_c fragmentation function together with the wave function corrections.

Program 1.

```

Needs["Hip`Work`"];
PrepareIndex[alf, bet, gam, del, rho, mu, nu, m1, m2, m3];
SetDotProduct[{K, K, M^2}]
m=M/2 + eps/2;
Mat1= a ((1+S1[K]/M)**Dg[alf]+Dg[alf]**(1-S1[K]/M))/2 +
      b ((1-S1[K]/M)**Dg[alf]+Dg[alf]**(1+S1[K]/M))/2 ;
Mat2 = ( (1+S1[K]/M)**Dg[alf] + Dg[alf]**(1-S1[K]/M) )/2;
SF[p_]:= (S1[p]+m)/(DP[p,p]-m^2)
a0=(1/2)*Q^3*Sqrt[M]*Psi;
a1=(1/2)*Q^3*Sqrt[M]*Dpsi;
a2=(1/2)*Q^3*Sqrt[M]*Psi*eps;
a = a0 + a1;
b = (-1/2)* Q^3*Sqrt[M]*Dpsi/3;
a3=(1/6)*Q^3*Sqrt[M]*M^2*Dpsi;
SetDotProduct[{s1, s1, -M*w1+M^2/4}, {s2, s2, -M*w2+M^2/4},
              {s3, s3, -M*w3+M^2/4}]
Expand[Mat1**Dg[m2]**SF[s2]**Dg[m1]**SF[-s3]**Dg[m3] ];
ta=Expand[Tr[%]];
Expand[Mat1**Dg[m1]**SF[s1]**Dg[m2]**SF[-s3]**Dg[m3] ];
tb=Expand[Tr[%]];
Expand[Mat1**Dg[m1]**SF[s1]**Dg[m3]**SF[-s2]**Dg[m2] ];
tc=Expand[Tr[%]];
q1q2=DP[q1, q2];
q1q3=DP[q1, q3];
q2q3=DP[q2, q3];
SetDotProduct[{s1, s2, q1q2/2}, {s1, s3, q1q3/2}, {s2, s3, q2q3/2},
              {s1, K, M*w1-M^2/2}, {s2, K, M*w2-M^2/2}, {s3, K, M*w3-M^2/2}]
K=q1+q2+q3;
s1=q1-K/2;
s2=q2-K/2;
s3=q3-K/2;
tabc=Expand[2*(ta+tb+tc)]; (* "2" accounts for crossed diagrams *)
%/.eps->0;
TA=Expand[%]>>c:\wnmath22\packages\ali\jpsideca\TAa;
D[tabc, eps];
%/.eps->0;
TD=Expand[%]>>c:\wnmath22\packages\ali\jpsideca\TDa;
(* THIS PART OF THE PROGRAM CALCULATES THE NEXT TO LEADING ORDER
AMPLITUDE FOR UPSILON TO DECAY INTO 3 PHOTONS WHICH COMES FROM
DIFFERENTIATING EACH PROPAGATOR TWICE. *)
Clear[q1, q2, q3, s1, s2, s3, tabc, K]
Sig[mu_, nu_]:= (I/2)* ( Dg[mu]**Dg[nu]-Dg[nu]**Dg[mu] )
Acoeff[H_]:= (1/4)*Tr[H]
Bcoeff[H_]:= (1/4)*Tr[H**Dg5]
Ccoeff[H_, mu_]:= (1/4)*Tr[H**Dg[mu]]
Dcoeff[H_, mu_]:= (1/4)*Tr[H**Dg[mu]**Dg5]
Ecoeff[H_, mu_, nu_]:= (1/8)*Tr[H**Sig[mu, nu]]
HH[H_]:=Simplify[Contract[ Acoeff[H]+Dg5*Bcoeff[H]+Ccoeff[H, mu]*Dg[mu]+
  Dcoeff[H, mu]*Dg5**Dg[mu]+Ecoeff[H, mu, nu]*Sig[mu, nu], {mu, nu} ]
(* HH[M] takes an arbitrary 4x4 matrix and breaks it up
into 16 gamma matrices. This helps simplify traces. *)
SetDotProduct[{K, K, M^2}]
eps=0;
DD=Together{ G{gam, del}-K{gam}*K{del}/M^2 };
SF[p_]:= (S1[p]+m)/(DP[p,p]-m^2)
D1[p_, alf_]:= -SF[p]**Dg[alf]**SF[p]
D2[p_, alf_, bet_]:= SF[p]**Dg[bet]**SF[p]**Dg[alf]**SF[p] +
  SF[p]**Dg[alf]**SF[p]**Dg[bet]**SF[p]
DF1[p_, rho_]:= HH[D1[p, rho]]

```



```

DF2[p_, rho_, lam_] := HH[D2[p, rho, lam]]
SetDotProduct[{s1, s1, -M*w1+M^2/4}, {s2, s2, -M*w2+M^2/4},
               {s3, s3, -M*w3+M^2/4}]

dd1=DF1[s1, gam];
dd2=DF1[s2, gam];
dd3=DF1[-s2, del];
dd4=DF1[-s3, del];
HH[dd2**Dg[m1]**dd4];
X1=Expand[Contract[8*DD, {gam, del}]];
HH[dd1**Dg[m2]**dd4];
Y1=Expand[Contract[8*DD, {gam, del}]];
HH[dd1**Dg[m3]**dd3];
Z1=Expand[Contract[8*DD, {gam, del}]];

dd1=DF2[s1, gam, del];
dd2=DF2[s2, gam, del];
dd3=DF2[-s3, gam, del];
dd4=DF2[-s2, gam, del];
R1=Expand[Contract[(1/2)*dd2*DD, {gam, del}]];
R2=Expand[Contract[(1/2)*dd3*DD, {gam, del}]];
S1=Expand[Contract[(1/2)*dd1*DD, {gam, del}]];
S2=Expand[Contract[(1/2)*dd3*DD, {gam, del}]];
T1=Expand[Contract[(1/2)*dd1*DD, {gam, del}]];
T2=Expand[Contract[(1/2)*dd4*DD, {gam, del}]];

Expand[Mat2**Dg[m2]**R1**Dg[m1]**SF[-s3]**Dg[m3] ];
ta1=Expand[Tr[%]];
Expand[Mat2**Dg[m2]**SF[s2]**Dg[m1]**R2**Dg[m3] ];
ta2=Expand[Tr[%]];
Expand[Mat2**Dg[m2]**X1**Dg[m3] ];
Expand[Tr[%]];
Contract[%, mu];
ta3=Expand[%];
ta=Expand[ta1+ta2+ta3];

Expand[Mat2**Dg[m1]**S1**Dg[m2]**SF[-s3]**Dg[m3] ];
tb1=Expand[Tr[%]];
Expand[Mat2**Dg[m1]**SF[s1]**Dg[m2]**S2**Dg[m3] ];
tb2=Expand[Tr[%]];
Expand[Mat2**Dg[m1]**Y1**Dg[m3] ];
Expand[Tr[%]];
Contract[%, mu];
tb3=Expand[%];
tb=Expand[tb1+tb2+tb3];

Expand[Mat2**Dg[m1]**T1**Dg[m3]**SF[-s2]**Dg[m2] ];
tc1=Expand[Tr[%]];
Expand[Mat2**Dg[m1]**SF[s1]**Dg[m3]**T2**Dg[m2] ];
tc2=Expand[Tr[%]];
Expand[Mat2**Dg[m1]**Z1**Dg[m2] ];
Expand[Tr[%]];
Contract[%, mu];
tc3=Expand[%];
tc=Expand[tc1+tc2+tc3];

q1q2=DP[q1, q2];
q1q3=DP[q1, q3];
q2q3=DP[q2, q3];
SetDotProduct[{s1, s2, q1q2/2}, {s1, s3, q1q3/2}, {s2, s3, q2q3/2},
               {s1, K, M*w1-M^2/2}, {s2, K, M*w2-M^2/2}, {s3, K, M*w3-M^2/2}]
tabc=Expand[2*(ta+tb+tc)]; (* "2" accounts for crossed diagrams *)

K=q1+q2+q3;
s1=q1-K/2;
s2=q2-K/2;
s3=q3-K/2;
Expand[tabc];
TC=Expand[Together[%]]>>c:\wnmath22\packages\ali\jpsideca\TCa;

```

Program 2.

```
Needs["Hip`Work`"];

(* AmpAD is the leading order J/psi->3 gamma amplitude.*)
AmpAD=b1*G[alf,m1]*G[m2,m3]+b2*G[alf,m2]*G[m1,m3]+b3*G[alf,m3]*G[m1,m2]+
G[alf,m1]*( X1213*q1[m2]*q1[m3] + X1223*q1[m2]*q2[m3] +
X1332*q1[m3]*q3[m2] + X1322*q1[m3]*q2[m2] +
X2223*q2[m2]*q2[m3] + X1233*q1[m2]*q3[m3] +
X3233*q3[m2]*q3[m3] ) +
G[alf,m2]*( X1321*q1[m3]*q2[m1] + X2123*q2[m1]*q2[m3] +
X2331*q2[m3]*q3[m1] + X1113*q1[m1]*q1[m3] +
X3133*q3[m1]*q3[m3] + X1123*q1[m1]*q2[m3] +
X2133*q2[m1]*q3[m3] ) +
G[alf,m3]*( X1231*q1[m2]*q3[m1] + X2132*q2[m1]*q3[m2] +
X3132*q3[m1]*q3[m2] + X1112*q1[m1]*q1[m2] +
X2122*q2[m1]*q2[m2] + X2231*q2[m2]*q3[m1] +
X1132*q1[m1]*q3[m2] ) +
G[m1,m2]*( X1a13*q1[alf]*q1[m3] + X1a23*q1[alf]*q2[m3] +
X132a*q1[m3]*q2[alf] + X2a23*q2[alf]*q2[m3] +
X133a*q1[m3]*q3[alf] + X233a*q2[m3]*q3[alf] +
X1a33*q1[alf]*q3[m3] + X3a33*q3[alf]*q3[m3] +
X2a33*q2[alf]*q3[m3] ) +
G[m1,m3]*( X1a12*q1[alf]*q1[m2] + X122a*q1[m2]*q2[alf] +
X123a*q1[m2]*q3[alf] + X1a32*q1[alf]*q3[m2] +
X2a32*q2[alf]*q3[m2] + X3a32*q3[alf]*q3[m2] +
X1a22*q1[alf]*q2[m2] + X2a22*q2[alf]*q2[m2] +
X223a*q2[m2]*q3[alf] ) +
G[m2,m3]*( X1a21*q1[alf]*q2[m1] + X2a21*q2[alf]*q2[m1] +
X213a*q2[m1]*q3[alf] + X1a31*q1[alf]*q3[m1] +
X2a31*q2[alf]*q3[m1] + X3a31*q3[alf]*q3[m1] +
X1a11*q1[alf]*q1[m1] + X112a*q1[m1]*q2[alf] +
X113a*q1[m1]*q3[alf] );

(* Now square it and perform pol sums: *)
AsqAD=Expand[Contract[AmpAD*AmpAD,{alf,m1,m2,m3}]]>>
C:\wnmath22\packages\ali\error\AsqAD.ma;
Expand[Contract[AmpAD*K[alf],alf]];
ApsqAD=Expand[Contract[%%,{m1,m2,m3}]]>>
C:\wnmath22\packages\ali\error\ApsqAD.ma;

SDP[{q1,q1,0},{q2,q2,0},{q3,q3,0}]
TA-<<C:\wnmath22\packages\ali\error\TA.ma;
TD-<<C:\wnmath22\packages\ali\error\TD.ma;
Expand[TA+eps*TD];
T=Expand[%];
Coefficient[T,G[alf,m1]*G[m2,m3]];
b1=Simplify[%];
Coefficient[T,G[alf,m2]*G[m1,m3]];
b2=Simplify[%];
Coefficient[T,G[alf,m3]*G[m1,m2]];
b3=Simplify[%];
X=Expand[T-b1*G[alf,m1]*G[m2,m3]-b2*G[alf,m2]*G[m1,m3]-
b3*G[alf,m3]*G[m1,m2]];
Y1=Coefficient[X,G[alf,m1]];
X1213=Simplify[Coefficient[Y1,q1[m2]*q1[m3]]];
X1223=Simplify[Coefficient[Y1,q1[m2]*q2[m3]]];
X1332=Simplify[Coefficient[Y1,q1[m3]*q3[m2]]];
X1322=Simplify[Coefficient[Y1,q1[m3]*q2[m2]]];
X2223=Simplify[Coefficient[Y1,q2[m2]*q2[m3]]];
X1233=Simplify[Coefficient[Y1,q1[m2]*q3[m3]]];
X3233=Simplify[Coefficient[Y1,q3[m2]*q3[m3]]];
Y2=Coefficient[X,G[alf,m2]];
X1321=Simplify[Coefficient[Y2,q1[m3]*q2[m1]]];
```

```

X2123=Simplify[Coefficient[Y2,q2[m1]*q2[m3]]];
X2331=Simplify[Coefficient[Y2,q2[m3]*q3[m1]]];
X1113=Simplify[Coefficient[Y2,q1[m1]*q1[m3]]];
X3133=Simplify[Coefficient[Y2,q3[m1]*q3[m3]]];
X1123=Simplify[Coefficient[Y2,q1[m1]*q2[m3]]];
X2133=Simplify[Coefficient[Y2,q2[m1]*q3[m3]]];
Y3=Coefficient[X,G[alf,m3]];
X1231=Simplify[Coefficient[Y3,q1[m2]*q3[m1]]];
X2132=Simplify[Coefficient[Y3,q2[m1]*q3[m2]]];
X3132=Simplify[Coefficient[Y3,q3[m1]*q3[m2]]];
X1112=Simplify[Coefficient[Y3,q1[m1]*q1[m2]]];
X2122=Simplify[Coefficient[Y3,q2[m1]*q2[m2]]];
X2231=Simplify[Coefficient[Y3,q2[m2]*q3[m1]]];
X1132=Simplify[Coefficient[Y3,q1[m1]*q3[m2]]];
Y4=Coefficient[X,G[m1,m2]];
X1a13=Simplify[Coefficient[Y4,q1[alf]*q1[m3]]];
X1a23=Simplify[Coefficient[Y4,q1[alf]*q2[m3]]];
X132a=Simplify[Coefficient[Y4,q1[m3]*q2[alf]]];
X2a23=Simplify[Coefficient[Y4,q2[alf]*q2[m3]]];
X133a=Simplify[Coefficient[Y4,q1[m3]*q3[alf]]];
X233a=Simplify[Coefficient[Y4,q2[m3]*q3[alf]]];
X1a33=Simplify[Coefficient[Y4,q1[alf]*q3[m3]]];
X3a33=Simplify[Coefficient[Y4,q3[alf]*q3[m3]]];
X2a33=Simplify[Coefficient[Y4,q2[alf]*q3[m3]]];
Y5=Coefficient[X,G[m1,m3]];
H1a12=SimplifySCoefficient[Y5,q1[alf]*q1[m2]]];
X122a=Simplify[Coefficient[Y5,q1[m2]*q2[alf]]];
X123a=Simplify[Coefficient[Y5,q1[m2]*q3[alf]]];
X1a32=Simplify[Coefficient[Y5,q1[alf]*q3[m2]]];
X2a32=Simplify[Coefficient[Y5,q2[alf]*q3[m2]]];
X3a32=Simplify[Coefficient[Y5,q3[alf]*q3[m2]]];
X1a22=Simplify[Coefficient[Y5,q1[alf]*q2[m2]]];
X2a22=Simplify[Coefficient[Y5,q2[alf]*q2[m2]]];
X223a=Simplify[Coefficient[Y5,q2[m2]*q3[alf]]];
Y6=Coefficient[X,G[m2,m3]];
X1a21=Simplify[Coefficient[Y6,q1[alf]*q2[m1]]];
X2a21=Simplify[Coefficient[Y6,q2[alf]*q2[m1]]];
X213a=Simplify[Coefficient[Y6,q2[m1]*q3[alf]]];
X1a31=Simplify[Coefficient[Y6,q1[alf]*q3[m1]]];
X2a31=Simplify[Coefficient[Y6,q2[alf]*q3[m1]]];
X3a31=Simplify[Coefficient[Y6,q3[alf]*q3[m1]]];
X1a11=Simplify[Coefficient[Y6,q1[alf]*q1[m1]]];
X112a=Simplify[Coefficient[Y6,q1[m1]*q2[alf]]];
X113a=Simplify[Coefficient[Y6,q1[m1]*q3[alf]]];

```

```

b1*G[alf,m1]*G[m2,m3]+b2*G[alf,m2]*G[m1,m3]+b3*G[alf,m3]*G[m1,m2]+
G[alf,m1]*( X1213*q1[m2]*q1[m3] + X1223*q1[m2]*q2[m3] +
X1332*q1[m3]*q3[m2] + X1322*q1[m3]*q2[m2] +
X2223*q2[m2]*q2[m3] + X1233*q1[m2]*q3[m3] +
X3233*q3[m2]*q3[m3] ) +
G[alf,m2]*( X1321*q1[m3]*q2[m1] + X2123*q2[m1]*q2[m3] +
X2331*q2[m3]*q3[m1] + X1113*q1[m1]*q1[m3] +
X3133*q3[m1]*q3[m3] + X1123*q1[m1]*q2[m3] +
X2133*q2[m1]*q3[m3] ) +
G[alf,m3]*( X1231*q1[m2]*q3[m1] + X2132*q2[m1]*q3[m2] +
X3132*q3[m1]*q3[m2] + X1112*q1[m1]*q1[m2] +
X2122*q2[m1]*q2[m2] + X2231*q2[m2]*q3[m1] +
X1132*q1[m1]*q3[m2] ) +
G[m1,m2]*( X1a13*q1[alf]*q1[m3] + X1a23*q1[alf]*q2[m3] +
X132a*q1[m3]*q2[alf] + X2a23*q2[alf]*q2[m3] +
X133a*q1[m3]*q3[alf] + X233a*q2[m3]*q3[alf] +
X1a33*q1[alf]*q3[m3] + X3a33*q3[alf]*q3[m3] +
X2a33*q2[alf]*q3[m3] ) +
G[m1,m3]*( X1a12*q1[alf]*q1[m2] + X122a*q1[m2]*q2[alf] +
X123a*q1[m2]*q3[alf] + X1a32*q1[alf]*q3[m2] +
X2a32*q2[alf]*q3[m2] + X3a32*q3[alf]*q3[m2] +
X1a22*q1[alf]*q2[m2] + X2a22*q2[alf]*q2[m2] +
X223a*q2[m2]*q3[alf] ) +
G[m2,m3]*( X1a21*q1[alf]*q2[m1] + X2a21*q2[alf]*q2[m1] +
X213a*q2[m1]*q3[alf] + X1a31*q1[alf]*q3[m1] +
X2a31*q2[alf]*q3[m1] + X3a31*q3[alf]*q3[m1] +
X1a11*q1[alf]*q1[m1] + X112a*q1[m1]*q2[alf] +
X113a*q1[m1]*q3[alf] );

```

```
X=Expand[%];
```

```
(* Have all terms been taken into account? If so the difference
between the above and T should be zero. *)
```

```
Expand[X-T]
```

```
0
```

```
AsqAD=<<<c:\wnmath22\AsqAD;
```

```
ApsqAD=<<<c:\wnmath22\ApsqAD;
```

```
Clear[w1,w2,w3,q1,q2,q3,s1,s2,s3]
```

```
SetDotProduct[{q1,q1,0},{q2,q2,0},{q3,q3,0},{K,K,M^2},
{K,q1,M*w1},{K,q2,M*w2},{K,q3,M*w3}]
```

```
s1=Expand[AsqAD];
```

```
s2=Expand[Cancel[ApsqAD/M^2]];
Expand[{s1-s2}];
```

```
Expand[%];
```

```
%/.eps^2->0;
```

```
XX=Expand[%];
```

```
XX0=Expand[XX/.eps->0]>>c:\wnmath22\packages\ali\error\XX0.ma;
```

```
XX1=Expand[D[XX,eps]]>>c:\wnmath22\packages\ali\error\XX1.ma;
```

```
XX0 = <<<c:\wnmath22\packages\ali\error\XX0.ma;
```

```
XX1 = <<<c:\wnmath22\packages\ali\error\XX1.ma;
```

```
a = a0+a1;
```

```
SetDotProduct[{q1,q2,q1q2},{q1,q3,q1q3},{q2,q3,q2q3}]
```

```
q1q2=( (w1+w2)^2 - w3^2 )/2;
```

```
q1q3=( (w1+w3)^2 - w2^2 )/2;
```

```
q2q3=( (w2+w3)^2 - w1^2 )/2;
```

```
w1=M*x1/2;
```

```
w2=M*x2/2;
```

```
w3=M-w1-w2;
```

```
x3=2-x1-x2;
```

```
Expand[XX0];
```

```
XX0=Expand[%*(1/3)*(1/6)]/. {a1^2->0,b^2->0,a1*b->0,b*a1->0};
```

```
x1=1-s/M^2;
```

```

x2=1-t/M^2;
x3=1-u/M^2;
a0=(1/2)*Q^3*Sqrt[M]*Psi;
a1=(1/2)*Q^3*Sqrt[M]*Dpsi;
a2=(1/2)*Q^3*Sqrt[M]*Psi*eps;
b = (-1/2)* Q^3*Sqrt[M]*Dpsi/3;
a3=(1/6)*Q^3*Sqrt[M]*M^2*Dpsi;
AAA=Together[Expand[XX0]]>>C:\wnmath22\packages\ali\error\AAA.ma

```

```
Clear[a, a0, a1, a2, b, a3];
```

```
a=a1+a0;
```

```
Expand[XX1];
```

```
XX1=Expand[?(1/3)*(1/6)]/.{a1->0,b->0};
```

```
XX1=Expand[?(2*a2/a0)];
```

```
a0=(1/2)*Q^3*Sqrt[M]*Psi;
```

```
a1=(1/2)*Q^3*Sqrt[M]*Dpsi;
```

```
a2=(1/2)*Q^3*Sqrt[M]*Psi*eps;
```

```
b = (-1/2)* Q^3*Sqrt[M]*Dpsi/3;
```

```
a3=(1/6)*Q^3*Sqrt[M]*M^2*Dpsi;
```

```
AAD=Together[XX1]>>C:\wnmath22\packages\ali\error\AAD.ma
```

```
Clear[x1,x2,x3,s,t,u,M]
```

```
AAA=<<C:\wnmath22\packages\ali\error\AAA.ma;
```

```
AAD=<<C:\wnmath22\packages\ali\error\AAD.ma;
```

```
K1=Factor[Expand[AAA /. {Dpsi->0,eps->0,M->Sqrt[s+t+u]}]]
```

$$\begin{aligned}
& (512 \text{ Psi } Q^6 \text{ Sqrt}[s + t + u]) \\
& \left((s^2 t^2 + s^2 t u + s^2 t^2 u + s^2 u^2 + s t^2 u + t^2 u^2) \right) \\
& / \left(9 (s + t)^2 (s + u)^2 (t + u)^2 \right)
\end{aligned}$$

```
K2=Factor[Expand[D[AAA,Dpsi]/. {Dpsi->0,eps->0,M->Sqrt[s+t+u]}]]
```

$$\begin{aligned}
& (512 \text{ Psi } Q^6 \text{ Sqrt}[s + t + u]) \\
& \left((-3 s^3 t^2 + s^2 t^2 - 3 s^3 t - 3 s^3 u - 7 s^2 t u - \right. \\
& \left. 7 s^2 t u - 3 t^3 u + s^2 u^2 - 7 s t^2 u + t^2 u^2 - \right. \\
& \left. 3 s^3 u - 3 t^3 u) \right) / \\
& \left(27 (s + t)^2 (s + u)^2 (t + u)^2 \right)
\end{aligned}$$

K3=Factor[Expand[D[AAD,eps]/. {Dpsi->0,eps->0,M->Sqrt[s+t+u]}]]

$$\begin{aligned}
 & (256 \text{Psi}^2 \text{Q}^6 (-(s^5 t^2) - 7 s^4 t^3 - 7 s^3 t^4 - s^2 t^5 + \\
 & 6 s^5 t u - s^4 t^2 u - 22 s^3 t^3 u - s^2 t^4 u + \\
 & 6 s^5 t u - s^5 t^2 u - s^4 t^2 u - 30 s^3 t^2 u - \\
 & 30 s^2 t^3 u - s^4 t^2 u - t^5 u - 7 s^4 u - \\
 & 22 s^3 t u - 30 s^2 t^2 u - 22 s t^3 u - \\
 & 7 t^4 u - 7 s^3 u - s^2 t u - s t^2 u - \\
 & 7 t^3 u - s^2 u + 6 s t u - t^2 u)) / \\
 & (9 (s+t)^3 (s+u)^3 (t+u)^3)
 \end{aligned}$$

(* The above:

(1) Has been divided by 3 for Jpsi pol. states.

(2) Has been divided by 6 for 3 identical photons.

(3) Has been multiplied by Q^6*M/4*psi(0)^2 . *)

(* Now get decay rate by dividing by the flux factor,
multiplying by Dlips, and integrating over x1 and x2. *)

Dlips=M^2/(128*Pi^3);

Flux=2*M;

Tot=Expand[(AAA+AAD)*Dlips/Flux];

T2=Factor[Expand[Dpsi*D[Tot,Dpsi]]]

$$\begin{aligned}
 & (2 \text{Dpsi}^2 \text{Psi}^2 \text{Q}^6 (16 - 46 x1 + 51 x1^2 - 28 x1^3 + \\
 & 7 x1^4 - 46 x2 + 91 x1 x2 - 62 x1^2 x2 + \\
 & 14 x1^3 x2 + 51 x2^2 - 62 x1 x2^2 + 21 x1^2 x2^2 - \\
 & 28 x2^3 + 14 x1 x2^3 + 7 x2^4)) / \\
 & (27 M^2 \text{Pi}^3 x1^2 x2^2 (-2 + x1 + x2)^2)
 \end{aligned}$$

```

T3=Factor[Expand[eps*D[Tot,eps]] ]
      2 6      2      3      4
(eps Psi Q (32 x1 - 112 x1 + 160 x1 - 120 x1 +
      5      6
48 x1 - 8 x1 + 32 x2 - 224 x1 x2 +
      2      3      4
472 x1 x2 - 448 x1 x2 + 212 x1 x2 -
      5      6      2      2
48 x1 x2 + 4 x1 x2 - 112 x2 + 472 x1 x2 -
      2 2      3 2      4 2
684 x1 x2 + 436 x1 x2 - 123 x1 x2 +
      5 2      3      3
12 x1 x2 + 160 x2 - 448 x1 x2 +
      2 3      3 3      4 3
436 x1 x2 - 166 x1 x2 + 20 x1 x2 -
      4      4      2 4
120 x2 + 212 x1 x2 - 123 x1 x2 +
      3 4      5      5      2 5
20 x1 x2 + 48 x2 - 48 x1 x2 + 12 x1 x2 -
      6      6
8 x2 + 4 x1 x2 ) ) /
      3 3 3 3      3
(9 M Pi x1 x2 (-2 + x1 + x2) )
T1=Factor[Expand[Tot-T2-T3] ]
      2 6      2      3      4
(2 Psi Q (2 - 6 x1 + 7 x1 - 4 x1 + x1 - 6 x2 +
      2      3      2
13 x1 x2 - 9 x1 x2 + 2 x1 x2 + 7 x2 -
      2      2 2      3      3      4
9 x1 x2 + 3 x1 x2 - 4 x2 + 2 x1 x2 + x2 ) ) \
      2 3 2 2      2
/ (9 M Pi x1 x2 (-2 + x1 + x2) )
d1=Together[Expand[T1*M^2/(Q^6*Psi^2)]];
d2=Together[Expand[T2*M^2/(Q^6*(Dpsi/Psi)*Psi^2)]];
d3=Together[Expand[T3*M^2/(Q^6*(eps/M)*Psi^2)]];
(* D1,D2,D3 are essentially d1,d2,d3 expressed in terms of s,t,u *)
Clear[s,t,u,x1,x2,x3,M]
x1=1-s/M^2;
x2=1-t/M^2;
x3=1-u/M^2;

```

M=Sqrt[s+t+u];

D1 = Together[Expand[d1]]

$$(2 (s^4 t^2 + 2 s^3 t^3 + s^2 t^4 + s^4 t u + 5 s^3 t^2 u + 5 s^2 t^3 u + s^4 t^2 u + s^4 t^2 u + 5 s^3 t^2 u + 9 s^2 t^2 u + 5 s^3 t^2 u + t^4 u + 2 s^3 u + 5 s^2 t u + 5 s^2 t^3 u + 2 t^3 u + s^2 u + s^4 t u + t^2 u)) / (9 \text{Pi} (s+t)^2 (s+u)^2 (t+u)^2)$$

Together[Expand[d1-D1]]

0

D2 = Together[Expand[d2]]

$$(-2 (3 s^5 t + 5 s^4 t^2 + 4 s^3 t^3 + 5 s^2 t^4 + 3 s t^5 + 3 s^5 u + 19 s^4 t u + 28 s^3 t^2 u + 28 s^2 t^3 u + 19 s t^4 u + 3 t^5 u + 5 s^4 u + 28 s^3 t u + 39 s^2 t^2 u + 28 s t^3 u + 5 t^4 u + 4 s^3 u + 28 s^2 t u + 28 s t^2 u + 4 t^3 u + 5 s^2 u + 19 s t u + 5 t^2 u + 3 s u + 3 t u)) / (27 \text{Pi} (s+t)^2 (s+u)^2 (t+u)^2)$$

Together[Expand[d2-D2]]

0

D3 = Together[Expand[d3]]

$$\begin{aligned} & (- (s^7 t^2) - 9 s^6 t^3 - 22 s^5 t^4 - 22 s^4 t^5 - 9 s^3 t^6 - \\ & s^2 t^7 + 6 s^7 t u + 9 s^6 t^2 u - 34 s^5 t^3 u - \\ & 74 s^4 t^4 u - 34 s^3 t^5 u + 9 s^2 t^6 u + 6 s t^7 u - \\ & s^7 u + 9 s^6 t u - 24 s^5 t^2 u - 144 s^4 t^3 u - \\ & 144 s^3 t^4 u - 24 s^2 t^5 u + 9 s t^6 u - t^7 u - \\ & 9 s^6 u - 34 s^5 t u - 144 s^4 t^2 u - \\ & 246 s^3 t^3 u - 144 s^2 t^4 u - 34 s t^5 u - \\ & 9 t^6 u - 22 s^5 u - 74 s^4 t u - 144 s^3 t^2 u - \\ & 144 s^2 t^3 u - 74 s t^4 u - 22 t^5 u - 22 s^4 u - \\ & 34 s^3 t u - 24 s^2 t^2 u - 34 s t^3 u - 22 t^4 u - \\ & 9 s^6 u + 9 s^5 t u + 9 s^4 t^2 u - 9 t^6 u - \\ & s^2 u + 6 s^7 t u - t^7 u) / \end{aligned}$$

$$(9 \text{ Pi}^3 (s+t)^3 (s+u)^3 (t+u)^3)$$

Together[Expand[d2-D2]]

0

Clear[s,t,u,x1,x2,x3,M]

DEN=(s-M^2)^3*(t-M^2)^3*(u-M^2)^3;

D3=(2*M^4/(9*Pi^3))*NUM/(2*DEN);

Clear[s,t,u,x1,x2,x3,M]

Integrate[d1,{x2,1-x1,1}];

spect1=Together[Expand[%]]

integ1=NIntegrate[spect1,{x1,0,1}];

spect1[x1]:=(2*(-16*x1 + 32*x1^2 - 26*x1^3 + 11*x1^4 -
2*x1^5 - 16*Log[1 - x1] + 40*x1*Log[1 - x1] -
34*x1^2*Log[1 - x1] + 10*x1^3*Log[1 - x1]))/
(9*Pi^3*(-2 + x1)^3*x1^2)

```

Integrate[d2, {x2, 1-x1, 1}];
spect2=Together[Expand[#]]
integ2=NIntegrate[spect2, {x1, 0, 1}];
spect2[x1_]:= (2*(-120*x1 + 236*x1^2 - 186*x1^3 +
77*x1^4 - 14*x1^5 - 120*Log[1 - x1] +
272*x1*Log[1 - x1] - 226*x1^2*Log[1 - x1] +
68*x1^3*Log[1 - x1]))/(27*Pi^3*(-2 + x1)^3*x1^2)

```

```

Integrate[d3, {x2, 1-x1, 1}];
spect3=Together[Expand[#]]
integ3=NIntegrate[spect3, {x1, 0, 1}];
spect3[x1_]:= (2*(-128*x1 + 416*x1^2 - 512*x1^3 +
280*x1^4 - 52*x1^5 - 2*x1^6 - 128*Log[1 - x1] +
480*x1*Log[1 - x1] - 712*x1^2*Log[1 - x1] +
548*x1^3*Log[1 - x1] - 238*x1^4*Log[1 - x1] +
51*x1^5*Log[1 - x1]))/(9*Pi^3*(-2 + x1)^4*x1^3)

```

```

x1=1-S;
Simplify[spect1]

```

$$\frac{(2 (1 + 4 S - 2 S^3 - S^4 - 2 S^5 + 2 S \operatorname{Log}[S] + 4 S^2 \operatorname{Log}[S] + 10 S^3 \operatorname{Log}[S]))}{(9 \operatorname{Pi}^3 (-1 + S)^2 (1 + S)^3)}$$

```

Simplify[spect2]

```

$$\frac{(2 (7 + 32 S - 18 S^3 - 7 S^4 - 14 S^5 + 6 \operatorname{Log}[S] + 24 S^2 \operatorname{Log}[S] + 22 S^3 \operatorname{Log}[S] + 68 S^3 \operatorname{Log}[S]))}{(27 \operatorname{Pi}^3 (-1 + S)^2 (1 + S)^3)}$$

```

Simplify[spect3]

```

$$\frac{(2 (2 - 16 S + 10 S^2 - 48 S^3 - 10 S^4 + 64 S^5 - 2 S^6 + \operatorname{Log}[S] - 3 S \operatorname{Log}[S] + 14 S^2 \operatorname{Log}[S] - 106 S^3 \operatorname{Log}[S] + 17 S^4 \operatorname{Log}[S] - 51 S^5 \operatorname{Log}[S]))}{(9 \operatorname{Pi}^3 (-1 - S)^4 (1 - S)^3)}$$

$$\text{WIDTH} = Q^6 \Psi^2 / M^2 * (\text{integ1} + \text{integ2} * (\text{Dpsi} / \Psi) + \text{integ3} * (\text{eps} / M))$$

$$- ((0.00311623 - \frac{0.00642662 \text{ eps}}{M} - \frac{0.0110489 \text{ Dpsi}}{\Psi}) \Psi^2)$$

$$Q^6 / M^2$$

Program 3.

```
Needs{"Hip`Work`"};
SetDotProduct[{q1, q1, 0}, {q2, q2, 0}, {q3, q3, 0}, {K, K, M^2},
               {q1, q2, u/2}, {q1, q3, t/2}, {q2, q3, s/2}]
PrepareIndex[alf, bet, gam, del, rho, mu, nu, m1, m2, m3];
m=M/2;
K=q1+q2+q3;
AA01=b1*G[alf, m1]*G[m2, m3]+b2*G[alf, m2]*G[m1, m3]+b3*G[alf, m3]*G[m1, m2]+
G[alf, m1]*( X1213*q1[m2]*q1[m3] + X1223*q1[m2]*q2[m3] +
             X1332*q1[m3]*q3[m2] + X1322*q1[m3]*q2[m2] +
             X1233*q1[m2]*q3[m3] + X3233*q3[m2]*q3[m3] +
             X2223*q2[m2]*q2[m3])+
G[alf, m2]*( X1113*q1[m1]*q1[m3] + X1321*q1[m3]*q2[m1] +
             X1123*q1[m1]*q2[m3] + X2123*q2[m1]*q2[m3] +
             X2331*q2[m3]*q3[m1] + X2133*q2[m1]*q3[m3] +
             X3133*q3[m1]*q3[m3])+
G[alf, m3]*( X1112*q1[m1]*q1[m2] + X2122*q2[m1]*q2[m2] +
             X1231*q1[m2]*q3[m1] + X2231*q2[m2]*q3[m1] +
             X1132*q1[m1]*q3[m2] + X2132*q2[m1]*q3[m2] +
             X3132*q3[m1]*q3[m2]) ;
AA02 = G[m1, m2]*(X1a13*q1[alf]*q1[m3]+X1a23*q1[alf]*q2[m3]+X132a*q1[m3]
*q2[alf]+
X2a23*q2[alf]*q2[m3] + X133a*q1[m3]*q3[alf] + X233a*q2[m3]*q3[alf]+
X1a33*q1[alf]*q3[m3] + X2a33*q2[alf]*q3[m3] + X3a33*q3[alf]*q3[m3])+
G[m1, m3]*(X1a12*q1[alf]*q1[m2]+X122a*q1[m2]*q2[alf]+X123a*q1[m2]*
q3[alf] + X1a32*q1[alf]*q3[m2] + X2a32*q2[alf]*q3[m2] +
X3a32*q3[alf]*q3[m2]+ X1a22*q1[alf]*q2[m2] +X2a22*q2[alf]*q2[m2]+
X223a*q2[m2]*q3[alf])+
G[m2, m3]*(X1a11*q1[alf]*q1[m1]+X112a*q1[m1]*q2[alf]+X1a21*q1[alf]*
q2[m1]+X2a21*q2[alf]*q2[m1]+X113a*q1[m1]*q3[alf]+X213a*q2[m1]*q3[alf]+
X1a31*q1[alf]*q3[m1] + X2a31*q2[alf]*q3[m1] +X3a31*q3[alf]*q3[m1] );
AA0-AA01+AA02;
AA2=a1*G[alf, m1]*G[m2, m3]+a2*G[alf, m2]*G[m1, m3]+a3*G[alf, m3]*G[m1, m2]+
G[alf, m1]*( Z1213*q1[m2]*q1[m3] + Z1223*q1[m2]*q2[m3] +
Z1332*q1[m3]*q3[m2] + Z1322*q1[m3]*q2[m2] + Z2223*q2[m2]*q2[m3] +
Z2332*q2[m3]*q3[m2] + Z1233*q1[m2]*q3[m3] + Z3233*q3[m2]*q3[m3] +
Z2233*q2[m2]*q3[m3] ) +
G[alf, m2]*( Z1321*q1[m3]*q2[m1] + Z2123*q2[m1]*q2[m3] +
Z2331*q2[m3]*q3[m1] + Z1113*q1[m1]*q1[m3] + Z1123*q1[m1]*q2[m3] +
Z1331*q1[m3]*q3[m1] + Z2133*q2[m1]*q3[m3] + Z3133*q3[m1]*q3[m3] +
Z1133*q1[m1]*q3[m3] ) +
G[alf, m3]*( Z1231*q1[m2]*q3[m1] + Z2132*q2[m1]*q3[m2] +
Z3132*q3[m1]*q3[m2] + Z1112*q1[m1]*q1[m2] + Z1221*q1[m2]*q2[m1] +
Z2122*q2[m1]*q2[m2] + Z2231*q2[m2]*q3[m1] + Z1132*q1[m1]*q3[m2] +
Z1122*q1[m1]*q2[m2] ) ;
AB2= G[m1, m2]*( Z1a13*q1[alf]*q1[m3] + Z1a23*q1[alf]*q2[m3] +
Z132a*q1[m3]*q2[alf] + Z2a23*q2[alf]*q2[m3] + Z133a*q1[m3]*q3[alf] +
Z233a*q2[m3]*q3[alf] + Z1a33*q1[alf]*q3[m3] + Z2a33*q2[alf]*q3[m3] +
Z3a33*q3[alf]*q3[m3] ) +
G[m1, m3]*( Z1a12*q1[alf]*q1[m2] + Z122a*q1[m2]*q2[alf] +
Z123a*q1[m2]*q3[alf] + Z1a32*q1[alf]*q3[m2] + Z2a32*q2[alf]*q3[m2] +
Z3a32*q3[alf]*q3[m2] + Z1a22*q1[alf]*q2[m2] + Z223a*q2[m2]*q3[alf] +
Z2a22*q2[alf]*q2[m2] ) +
G[m2, m3]*( Z1a21*q1[alf]*q2[m1] + Z2a21*q2[alf]*q2[m1] +
Z213a*q2[m1]*q3[alf] + Z1a31*q1[alf]*q3[m1] + Z2a31*q2[alf]*q3[m1] +
Z3a31*q3[alf]*q3[m1] + Z112a*q1[m1]*q2[alf] + Z113a*q1[m1]*q3[alf] +
Z1a11*q1[alf]*q1[m1] ) ;
Expand[AA01*K[alf]];
b0=Contract[% , alf]>>c:\wnmath22\packages\all\jpsideca\b01
```

```

Expand[AA02*K[alf]];
b0=Contract[%,alf]>>c:\wnmath22\packages\ali\jpsideca\b02
Expand[AA2*K[alf]];
c2=Contract[%,alf]>>c:\wnmath22\packages\ali\jpsideca\c2
Expand[AB2*K[alf]];
d2=Contract[%,alf]>>c:\wnmath22\packages\ali\jpsideca\d2
(* ApsqAC1 = ApsqACa+ApsqACb *)
b01=<<<c:\wnmath22\packages\ali\jpsideca\b01;
c2=<<<c:\wnmath22\packages\ali\jpsideca\c2;
Expand[2*b01*c2]; (* "2" because it's an interference term *)
Contract[%,m1];
Contract[%,m2];
Contract[%,m3];
%>>c:\wnmath22\packages\ali\error\ApsqACa.ma;
b02=<<<c:\wnmath22\packages\ali\jpsideca\b02;
c2=<<<c:\wnmath22\packages\ali\jpsideca\c2;
Expand[2*b02*c2]; (* "2" because it's an interference term *)
Contract[%,m1];
Contract[%,m2];
Contract[%,m3];
%>>c:\wnmath22\packages\ali\error\ApsqACb.ma;
(* ApsqAC2 = ApsqACc+ApsqACd *)
b01=<<<c:\wnmath22\packages\ali\jpsideca\b01;
d2=<<<c:\wnmath22\packages\ali\jpsideca\d2;
Expand[2*b01*d2]; (* "2" because it's an interference term *)
Contract[%,m1];
Contract[%,{m2,m3}]>>c:\wnmath22\packages\ali\error\ApsqACc.ma;
b02=<<<c:\wnmath22\packages\ali\jpsideca\b02;
d2=<<<c:\wnmath22\packages\ali\jpsideca\d2;
Expand[2*b02*d2]; (* "2" because it's an interference term *)
Contract[%,m1];
Contract[%,{m2,m3}];
%>>c:\wnmath22\packages\ali\error\ApsqACd.ma;
(* "2" because it's an interference term *)
C1 = Contract[Expand[2*AA0*AA2 ],{alf,m1,m2,m3}];
C2 = Contract[Expand[2*AA0*AB2 ],{alf,m1,m2,m3}];
C1+C2>>c:\wnmath22\packages\ali\jpsideca\AsqAC;
<<<c:\wnmath22\packages\ali\error\TA.ma;
T=Expand[%];
a = a0;
(*b and a1 terms are being multiplied by a3 which contains Dpsi
in it *)
b = 0; (*coefficient of Dpsi*)
a1 = 0; (*coefficient of Dpsi*)
Coefficient[T,G[alf,m1]*G[m2,m3]];
b1=Simplify[%];
Coefficient[T,G[alf,m2]*G[m1,m3]];
b2=Simplify[%];
Coefficient[T,G[alf,m3]*G[m1,m2]];
b3=Simplify[%];
X=Expand[T-b1*G[alf,m1]*G[m2,m3]-b2*G[alf,m2]*G[m1,m3]-
b3*G[alf,m3]*G[m1,m2]];

```

```

Y1=Coefficient[X,G[alf,m1]];
X1213=Simplify[Coefficient{Y1,q1[m2]*q1[m3]}];
X1223=Simplify[Coefficient{Y1,q1[m2]*q2[m3]}];
X1332=Simplify[Coefficient{Y1,q1[m3]*q3[m2]}];
X1322=Simplify[Coefficient{Y1,q1[m3]*q2[m2]}];
X2223=Simplify[Coefficient{Y1,q2[m2]*q2[m3]}];
X1233=Simplify[Coefficient{Y1,q1[m2]*q3[m3]}];
X3233=Simplify[Coefficient{Y1,q3[m2]*q3[m3]}];

Y2=Coefficient[X,G[alf,m2]];
X1113=Simplify[Coefficient{Y2,q1[m1]*q1[m3]}];
X1321=Simplify[Coefficient{Y2,q1[m3]*q2[m1]}];
X1123=Simplify[Coefficient{Y2,q1[m1]*q2[m3]}];
X2123=Simplify[Coefficient{Y2,q2[m1]*q2[m3]}];
X2331=Simplify[Coefficient{Y2,q2[m3]*q3[m1]}];
X2133=Simplify[Coefficient{Y2,q2[m1]*q3[m3]}];
X3133=Simplify[Coefficient{Y2,q3[m1]*q3[m3]}];

Y3=Coefficient[X,G[alf,m3]];
X1112=Simplify[Coefficient{Y3,q1[m1]*q1[m2]}];
X2122=Simplify[Coefficient{Y3,q2[m1]*q2[m2]}];
X1231=Simplify[Coefficient{Y3,q1[m2]*q3[m1]}];
X2231=Simplify[Coefficient{Y3,q2[m2]*q3[m1]}];
X1132=Simplify[Coefficient{Y3,q1[m1]*q3[m2]}];
X2132=Simplify[Coefficient{Y3,q2[m1]*q3[m2]}];
X3132=Simplify[Coefficient{Y3,q3[m1]*q3[m2]}];

Y4=Coefficient[X,G[m1,m2]];
X1a13=Simplify[Coefficient{Y4,q1[alf]*q1[m3]}];
X1a23=Simplify[Coefficient{Y4,q1[alf]*q2[m3]}];
X132a=Simplify[Coefficient{Y4,q1[m3]*q2[alf]}];
X2a23=Simplify[Coefficient{Y4,q2[alf]*q2[m3]}];
X133a=Simplify[Coefficient{Y4,q1[m3]*q3[alf]}];
X233a=Simplify[Coefficient{Y4,q2[m3]*q3[alf]}];
X1a33=Simplify[Coefficient{Y4,q1[alf]*q3[m3]}];
X2a33=Simplify[Coefficient{Y4,q2[alf]*q3[m3]}];
X3a33=Simplify[Coefficient{Y4,q3[alf]*q3[m3]}];

Y5=Coefficient[X,G[m1,m3]];
X1a12=Simplify[Coefficient{Y5,q1[alf]*q1[m2]}];
X122a=Simplify[Coefficient{Y5,q1[m2]*q2[alf]}];
X123a=Simplify[Coefficient{Y5,q1[m2]*q3[alf]}];
X1a32=Simplify[Coefficient{Y5,q1[alf]*q3[m2]}];
X2a32=Simplify[Coefficient{Y5,q2[alf]*q3[m2]}];
X3a32=Simplify[Coefficient{Y5,q3[alf]*q3[m2]}];
X1a22=Simplify[Coefficient{Y5,q1[alf]*q2[m2]}];
X2a22=Simplify[Coefficient{Y5,q2[alf]*q2[m2]}];
X223a=Simplify[Coefficient{Y5,q2[m2]*q3[alf]}];

Y6=Coefficient[X,G[m2,m3]];
X1a11=Simplify[Coefficient{Y6,q1[alf]*q1[m1]}];
X112a=Simplify[Coefficient{Y6,q1[m1]*q2[alf]}];
X1a21=Simplify[Coefficient{Y6,q1[alf]*q2[m1]}];
X2a21=Simplify[Coefficient{Y6,q2[alf]*q2[m1]}];
X113a=Simplify[Coefficient{Y6,q1[m1]*q3[alf]}];
X213a=Simplify[Coefficient{Y6,q2[m1]*q3[alf]}];
X1a31=Simplify[Coefficient{Y6,q1[alf]*q3[m1]}];
X2a31=Simplify[Coefficient{Y6,q2[alf]*q3[m1]}];
X3a31=Simplify[Coefficient{Y6,q3[alf]*q3[m1]}];

```

```

b1*G[alf,m1]*G[m2,m3]+b2*G[alf,m2]*G[m1,m3]+b3*G[alf,m3]*G[m1,m2]+
G[alf,m1]*( X1213*q1[m2]*q1[m3] + X1223*q1[m2]*q2[m3] +
X1332*q1[m3]*q3[m2] + X1322*q1[m3]*q2[m2] +
X1233*q1[m2]*q3[m3] + X3233*q3[m2]*q3[m3] +
X2223*q2[m2]*q2[m3])+
G[alf,m2]*( X1113*q1[m1]*q1[m3] + X1321*q1[m3]*q2[m1] +
X1123*q1[m1]*q2[m3] + X2123*q2[m1]*q2[m3] +
X2331*q2[m3]*q3[m1] + X2133*q2[m1]*q3[m3] +
X3133*q3[m1]*q3[m3])+
G[alf,m3]*( X1112*q1[m1]*q1[m2] + X2122*q2[m1]*q2[m2] +
X1231*q1[m2]*q3[m1] + X2231*q2[m2]*q3[m1] +
X1132*q1[m1]*q3[m2] + X2132*q2[m1]*q3[m2] +
X3132*q3[m1]*q3[m2])+
G[m1,m2]*(X1a13*q1[alf]*q1[m3]+X1a23*q1[alf]*q2[m3]+X132a*q1[m3]*
q2[alf]+X2a23*q2[alf]*q2[m3] + X133a*q1[m3]*q3[alf] + X233a*q2[m3]*
q3[alf]+
X1a33*q1[alf]*q3[m3] + X2a33*q2[alf]*q3[m3] + X3a33*q3[alf]*q3[m3])+
G[m1,m3]*(X1a12*q1[alf]*q1[m2]+X122a*q1[m2]*q2[alf]+X123a*q1[m2]*
q3[alf] +
X1a32*q1[alf]*q3[m2] + X2a32*q2[alf]*q3[m2] + X3a32*q3[alf]*q3[m2]+
X1a22*q1[alf]*q2[m2] +X2a22*q2[alf]*q2[m2]+X223a*q2[m2]*q3[alf])+
G[m2,m3]*(X1a11*q1[alf]*q1[m1]+X112a*q1[m1]*q2[alf]+X1a21*q1[alf]*
q2[m1]+
X2a21*q2[alf]*q2[m1]+X113a*q1[m1]*q3[alf]+X213a*q2[m1]*q3[alf]+
X1a31*q1[alf]*q3[m1]+X2a31*q2[alf]*q3[m1]+X3a31*q3[alf]*q3[m1] );

```

```
X=Expand[%-T]
```

```
0
```

```
<<c:\wnmath22\packages\ali\error\TC.ma;
```

```
T=Expand[%];
```

```
Coefficient[T,G[alf,m1]*G[m2,m3]];
```

```
a1=Simplify[%];
```

```
Coefficient[T,G[alf,m2]*G[m1,m3]];
```

```
a2=Simplify[%];
```

```
Coefficient[T,G[alf,m3]*G[m1,m2]];
```

```
a3=Simplify[%];
```

```
X=Expand[T-a1*G[alf,m1]*G[m2,m3]-a2*G[alf,m2]*G[m1,m3]-
a3*G[alf,m3]*G[m1,m2]];
```

```
Y1=Coefficient[X,G[alf,m1]];
```

```
Z1213=Simplify[Coefficient[Y1,q1[m2]*q1[m3]]];
```

```
Z1223=Simplify[Coefficient[Y1,q1[m2]*q2[m3]]];
```

```
Z1332=Simplify[Coefficient[Y1,q1[m3]*q3[m2]]];
```

```
Z1322=Simplify[Coefficient[Y1,q1[m3]*q2[m2]]];
```

```
Z2223=Simplify[Coefficient[Y1,q2[m2]*q2[m3]]];
```

```
Z2332=Simplify[Coefficient[Y1,q2[m3]*q3[m2]]];
```

```
Z1233=Simplify[Coefficient[Y1,q1[m2]*q3[m3]]];
```

```
Z3233=Simplify[Coefficient[Y1,q3[m2]*q3[m3]]];
```

```
Z1332=Simplify[Coefficient[Y1,q1[m3]*q3[m2]]];
```

```
Z2233=Simplify[Coefficient[Y1,q2[m2]*q3[m3]]];
```

```
Y2=Coefficient[X,G[alf,m2]];
```

```
Z1321=Simplify[Coefficient[Y2,q1[m3]*q2[m1]]];
```

```
Z2123=Simplify[Coefficient[Y2,q2[m1]*q2[m3]]];
```

```
Z2331=Simplify[Coefficient[Y2,q2[m3]*q3[m1]]];
```

```
Z1113=Simplify[Coefficient[Y2,q1[m1]*q1[m3]]];
```

```
Z1123=Simplify[Coefficient[Y2,q1[m1]*q2[m3]]];
```

```
Z1331=Simplify[Coefficient[Y2,q1[m3]*q3[m1]]];
```

```
Z2133=Simplify[Coefficient[Y2,q2[m1]*q3[m3]]];
```

```
Z3133=Simplify[Coefficient[Y2,q3[m1]*q3[m3]]];
```

```
Z1133=Simplify[Coefficient[Y2,q1[m1]*q3[m3]]];
```

```
Y3=Coefficient[X,G[alf,m3]];
```

```
Z1231=Simplify[Coefficient[Y3,q1[m2]*q3[m1]]];
```

```
Z2132=Simplify[Coefficient[Y3,q2[m1]*q3[m2]]];
```

```
Z3132=Simplify[Coefficient[Y3,q3[m1]*q3[m2]]];
Z1112=Simplify[Coefficient[Y3,q1[m1]*q1[m2]]];
Z1221=Simplify[Coefficient[Y3,q1[m2]*q2[m1]]];
Z2122=Simplify[Coefficient[Y3,q2[m1]*q2[m2]]];
Z2231=Simplify[Coefficient[Y3,q2[m2]*q3[m1]]];
Z1132=Simplify[Coefficient[Y3,q1[m1]*q3[m2]]];
Z1122=Simplify[Coefficient[Y3,q1[m1]*q2[m2]]];
Y4=Coefficient[X,G[m1,m2]];
Z1a13=Simplify[Coefficient[Y4,q1[alf]*q1[m3]]];
Z1a23=Simplify[Coefficient[Y4,q1[alf]*q2[m3]]];
Z132a=Simplify[Coefficient[Y4,q1[m3]*q2[alf]]];
Z2a23=Simplify[Coefficient[Y4,q2[alf]*q2[m3]]];
Z133a=Simplify[Coefficient[Y4,q1[m3]*q3[alf]]];
Z233a=Simplify[Coefficient[Y4,q2[m3]*q3[alf]]];
Z1a33=Simplify[Coefficient[Y4,q1[alf]*q3[m3]]];
Z2a33=Simplify[Coefficient[Y4,q2[alf]*q3[m3]]];
Z3a33=Simplify[Coefficient[Y4,q3[alf]*q3[m3]]];
Y5=Coefficient[X,G[m1,m3]];
Z1a12=Simplify[Coefficient[Y5,q1[alf]*q1[m2]]];
Z122a=Simplify[Coefficient[Y5,q1[m2]*q2[alf]]];
Z123a=Simplify[Coefficient[Y5,q1[m2]*q3[alf]]];
Z1a32=Simplify[Coefficient[Y5,q1[alf]*q3[m2]]];
Z2a32=Simplify[Coefficient[Y5,q2[alf]*q3[m2]]];
Z3a32=Simplify[Coefficient[Y5,q3[alf]*q3[m2]]];
Z1a22=Simplify[Coefficient[Y5,q1[alf]*q2[m2]]];
Z223a=Simplify[Coefficient[Y5,q2[m2]*q3[alf]]];
Z2a22=Simplify[Coefficient[Y5,q2[alf]*q2[m2]]];
```



```

<<c:\wnmath22\packages\ali\jpsideca\ApsqAC;
ApsqAC=Together[%/M^2]>>c:\wnmath22\packages\ali\jpsideca\ApsqAC2.ma;
AsqAC= <<c:\wnmath22\packages\ali\jpsideca\AsqAC1.ma;
ApsqAC=<<c:\wnmath22\packages\ali\jpsideca\ApsqAC2.ma;
six=Expand[AsqAC-ApsqAC]
?>>c:\wnmath22\packages\ali\jpsideca\Diff.ma;
w1=M*x1/2;
w2=M*x2/2;
w3=M-w1-w2;
x3=2-x1-x2;
six = <<c:\wnmath22\packages\ali\jpsideca\Diff.ma;
XX2=Expand[six*(1/3)*(1/6)*a3];
a0=(1/2)*Q^3*Sqrt[M]*Psi;
a3=(1/6)*Q^3*Sqrt[M]*M^2*Dpsi;
AAC=Together[XX2]>>c:\wnmath22\packages\ali\jpsideca\AAC.ma
XX=<<c:\wnmath22\packages\ali\jpsideca\AAC.ma;
x1=1-s/M^2;
x2=1-t/M^2;
x3=1-u/M^2;
M=Sqrt[s+t+u];
AAC = Simplify[XX] >> c:\wnmath22\packages\ali\jpsideca\aac.ma
AAC=<<c:\wnmath22\packages\ali\jpsideca\AAC.ma
        6
(256 Dpsi Psi Q Sqrt[s + t + u]
      5 2      4 3      3 4      2 5      5
(15 s t + 35 s t + 35 s t + 15 s t - 42 s t u -
      4 2      3 3      2 4      5      5 2
33 s t u + 26 s t u - 33 s t u - 42 s t u + 15 s u -
      4 2      3 2 2      2 3 2      4 2
33 s t u + 46 s t u + 46 s t u - 33 s t u +
      5 2      4 3      3 3      2 2 3      3 3
15 t u + 35 s u + 26 s t u + 46 s t u + 26 s t u +
      4 3      3 4      2 4      2 4      3 4
35 t u + 35 s u - 33 s t u - 33 s t u + 35 t u +
      2 5      5      2 5
15 s u - 42 s t u + 15 t u ) /
      3      3      3
(27 (s + t) (s + u) (t + u) )
(* The above:
(1)Has been divided by 3 for Jpsi pol. states.
(2)Has been divided by 6 for 3 identical photons.
(3)Has been multiplied by Q^6*M/4*psi(0)*(1/6)*M^5/2*Dpsi/M^2 *)
(* Now get decay rate by dividing by the flux factor,
multiplying by Dlips, and integrating over x1 and x2. *)
Dlips=M^2/(128*Pi^3);
Flux=2*M;
T4=AAC*Dlips/Flux;
d4=Factor[Together[Expand[T4*M^2/(Q^6*(Dpsi/Psi)*Psi^2)]]]
s = M^2 (1-x1);
t = M^2 (1-x2);
u = M^2 (1-x3);

```

```

Y6=Coefficient[X,G[m2,m3]];
Z1a21=Simplify[Coefficient[Y6,q1[alf]*q2[m1]]];
Z2a21=Simplify[Coefficient[Y6,q2[alf]*q2[m1]]];
Z213a=Simplify[Coefficient[Y6,q2[m1]*q3[alf]]];
Z1a31=Simplify[Coefficient[Y6,q1[alf]*q3[m1]]];
Z2a31=Simplify[Coefficient[Y6,q2[alf]*q3[m1]]];
Z3a31=Simplify[Coefficient[Y6,q3[alf]*q3[m1]]];
Z112a=Simplify[Coefficient[Y6,q1[m1]*q2[alf]]];
Z113a=Simplify[Coefficient[Y6,q1[m1]*q3[alf]]];
Z1a11=Simplify[Coefficient[Y6,q1[alf]*q1[m1]]];

Z2332*q2[m3]*q3[m2] + Z1233*q1[m2]*q3[m3] + Z3233*q3[m2]*q3[m3] +
Z2233*q2[m2]*q3[m3] ) +
G[alf,m2]*( Z1321*q1[m3]*q2[m1] + Z2123*q2[m1]*q2[m3] +
Z2331*q2[m3]*q3[m1] + Z1113*q1[m1]*q1[m3] + Z1123*q1[m1]*q2[m3] +
Z1331*q1[m3]*q3[m1] + Z2133*q2[m1]*q3[m3] + Z3133*q3[m1]*q3[m3] +
Z1133*q1[m1]*q3[m3] ) +
G[alf,m3]*( Z1231*q1[m2]*q3[m1] + Z2132*q2[m1]*q3[m2] +
Z3132*q3[m1]*q3[m2] + Z1112*q1[m1]*q1[m2] + Z1221*q1[m2]*q2[m1] +
Z2122*q2[m1]*q2[m2] + Z2231*q2[m2]*q3[m1] + Z1132*q1[m1]*q3[m2] +
Z1122*q1[m1]*q2[m2] ) +
G[m1,m2]*( Z1a13*q1[alf]*q1[m3] + Z1a23*q1[alf]*q2[m3] +
Z132a*q1[m3]*q2[alf] + Z2a23*q2[alf]*q2[m3] + Z133a*q1[m3]*q3[alf] +
Z233a*q2[m3]*q3[alf] + Z1a33*q1[alf]*q3[m3] + Z2a33*q2[alf]*q3[m3] +
Z3a33*q3[alf]*q3[m3] ) +
G[m1,m3]*( Z1a12*q1[alf]*q1[m2] + Z122a*q1[m2]*q2[alf] +
Z123a*q1[m2]*q3[alf] + Z1a32*q1[alf]*q3[m2] + Z2a32*q2[alf]*q3[m2] +
Z3a32*q3[alf]*q3[m2] + Z1a22*q1[alf]*q2[m2] + Z223a*q2[m2]*q3[alf] +
Z2a22*q2[alf]*q2[m2] ) +
G[m2,m3]*( Z1a21*q1[alf]*q2[m1] + Z2a21*q2[alf]*q2[m1] +
Z213a*q2[m1]*q3[alf] + Z1a31*q1[alf]*q3[m1] + Z2a31*q2[alf]*q3[m1] +
Z3a31*q3[alf]*q3[m1] + Z112a*q1[m1]*q2[alf] + Z113a*q1[m1]*q3[alf] +
Z1a11*q1[alf]*q1[m1] );
Amp=Expand[%];
Expand[T-%]
0
ApsqACa=<<<c:\wnmath22\packages\ali\error\ApsqACa.ma;
Aa=Expand[%];
%>>c:\wnmath22\packages\ali\jpsideca\trial1.ma;
ApsqACb=<<<c:\wnmath22\packages\ali\error\ApsqACb.ma;
Ab=Expand[%];
%>>c:\wnmath22\packages\ali\jpsideca\trial2.ma;
ApsqACc=<<<c:\wnmath22\packages\ali\error\ApsqACc.ma;
Ac=Expand[%];
%>>c:\wnmath22\packages\ali\jpsideca\trial3.ma;
ApsqACd=<<<c:\wnmath22\packages\ali\error\ApsqACd.ma;
Ad=Expand[%];
%>>c:\wnmath22\packages\ali\jpsideca\trial4.ma;
<<<c:\wnmath22\packages\ali\jpsideca\AsqAC;
Ba=Expand[%];
AsqAC=Together[Ba]>>c:\wnmath22\packages\ali\jpsideca\AsqAC1.ma;
<<<c:\wnmath22\packages\ali\jpsideca\trial1.ma;
trial1=Together[%];
<<<c:\wnmath22\packages\ali\jpsideca\trial2.ma;
trial2=Together[%];
<<<c:\wnmath22\packages\ali\jpsideca\trial3.ma;
trial3=Together[%];
<<<c:\wnmath22\packages\ali\jpsideca\trial4.ma;
trial4=Together[%];
Together[trial1+trial2+trial3+trial4]>>
c:\wnmath22\packages\ali\jpsideca\ApsqAC;

```

```

x3 = 2 - x1 - x2;
D4 = d4;
spect4=Integrate{D4, {x2, 1-x1, 1}}
integ4=NIntegrate[spect4, {x1, 0, 1}]
x1=1-S;
Simplify[spect4]
Clear[spect4]
spect4[S_]:= (2*(-41 - 58*S - 293*S^2 -
      86*S^3 + 301*S^4 + 130*S^5 +
      33*S^6 + 14*S^7 - 15*Log[S] -
      51*S*Log[S] - 406*S^2*Log[S] -
      214*S^3*Log[S] -
      395*S^4*Log[S] - 167*S^5*Log[S]))/
(27*Pi^3*(-1 + S)^2*(1 + S)^5)
S = 1-x1;
(2 (1248 x1 - 3344 x12 + 3568 x13 - 1936 x14 + 622 x15 - 131 x16 +
  14 x17 + 1248 Log[1 - x1] - 3920 x1 Log[1 - x1] +
  5088 x12 Log[1 - x1] - 3464 x13 Log[1 - x1] +
  1230 x14 Log[1 - x1] - 167 x15 Log[1 - x1])) /
(27 Pi3 (-2 + x1)5 x12)

```

Program 4.

```

Needs["Hip`Work`"];
PrepareIndex[alp,bet,mu,nu,rho,lambda];
Clear[Q,l,n,z,m,M,M0,M2,M4,x,ln,lQ];
SetDotProduct[{{Q,Q,M^2},{n,n,0},{l,l,m^2},{Q,l,lQ},{l,n,ln},{Q,n,l}}];
m = M/2;
(* M0 is the matrix element of two quark field operators at origin *)
M0 = (a1 M^2 + a2 M Sl[Q]);
M2 = (b/2) M^2 *( Slash[Q]**Dg[rho] - Dg[rho]**Slash[Q] );
M4 = (d1/2) M (-M^3 G[rho,lambda] + M Q[rho] Q[lambda] - M^2 Sl[Q] *
  G[rho,lambda] + Sl[Q] Q[rho] Q[lambda] );
d2[k_,mu_,nu_] := -DP[k,n] G[mu,nu] + (k[mu]*n[nu]+k[nu]*n[mu] )
d3[k_,mu_,nu_,rho_] := -2 k[rho] d2[k,mu,nu] DP[k,n] + DP[k,k]*
  (-k[mu]*n[nu]*n[rho]-k[nu] n[rho]+(G[rho,mu] n[nu]+
    G[rho,nu] n[mu] ) * DP[k,n]);
d4[k_,mu_,nu_,alp_,bet_] := DP[k,k] DP[k,n] ( -2 (DP[k,n] G[alp,bet] +
  k[alp] n[bet] ) d2[k,mu,nu] +
  (2 k[bet] DP[k,n]+DP[k,k] n[bet]) ( G[mu,alp] n[nu] +
  G[alp,nu] n[mu] ) -
  2 k[alp] DP[k,n] (-n[bet] G[mu,nu] + n[nu] G[bet,mu] +
  n[mu] G[bet,nu])-
  DP[k,k] (n[alp] n[nu] G[mu,bet] + n[alp] n[mu] G[nu,bet]) -
  2 k[bet] ( n[alp] k[mu] n[nu] + n[alp] k[nu] n[mu] ) ) -
  2 ( 2 k[bet] DP[n,k]+n[bet] DP[k,k] ) d3[k,mu,nu,alp]
AB1 = - Tr[Sl[n]**(Sl[Q+1]+m)**Dg[alp]**M0**Dg[bet]**
  (-Sl[l]+m)**Dg[mu]**M0**Dg[nu]**(Sl[Q+1]+m) ];
AB2 = Tr[Sl[n]**(Sl[Q+1]+m)**Dg[alp]**M0**Dg[bet]**
  (-Sl[l]+m)**Dg[mu]**M2**Dg[nu]**(Sl[Q+1]+m)];
AB3 = Tr[Sl[n]**(Sl[Q+1]+m)**Dg[alp]**M4**Dg[bet]**
  (-Sl[l]+m)**Dg[mu]**M0**Dg[nu]**(Sl[Q+1]+m)];
Expand[AB1 * d2[k,bet,alp] ];
Contract[%,{alp,bet}];
Expand[% * d2[k,mu,nu]];
AC1=Contract[%,{mu,nu}];
Expand[AB2 * d2[k,alp,bet]];
AC2 = Contract[%,{alp,bet}];
Expand[AC2 * d3[k,mu,nu,rho] ];
AC2 = Contract[%,{rho,mu,nu}];
Expand[AB3 * d2[k,mu,nu]];
AC3 = Contract[%,{mu,nu}];
d4[k,bet,alp,rho,lambda];
Expand[AC3 * %];
AC3 = Contract[%,{rho,lambda,bet,alp}];
lQ = (M^2 x + m^2) / (2(1/z-1)) + (1/z-1) M^2/2;
ln = (1/z-1);
Denom1 = (DP[Q+1,Q+1]-m^2)^2 * (DP[k,k])^2 * (DP[k,n])^2 ;
Denom2 = (DP[Q+1,Q+1]-m^2)^2 * (DP[k,k])^3 * (DP[k,n])^3 ;
Denom3 = (DP[Q+1,Q+1]-m^2)^2 * (DP[k,k])^4 * (DP[k,n])^4 ;
k = Q/2 + 1;
AG1 = Simplify [AC1 / Denom1];
AG2 = Simplify [AC2 / Denom2];
AG3 = Simplify [AC3 / Denom3];
S1 = Integrate[AG1,{x,0,Infinity}];
S2 = Integrate[AG2,{x,0,Infinity}];
S3 = Integrate[AG3,{x,0,Infinity}];
a1 = 1/(2 M^(3/2)) Wfunc;
a2 = a1 + 1/(M^(7/2)) D2Wfunc;

```

```

b = D2Wfunc / (3 M^(7/2));
d1 = D2Wfunc / (6 M^(7/2));
Wfunc = R0/Sqrt[4 Pi];
D2Wfunc = DRs / Sqrt[4 Pi];
Cf = 16/(3*36);
g = Sqrt[4 Pi alphas];
Result1 = Factor[Cf (M z g^2)^2* S1/ ((1-z) *
(16 Pi^2))];
Result2 = 2 * Together[Factor[Cf (M z g^2)^2* S2/ ((1-z) *
(16 Pi^2))]];
Result3 = 2 * Together[Factor[Cf (M z g^2)^2* S3/ ((1-z) *
(16 Pi^2))]];
Re0 = R0^2 * Factor[Coefficient[Result1,R0,2] ]
      2 2 2 2 3 4
64 alphas R0 (-1 + z) z (48 + 8 z - 8 z + 3 z )
-----
      3 6
      81 M Pi (-2 + z)
Re1 = R0 * Factor[Coefficient[Result1,R0,1] ]
      2 2
1024 alphas DRs R0 (-1 + z) z (2 + z)
-----
      5 5
      27 M Pi (2 - z)
Re2 = R0 * Factor[Coefficient[Result2,R0,1]]
-(512*alphas^2*DRs*R0*(-1 + z)^2*z^2*(-24 + 4*z + 2*z^2 + 3*z^3))/
(243*M^5*Pi*(-2 + z)^6);
Re3 = R0 * Factor[Coefficient[Result3,R0,1]]
      2 2
(512 alphas DRs R0 (-1 + z) z
      2 3 4 5 6
(-192 + 336 z - 416 z + 192 z - 76 z + 33 z - 6 z )) /
      5 8
(243 M Pi (-2 + z) )
Wfncor = Factor[Simplify [Rel + Re2 + Re3]]
      2 2
(512 alphas DRs R0 (-1 + z) z
      2 3 4 5 6
(96 + 144 z - 528 z + 296 z - 102 z + 43 z - 9 z )) /
      5 8
(243 M Pi (-2 + z) )

```